Linear Quadratic Regulator Control of Greenhouse Indoor Climate Incorporating Feedback Linearization

Kidist Ameha Mengesha

A Thesis Submitted to

The Department of Electrical Power and Control Engineering

School of Electrical Engineering and Computing

Presented in Partial Fulfillment of the Requirement for the Master of Science Degree in Electrical Power and Control Engineering (Specialization in Control Engineering)

Office of Graduate Studies

Adama Science and Technology University

July 2021

Adama, Ethiopia

Linear Quadratic Regulator Control of Greenhouse Indoor Climate Incorporating Feedback Linearization

Kidist Ameha Mengesha

Advisor: Prof. Gang Gyoo Jin

A Thesis Submitted to
The Department of Electrical Power and Control Engineering
School of Electrical Engineering and Computing

Presented in Partial Fulfillment of the Requirement for the Master of Science Degree in Electrical Power and Control Engineering (Specialization in Control Engineering)

Office of Graduate Studies
Adama Science and Technology University

July 2021
Adama, Ethiopia

APPROVAL SHEET

I, the advisor of the thesis entitled "Linear Quadratic Regulator Control of Greenhouse Indoor Climate Incorporating Feedback Linearization" and developed by Kidist Ameha Mengesha, hereby certify that the recommendation and suggestions made by the board of examiners are appropriately incorporated into the final version of the thesis.

______________________	________________	________________
Advisor	Signature	Date

We, the undersigned, members of the Board of Examiners of the thesis by Kidist Ameha Mengesha have read and evaluated the thesis entitled "Linear Quadratic Regulator Control of Greenhouse Indoor Climate Incorporating Feedback Linearization" and examined the candidate during the open defense. This is, therefore, to certify that the thesis is accepted for partial fulfillment of the requirement of the degree of Master of Science in Control Engineering.

______________________	________________	________________
Chairperson	Signature	Date
______________________	________________	________________
Internal Examiner	Signature	Date
______________________	________________	________________
External Examiner	Signature	Date

Finally, approval and acceptance of the thesis are contingent upon submission of its final copy to the Office of Postgraduate Studies (OPGS) through the Department Graduate Council (DGC) and School Graduate Committee (SGC).

______________________	________________	________________
Department Head	Signature	Date
______________________	________________	________________
School Dean	Signature	Date
______________________	________________	________________
Office of Postgraduate Studies, Dean	Signature	Date

DECLARATION AND RECOMMENDATION

Declaration

I hereby declare that this Master Thesis entitled "Linear Quadratic Regulator Control of Greenhouse Indoor Climate Incorporating Feedback Linearization" is my original work. That is, it has not been submitted for the award of any academic degree, diploma, or certificate in any other university. All sources of materials that are used for this thesis have been duly acknowledged through citation.

Kidist Ameha Mengesha		4.08.2021
Name of the student	Signature	Date

Recommendation

I, the advisor of this thesis, hereby certify that I have read the revised version of the thesis entitled "Linear Quadratic Regulator Control of Greenhouse Indoor Climate Incorporating Feedback Linearization" prepared under my guidance by Kidist Ameha Mengesha submitted in partial fulfillment of the requirements for the degree of Master of Science in Control Engineering. Therefore, I recommend the submission of the revised version of the thesis to the department following the applicable procedures.

Prof. Gang Gyoo Jin	____________________	____________________
Advisor	Signature	Date

ACKNOWLEDGMENTS

First and foremost, I would like to thank the almighty God who gave me strength, patience, and courage to complete the thesis successfully.

I am incredibly grateful to my esteemed advisor, **Professor Gang Gyoo Jin**, for his invaluable advice, continuous support, and patience during my thesis. His immense knowledge and ample experience have encouraged me in my academic research and daily life. Regardless of his often-high workload, he always makes time to answer questions and give encouraging advice.

I would also like to thank the production manager of Florensis Ethiopia PLC, **Mr. Netsanet Tadesse,** and all the staff for their cooperation in providing all the required data related to my work.

Furthermore, I would like to thank **Mr. Hinsermu Alemayehu Garbaabaa (MSc.)** for his support during my thesis work.

I would like to thank the EPCE department head **Mr. Mesfin Megra (MSc.),** and laboratory staff members for making open computer labs for discussion when I have a meeting with my advisor and for making me feel very welcome during my thesis. Moreover, I would like to appreciate the department for preparing the progress and mock presentations.

Finally, I have a special thanks to my whole family and friends for their love, encouragement, and sacrifices.

ABSTRACT

Greenhouses are highly vulnerable to internal and external climate factors like sunlight, temperature, humidity, and carbon dioxide. An appropriate control mechanism of the greenhouse environment is required to maximize the growth and quality of the plants. Even though controlling the indoor climate of a greenhouse is difficult due to the system nonlinearity and existence of coupling relation among system parameters, the designed controller should have good tracking and rejection performances. With this as a starting point, feedback linearization linear quadratic regulator (LQR) control of greenhouse indoor climate is implemented in this thesis. The nonlinear multi-input multi-output (MIMO) dynamic model of greenhouse climate is obtained and transformed to its equivalent linear model using input-output feedback linearization. Then, a proportional-integral (PI)-type LQR controller is designed based on the linearized model to obtain a fast response with less overshoot. In addition, a genetic algorithm (GA)-based practical proportional integral derivative (PID) controller that minimizes the performance indices such as integral absolute error (IAE) and integral square error (ISE) is implemented for comparison purposes. The setpoint tracking and disturbance rejection performance tests are performed by considering different psychrometric processes for the daytime summer season operations. The performance of these controllers is evaluated using performance measures such as overshoot, settling time, recovery time, and perturbance peak values. In the tracking test, the closed-loop response of indoor temperature at 28℃ and 20g [water]/kg [dry air] using the LQR temperature controller gives 1.6369min, 3.0330min, 0, and 1.8523 of rise time, settling time, overshoot, and IAE, which is very small as compared to the PID, respectively. Also, the LQR humidity controller gives a 0 overshoot with 0.5814 of IAE even though the settling time (3.8772min) is slightly greater than the PID. In the rejection test, when both the intercepted solar radiant energy and outside temperature are increased while setpoints are fixed at 28℃ and 18g [water]/kg [dry air], the LQR recovers the output responses of temperature and humidity quickly with a recovery time of 4.2819min and 3.7231min, respectively. These values are very small compared to the PID controller. In general, the performance measures of the implemented controllers in both performance tests informed that the LQR indoor temperature and humidity controller is better than the PID controller for this designed system.

Keywords: *Greenhouse Climate, LQR, Feedback Linearization, PID Controller, and Genetic Algorithm*

TABLE OF CONTENTS

LIST OF TABLES

LIST OF FIGURES

LIST OF ACRONYMS

DIS	Disturbance
GA	Genetic Algorithm
GH	Greenhouse
IAE	Integral Absolute Error
ISE	Integral Square Error
LQR	Linear Quadratic Regulator
MIMO	Multi-Input Multi-Output
PI	Proportional Integral
PID	Proportional Integral Derivative
PSO	Particle Swarm Optimization
RBF	Radial Basis Function
RK4	Rang Kutta Fourth Order
SFC	State Feedback Controller
SP	Setpoint

LIST OF SYMBOLS

A	Surface area
Co	The thermal capacity of the greenhouse
Cp	Specific heat of the air
H_{in}	Inside humidity ratio
H_{out}	Outside humidity ratio
I	Solar radiation
Q_C	Heat loss conducted through the walls
Q_e	Heat loss due to water evaporation
Q_{fog}	Heat loss due to the fog system
Q_h	Heat emanated by the floor heating system
Q_s	Solar energy entering the greenhouse
Q_V	Heat loss due to the ventilation
$q_{\%fog}$	Percentage of the maximum capacity of the fog system
S	Intercepted solar radiant energy
T_{in}	Indoor air temperature
T_{out}	Outside air temperature
t	Time
t_v	The inverse of the number of air changes per unit time
V_H	Actively mixing air volume humidity
V_R	Ventilation rate
V_T	Temperature active mixing volume
UA	Heat transfer coefficient of the enclosure
W_{airin}	Rates of moisture transfer from the inside air leaving the greenhouse
W_{airout}	Rates of moisture transfer from the outside air entering the greenhouse
W_e	Rates of moisture due to evaporation water from the floor
W_{fog}	Water capacity of the fog system
α	The overall coefficient to account for shading and leaf area index

α'	Contribution of evapotranspiration to the balance of the absolute humidity
α_c	Cover absorptivity of the solar radiation
β_T	The overall coefficient to account for thermodynamic constants and other factors affecting evapotranspiration
ρ	Air density
τ_c	Cover transmittance
λ	Latent heat of vaporization

CHAPTER ONE

INTRODUCTION

1.1 Background

Supplying agricultural products outside the cultivation season is the main aim of greenhouse industries. Since the open fields are not suitable, they provide an appropriate internal environment for plants to obtain more fruiting and growth. Controlling the greenhouse environment implies controlling the basic environmental parameters of the greenhouse, such as air temperature, humidity, air composition, and light [1]. The comfort in a greenhouse depends on these environmental parameters. The cooling and heating uniformity is also an essential design consideration of greenhouse to maintain the desired setpoint conditions of greenhouse environment parameters.

The difficulty in the distribution of cooling and heating may result from a non-uniformly controlled environment. Since the environment is not uniform, managing the plant climate system becomes more difficult. Additionally, the non-uniform environment causes potential disease problems and differential plant growth rates [2].

The coupling relation of the greenhouse parameters, basically between the air temperature and humidity, is the principal cause for the problematic distribution of either heating or cooling. The inside air temperature and internal humidity are the fundamental factors that affect the microclimate of the greenhouse industry.

This internal coupling characteristic of temperature and humidity exists through psychrometric laws and the thermally dynamic nature [3]. Psychrometry deals with moist air's physical and thermodynamic behaviors. A mixture of dry air and water vapor is called moist air. The psychrometric processes are the basic requirements for designing environmental control systems for plants, crops, animals, or humans. The psychrometric properties of air include dry air, moist air, saturated air, dew point temperature, dry and wet bulb temperature, relative and percentage humidity, and relative ratio. The properties of moist air can be represented in a graphical format using a psychrometric chart. A psychrometric chart is used in many greenhouse industries for troubleshooting greenhouse environmental problems [4].

Several control techniques were proposed to solve the non-uniform distribution of cooling and heating, namely PID, fuzzy logic control, predictive control, and adaptive control. These techniques were applied to control either the nonlinear or the linearized dynamic system of a greenhouse. The results obtained from those methods indicate that the effectiveness of those control systems in tracking setpoint changes. However, the speed of the responses and the system's stability are significant problems of those methods. As a result, a poor setpoint tracking performance was obtained. In their study, they did not consider the performance of the controllers in rejecting disturbances, as there were external disturbances in the greenhouse.

In this thesis, the greenhouse indoor climate is modeled mathematically. Then, the input-output feedback linearization is applied to transform the nonlinear system into its equivalent linear system. A PI-type LQR controller is designed based on the linear model and then combine with the nonlinear cancellation part to obtain the control input. For comparison purposes, the PID controller is designed and GA is used for tuning the PID gains. In the tuning process, the IAE and ISE performance indices are used as objective functions that are minimized by GA. The overall system simulation is performed in MATLAB software based on both setpoint tracking and disturbance rejection tests.

1.2 Statement of the Problem

Nowadays, greenhouse facilities have become more popular in different parts of the world. However, a common challenge remains in managing the interior climate. The internal environment of the greenhouse is essential to obtain better plant growth with good quality. This environment is affected by different parameters such as temperature, humidity, light intensity, and carbon dioxide concentration. The control of such parameters mainly depends upon the climatic seasons like summer (warm) and winter (cold) seasons. The inside air temperature is cooled in summer whereas heated in winter to make a favorable environment. Even though majorities of plants are grown quickly in the summer season, cooling the greenhouse air faces challenges because of less advanced technology in the greenhouse cooling system.

Air temperature and humidity are the major factors that affect the greenhouse microclimate since plants are more sensitive to these environmental parameters. The system is complex due to the nonlinear coupling between indoor air temperature and humidity through psychrometric process law. Coupling may lead to little change in air temperature that causes a change in humidity. The existence of coupling among these system parameters results in a stability and tracking problem in the system. Setpoint tracking is an important performance measuring in greenhouse controller design because the setpoint of such parameters can be changed by the operators depending upon the types of plants, plant-grown stages, and the season.

Additionally, disturbance rejection is also used as performance testing of the greenhouse microclimate controller. The inside environment is also highly affected due to external disturbances such as solar radiation, wind, outside air temperature, and external humidity. Either increasing or decreasing such factors affects the greenhouse indoor climate, especially in the summer season. To overcome the problems mentioned above during the summer season, a transformation from coupling to decoupling system is required for the nonlinear MIMO greenhouse system.

Furthermore, an optimal control method for the decoupled system is also needed for obtaining fast response and good stability of the system during both tracking and rejection problems. In this thesis work, the input-output feedback linearization technique and PI-type LQR controller are proposed and developed. As the PID controller is widely used in many greenhouse industries, the GA-based practical PID controller is also designed for comparison purposes. The proposed control method and the optimized PID is implemented and simulated using MATLAB software.

1.3 Objectives of the Study

1.3.1 General Objectives

The main objective of this thesis is to present an LQR control for greenhouse indoor climate incorporating with feedback linearization technique.

1.3.2 Specific Objectives

The specific objectives of the thesis are:

- To obtain the nonlinear model of greenhouse indoor climate and convert it to an equivalent linear model using the feedback linearization scheme
- To design a PI-type LQR controller that provides good setpoint tracking and disturbance rejection performance
- To check the controllability and stability of the closed-loop system
- To compare the responses of the proposed method with those of the GA-tuned PID controller based on system performance measures

1.4 Scope of the Study

The thesis focuses on the mathematical modeling and design of an indoor climate of a greenhouse system. The simulation of feedback linearization LQR control of greenhouse indoor climate is performed. The designed system is only applied for the daytime operation of the summer season. A GA-based PID controller is also intended for comparison purposes. In GA tuning, the IAE and ISE performance indices are minimized. Furthermore, the setpoint tracking and disturbance rejection performance tests are performed. The performances of the proposed and the optimized PID methods are discussed using performance measures.

1.5 Limitations of the Study

This thesis work is only applicable for the daytime summer season operations. Even though the greenhouse has many environmental parameters, the indoor temperature and humidity are controlled in this study. Although the greenhouse microclimate is affected by several external disturbances, only three disturbances (intercepted solar radiant energy, outside temperature, and external humidity) are considered in this proposed system. Furthermore, the setpoint tracking test is performed using the different setpoint conditions of the cutting flower. Accordingly, this thesis is only applicable for cutting flowers since the temperature and humidity requirements are different from plant to plant.

1.6 Motivation of the Study

Nowadays, greenhouse industries are built in most parts of the world to grow different plants such as vegetables, fruits, crops, and flowers. Greenhouses with a controlled environment can help greenhouse owners to get better-quality control and increase plant growth with advanced control techniques. Plenty of related research has been conducted, especially in the area of microclimate control of greenhouse. The future will have a massive market in greenhouses, and it is essential to be more professional in greenhouse microclimate design, modeling, and control.

1.7 Significance of the Study

The main contribution of this thesis is to model and control the greenhouse indoor air temperature and humidity using an LQR controller incorporating feedback linearization. Due to the complexity and nonlinearity of greenhouse dynamic systems, it is difficult to use classical controllers. To overcome this, an input-output feedback linearization technique is used to convert the nonlinear model to an equivalent linear model. Then, a PI-type LQR is designed based on the linear model and combine with the nonlinear cancellation part to obtain the control input. The main advantage of using LQR is to provide good setpoint tracking and disturbance rejection performance since it can stabilize the given system by selecting eigenvalue locations of the closed-loop system. As the system uses an automated way of finding a state feedback controller, the plant growth and quality are increased. Finally, this thesis can also be an input for people who are engaged in the work of the greenhouse microclimate control system.

1.8 Thesis Organization

This thesis has been organized into six chapters. The first chapter presents the background of the study, statement of the problems, objectives, significance, scope, and limitation of the research. The second chapter describes the overview of the greenhouse system and a review of previous work. It also contains information on the classification of greenhouse based on structure, glazing, and environmental control. The psychrometric chart is explained in this chapter. Moreover, the feedback linearization technique is explained in detail. At the end of this chapter, the pros and cons of previous works are presented. The third chapter presents the methodology and system modeling. The fourth chapter explains the overall controller design. Moreover, stability analysis of the proposed system and the design of the PID controller tuned by GA is presented in this chapter. The proposed system results and discussions are presented and discussed in chapter five. The last chapter presents the conclusions drawn from this work and recommends possible directions for future studies.

CHAPTER TWO

THEORETICAL BACKGROUND AND LITERATURE REVIEW

This chapter mainly covers five main sections. The first section is about the overview of the greenhouse systems. The second section contains the main classifications of greenhouse based on structure, glazing, and environmental control. In the third section, the psychrometric chart and its explanation are described in detail. The feedback linearization technique is described in section four. The last section is about the review of closely related works, especially in indoor climate control of greenhouse with different control techniques along with their merits and demerits.

2.1 Overview of Greenhouse Systems

Greenhouses are covered structures that help crops to grow under a controlled environment. During the off-season, producing foods and ornamentals are impossible by outdoor production. Therefore, greenhouse technologies are essentials in creating a controlled environment to increase crop yields. Also, the growing cost inside a greenhouse is greater than outside growing, which makes the greenhouse industry obtain high production costs. Monitoring and controlling environmental parameters such as temperature, relative humidity, lighting, air quality, CO_2 levels, water, ratio, plant nutrients, and pest control are necessary to obtain high production at low expense and make the environment competitive [1] [5].

Greenhouses are a technology-based industry. The more advanced technology used, the higher potential to achieve a controlled growing environment. This capacity to tightly control the conditions within which the crop is grown is strongly associated with the health and productivity of the crop. Greenhouse technology gives a suitable and controlled environment for the plants to grow seasons outside the cultivation seasons. The technology protects plants from the warmth in summer, and from the cold in winter [6]. The greenhouse technology is more favored to vegetable crops and flowers like tomato, rose, carnation, cauliflower, capsicum, gerbera, cabbage, and chilies. Since commercial farming requires investment in building up the entire framework, applying such technology is suitable for them [7].

2.2 Classification of Greenhouse

Greenhouses are differentiated and classified depending on several criteria. Based on working and principal applications, the greenhouse can be classified as crop cultivation, solar energy collector, and crop drying [8], as shown in Figure 2.1. In this study, the Classification of greenhouse based on the type of structures, type of glazing, and environmental control is explained in detail.

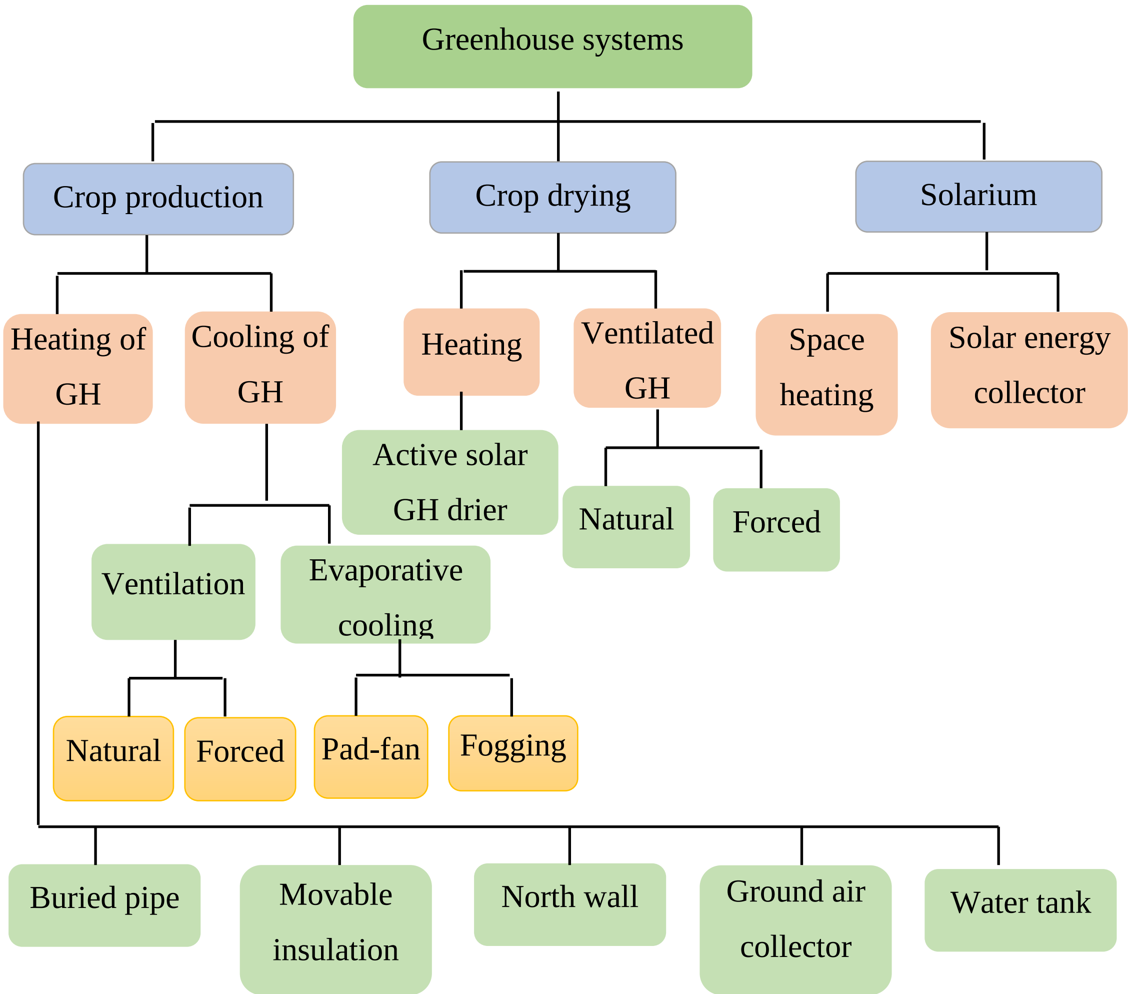

Figure 2.1 Classification of greenhouse based on working and principal applications [8]

2.2.1 Classification Based on the Structure

2.2.1.1 Quonset Greenhouse

Based on structure, a greenhouse is categorized as a Quonset greenhouse. In this greenhouse type, the trusses are sustained through pipe purling that runs along the length of the greenhouse. The enclosure material that used in such a greenhouse is polyethylene.

When compared with gutter-connected greenhouses, it is less expensive and preferable in a given small confined area. The standing and interlocking styles are the basic connection styles that are used in such greenhouses. In the case of interlocking, it is required to grow plants between the overlapping portion of neighboring houses by overlapping truss members. In this type, a single large cultural space exists for a set of houses. This arrangement is better adapted to the automation and movement of labor [9].

Figure 2.2 Quonset Type Greenhouse [10]

2.2.1.2 Gable Roof Greenhouse

Gable-roofed greenhouses are common types of greenhouses. They gain maximum amounts of sunlight while supplying ample space to grow many plants [10].

Figure 2.3 Gable roof type of greenhouse [10]

2.2.2 Classification Based on Glazing

2.2.2.1 Glass Glazing

Glass glazing is the oldest one among all other types of greenhouses glazing materials. As its name implies, the glass is used as a glazing material in this type of greenhouse, as shown in Figure 2.4. It is more effective for winter cultivation as compared to summer cultivation. This is because the temperature is high in the daytime of the summer season. Due to its high installation cost, complicated construction, and frequent damage of glasses through high wind velocity, a glass glazing greenhouse is not preferred [11]. However, the double-pane tempered glass is the best glass glazing type due to its robustness. Also, it breaks into small square pieces in case of damage which minimizes the chances of injury, and tiny parts will not damage your plants [11].

Figure 2.4 Glass glazing greenhouse [12]

2.2.2.2 Fiberglass Reinforced Plastic Glazing

This type of greenhouse is available in two configurations. These are corrugated and flat panels. The corrugated is used as their corrugated shape that lends strength and rigidity to the panels for the greenhouse ceiling. In contrast, the flat is commonly used for windows, sidewalls, and vents [3]. FRPs are soft to be bent in a curve that fits the Quonset type greenhouse framework although they are categorized as rigid plastic, it is also classified as a plain sheet and corrugated sheet [13].

Figure 2.5 Corrugated sheets [14]

2.2.2.3 Plastic Film

A flat solid could be a nice diffuser of daylight, granting intense lightweight at the cover level of the greenhouse. It conjointly produces few shadows as a result of fewer braces and trusses square measure usually utilized in constructing a synthetic resin greenhouse. It is a good selection for first-time greenhouse growers. It is conjointly additional classified as Ultraviolet stabilized low-density synthetic resin and Silpaulin [8].

Figure 2.6 Plastic (polyethylene) film [15]

2.2.3 Classification Based on Environmental Control

The greenhouse environment is affected by many factors such as temperature, solar radiation, carbon dioxide, and humidity. Thus, appropriate control of these factors is required. Every greenhouse has its environmental control system. This system helps to obtain a uniform controlled environment. When the environment is non-uniform, many problems occur in the plants, such as potential diseases, ineradicable results with hormonal or nutrition applications, and variation of plant growth rate. As a result, it is difficult to manage the plant production system [16].

During the summer season, reducing a large amount of heat is the basic concern of the greenhouse environment control system. The main sources of this heat are the incoming solar radiation and heat gain through air exchange. So, reducing such sources of heat and maximizing the fraction of energy partitioned into latent heat can minimize the heat amount of heat in the greenhouse. The best methods to reduce solar radiation are whitewash and shade nets.

Also, the extra heat through air exchange between outside and inside is removed by ventilation during low outside temperatures. The other common technique is evaporative cooling. This technique increases the latent heat fraction of dissipated energy to decrease sensible heat load [17]. A detailed explanation of ventilation, cooling systems and is described below.

2.2.3.1 Ventilation

Two types of ventilation are used in a greenhouse. These are either mechanical or natural ventilation. In the case of mechanical ventilation, the fans are operated using exhaust fans, inlet openings, and electricity [18]. So, a proper design is required to obtain enough cooling under a variety of climatic conditions [19].

The thermal buoyancy and wind effect are the basic natural ventilation phenomena depending on these phenomena. When incoming solar radiation is high, ventilation affects inside greenhouse temperature. Removing excess amounts of heat is necessary to exchange air between inside and outside of a greenhouse in a homogenous manner [19]. The temperature gradients between outside and inside greenhouse and wind create a pressure difference in the greenhouse. As a result, natural ventilation occurs through openings in the greenhouse structure to control the humidity and temperature within the greenhouse. Also, it can provide sufficient air exchange [20].

Fans, roof vents, and front doors are combined to create good ventilation in the greenhouse. The improvement of ventilation is an effective method to reduce the difference between indoor and outdoor air temperature [20].

Figure 2.7 Naturally ventilated greenhouse [21]

2.2.3.2 Cooling System

The temperature control of the greenhouse may be required an additional cooling system when the cooling ability of the ventilation system becomes insufficient for controlling the greenhouse. Pad-fan and fog systems are those additional cooling systems that are worked using water evaporation [20]. In fogging systems, small water droplets with high pressure are sprayed into the air above the plants [22]. This helps to maximize the water surface in contact with the air. When the inside greenhouse is cooled, the relative humidity becomes high during the fogging system [9]. These two cooling systems are described as follows.

1. Fan and Pad Cooling System

The appropriate size of fan and pad systems should be chosen to achieve maximum cooling efficiency. Since these systems cannot be justified all the time, passive ventilation may be used with an open-sided greenhouse. For a given crop, it helps to provide adequate cooling without using any energy. A closed greenhouse with a fan and pad system may be necessary where biosecurity or insect exclusion is a priority in the given greenhouse [23].


Figure 2.8 Fan and pad greenhouse evaporative cooling system [21]

The pads minimize air temperature by passing the air through it. The pad gains heat from plants, soil, and solar radiation when the air moves across the house to the fans. This leads to a gradual increase in air temperature. As a result, the air moves down the greenhouse and increases the temperature. Due to the temperature difference among the fan and pad sides of the greenhouse, there is a temperature gradient across the length of the greenhouse.

Some minerals and algae may develop and cause low efficiency and less air movement in the cooling pads. So, they need frequent maintenance to be efficient. The fan and pad cooling systems can be influenced by many factors [23], the main factors are listed below:

- Greenhouse location and orientation
- Types of cooling pad
- Water flow rate
- Problem with cooling pads
- Operational considerations

2. Fog Cooling System

A pump unit and fogging lines are the basic elements of fogging system in the greenhouse. The pump unit consists of a pump, a water reservoir, a water softener, a fine filter, a pressure adjusting regulator, a valve, and the fogging lines consist of the main pipeline, distributor line, LDPE (low-density polyethylene) pipe [17].

Small size water droplets that contain fog is generated using a high-pressure pumping apparatus. During evaporation, the size of these droplets is very small to stay suspended in the air. When the fog is distributed throughout the greenhouse, that cools the air everywhere, and the risk of disease and pest attack is reduced when the foliage is not wet by the cooling system. Hence, the plants stay dry throughout the process. This system is also used for seed germination and propagation as it removes the need for a mist system. Both types of summer cooling systems can reduce the greenhouse air temperature [23].

Since the size of water droplets is very small in fog, the fog system can reduce the incoming air temperature by 100% while the fan-pad reduce 80% of the difference between the dry and wet bulb temperatures. As a result, complete evaporation of water is taken place in the fog system [17].

Figure 2.9 Fogging system for cooling a greenhouse [24]

2.2.3.3 Shading

One of the procedures for cooling the greenhouse is shading. It is used to reduce the amount of solar radiation that reaches plants. By reducing the solar load on the greenhouse, the air temperature difference is smaller, making the absolute air temperatures inside the greenhouse closer to the outside temperatures [17].

Direct solar radiation is the primary source of heat gain in greenhouses. Due to the reduction of light and the possible effects of ventilation rate, the development and photosynthesis of greenhouse plants might be affected by shading. Hence, care has to be taken when deciding on the type of shading and associated control strategies [17].

A proper selection and installation of shed nets can contribute to increasing crop productions in periods or places where temperature and solar radiation are adverse. The shading plays a large role by protecting the plants from high solar radiation in the greenhouse system [25].

Figure 2.10 Aluminum Shade net for Greenhouse [26]

2.3 Psychrometric Chart

The mixture of different gases, water vapor, and many pollutants make an atmospheric air. The pollutants should be filtered out before processing of air. Thus, the process of air is a mixture of various gases that contain air and water vapor. This mixture yields moist air. Moist air is a mixture of dry air and water vapor. The thermal and physical behavior of this moist air is called psychrometry. The state points of this moist air are represented in a graphical form which is known as a psychrometric chart. The environmental problems of a greenhouse and livestock building can be solved using this chart. The air temperature and humidity problems can be solved by understanding the use and shape of the psychrometric chart. Figure 2.11 depicts an odd-shaped graph of a psychrometric chart that contains a lot of information about the attributes of moist air [4].

A humidity ratio and dry-bulb temperature are scaled on the vertical and horizontal axis of the psychrometric chart, respectively. The dry-bulb temperature is the temperature of air recorded by a standard thermometer with clean and dry sensing elements used during the healing process [27]. Humidity ratio is used for comparing the water vapor to dry air by weight. Different properties of moist air are included in the chart, such as dewpoint temperature, relative humidity, enthalpy, specific volume, and wet-bulb temperature [24].

For evaporative cooling, the wet-bulb line is used to represent the removal of sensible heat by the addition of moisture to the air at a constant wet-bulb temperature. This process is used to increase the relative humidity and decrease the air temperature [4]. The design and analysis of the air conditioning greenhouse environment have required the identification of various processes that are performed on the air. After various processes are identified, the laws of conservation of mass and energy can be used to analyze the processes [24] [27].

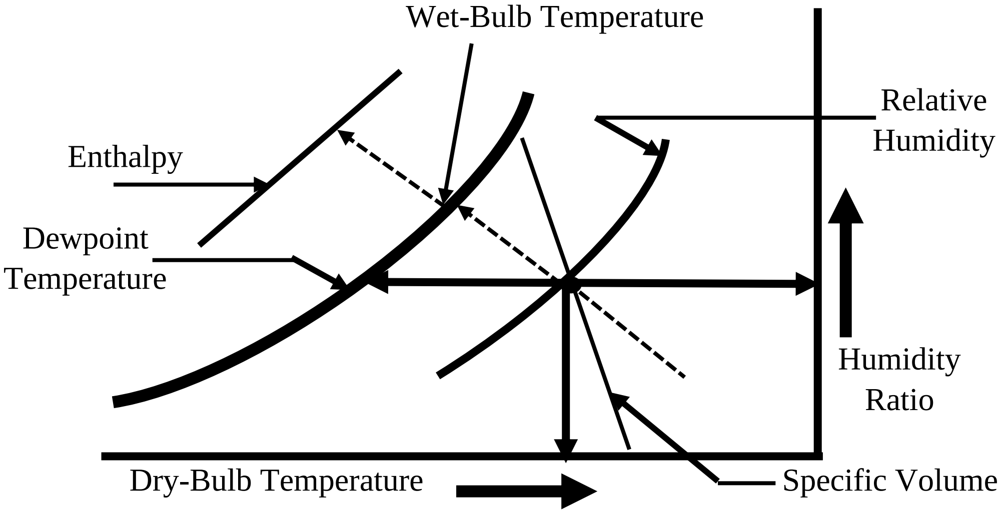

Figure 2.11 A simple representation of the psychrometric chart

These processes are called psychrometric processes such as humidification, dehumidification, sensible heating, sensible cooling, heating and humidification, heating and dehumidification, cooling and humidification, and cooling and dehumidification. In the sensible cooling process, the moist air flows over a cooling coil. This reduces the temperature in the air with a constant moisture content of the air. During the cooling and dehumidification process, both the temperature and humidity ratio of air become decrease due to the condensation of some of the water vapor in the air—the temperature decreases as its humidity rise in the cooling and humidification process. Hence, the evaporative cooling produces a low temperature as compared to the dry-bulb temperature of the air; however, it is higher than its dewpoint temperature to avoid condensation [27].

2.4 Feedback Linearization

Feedback linearization is one of the well-known approaches used in controlling nonlinear systems. The approach involves converting the nonlinear system into an equivalent linear system that could be controlled easily using existing linear control theory. Consider a SISO nonlinear system of the following form [28]:

$$\dot{\mathbf{x}} = \mathbf{f}(\mathbf{x}) + \mathbf{g}(\mathbf{x})\mathrm{u} \tag{2.1a}$$

$$\mathrm{y} = \mathrm{h}(\mathbf{x}) \tag{2.1b}$$

where $\mathbf{x}\in\Re^n$ is the state vector, $u\in\Re$ the control input, $y\in\Re$ the output. **f**: $D\rightarrow\Re^n$, **g**: $D\rightarrow\Re^n$, h: $D\rightarrow\Re$ are nonlinear functions and sufficiently smooth on a domain $D\subset\Re^n$ [28]. To apply the idea of nonlinearity cancellation to Equation (2.1a), it has to be converted into a controllable linear state equation of the following structure:

$$\dot{\mathbf{x}} = \mathbf{Ax} + \mathbf{B}\gamma(\mathbf{x})[u - \alpha(\mathbf{x})] \tag{2.2}$$

where $\mathbf{A}\in\Re^{n\times n}$ and $\mathbf{B}\in\Re^n$ are the system matrices, the pair (**A**, **B**) is controllable, $\alpha(\mathbf{x})$ and $\gamma(\mathbf{x})$ are the functions, and $\gamma(\mathbf{x})$ is nonsingular for $\forall\mathbf{x}\in D$.

Letting $v= \gamma(\mathbf{x})[u-\alpha(\mathbf{x})]$ in Equation (2.2) gives

$$\dot{\mathbf{x}} = \mathbf{Ax} + \mathbf{B}v \tag{2.3}$$

For the regulator problem, we can design $v= -\mathbf{Kx}$ such that all the poles of (**A-BK**) have a negative real part. The final goal is to obtain a control input via the state-feedback of the form:

$$\begin{aligned} u &= \alpha(\mathbf{x}) + \gamma^{-1}(\mathbf{x})v \\ &= \alpha(\mathbf{x}) - \beta(\mathbf{x})\mathbf{Kx} \end{aligned} \tag{2.4}$$

where $\beta(\mathbf{x})= \gamma^{-1}(\mathbf{x})$. Figure 2.12 shows the block diagram of a SISO system with feedback linearization.

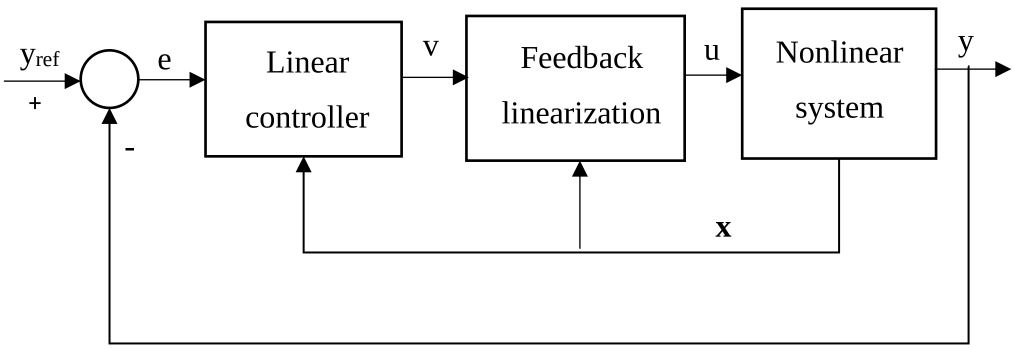

Figure 2.12 Block diagram of a SISO system with feedback linearization [29]

Feedback linearization is conveniently divided into two categories: input-output linearization and input-state linearization [30].

A. Input-output feedback linearization: The input-output map of the system is linearized, while the state equation may be partially linearized. If the system is partly linearized, the control design has practical meaning only when the internal dynamics are stable. In this method, the output y is differentiated until the input u appears in the r^{th} derivative of y. Then u is designed from the linearized system [28].

B. **Input-state feedback linearization**: The state equation is completely linearized. This feedback linearization technique may fail in designing a controller since the output is nonlinear. Hence it is hard to obtain satisfactory performance [31].

The nonlinearity cancellation via feedback linearization requires a certain structural property of the system and whether or not it is possible is determined by a factor called the *relative degree* of the system, according to Definition 2.1 [28] [30]:

Definition 2.1 (Relative degree of SISO systems)

A SISO nonlinear system of Equation (2.1) is said to have a relative degree r, $1 \le r \le n$ at $\mathbf{x}$ in a region $D_0 \subset D$ if and only if [28]:

$$L_g L_f^{i-1} h(\mathbf{x}) = 0 \; (i = 1, 2, \cdots r-1) \text{ but } L_g L_f^{r-1} h(\mathbf{x}) \neq 0 \tag{2.5}$$

where the following notation known as the *lie derivative* is used to calculate the multiple derivatives of h concerning the same vector field f:

$$\begin{aligned}
&L_f^0 h(\mathbf{x}) = h(\mathbf{x}) \\
&L_f h(\mathbf{x}) = \frac{\partial h}{\partial \mathbf{x}} \mathbf{f}(\mathbf{x}) \\
&L_f^2 h(\mathbf{x}) = L_f L_f h(\mathbf{x}) = \frac{\partial (L_f h)}{\partial \mathbf{x}} \mathbf{f}(\mathbf{x}) \\
&\vdots \\
&L_f^k h(\mathbf{x}) = L_f L_f^{k-1} h(\mathbf{x}) = \frac{\partial (L_f^{k-1} h)}{\partial \mathbf{x}} \mathbf{f}(\mathbf{x}) \;\text{ and} \\
&L_g L_f h(\mathbf{x}) = \frac{\partial (L_f h)}{\partial \mathbf{x}} \mathbf{g}(\mathbf{x})
\end{aligned}$$

Note that if r= n, then the system is fully feedback linearizable, if r<n, it is partially feedback linearizable, and if r>n, feedback linearization is impossible.

In this thesis, we use input-output feedback linearization for convenience since both types of feedback linearization are the same when the system is fully feedback linearizable.

2.4.1 Input-Output Feedback Linearization of MIMO Nonlinear Systems

The primary objective of feedback linearization is to design a nonlinear control law by assuming that the inner-loop control is, in the most suitable case, precisely linearizes the nonlinear system after appropriate state space modification of coordinates [29]. It is a common technique used in controlling nonlinear systems. For MIMO nonlinear systems, feedback linearization is used to cancel the interactions between variables. Besides, it is used to remove nonlinearities in the input-output relations [32].

Input-output feedback linearization can be applied to an MIMO nonlinear dynamic system of the form:

$$\dot{\mathbf{x}} = \mathbf{f}(\mathbf{x}) + \sum_{i=1}^{m} \mathbf{g}_i(\mathbf{x})u_i \tag{2.6a}$$

$$\begin{aligned} y_1 &= h_1(\mathbf{x}) \\ y_2 &= h_2(\mathbf{x}) \\ &\vdots \\ y_m &= h_m(\mathbf{x}) \end{aligned} \tag{2.6b}$$

where

$\mathbf{x} = [\mathbf{x}_1\, \mathbf{x}_2 \ldots \mathbf{x}_n]^T \in \Re^n$ is the state vector,

$\mathbf{u} = [u_1\, u_2 \ldots u_p]^T \in \Re^p$ is the control input,

$\mathbf{y} = [y_1\, y_2 \ldots y_m]^T \in \Re^m$ is the output,

$\mathbf{f}(\mathbf{x})$ and $\mathbf{g}_i(\mathbf{x})$ are n-dimensional smooth vector functions and

$h_i(\mathbf{x})$ (i = 1, 2...m) are smooth nonlinear functions [29] [33].

Let assume r_i is the smallest integer such that at least one of the inputs appears in $y_i^{(ri)}$, that is

$$y_i^{(r_i)} = L_f h_i(\mathbf{x}) + \sum_{j=1}^{m} L_{g_j} L_f^{r_i-1} h_i(\mathbf{x}) u_j \tag{2.7}$$

with $L_{g_j} L_f^{r_i-1} h_i(\mathbf{x}) \neq 0$ at least one j [29] [31].

The above equation can be written in a simple form as shown in Equation (2.8).

$$\begin{bmatrix} y_1^{(r_1)} \\ y_2^{(r_2)} \\ \vdots \\ y_m^{(r_m)} \end{bmatrix} = \mathbf{A}(\mathbf{x}) + \mathbf{E}(\mathbf{x})\mathbf{u} \tag{2.8}$$

where

$$\mathbf{A}(\mathbf{x}) = \begin{bmatrix} L_f^{r_1} h_1(\mathbf{x}) \\ \vdots \\ L_f^{r_m} h_m(\mathbf{x}) \end{bmatrix}, \text{ and } \mathbf{E}(\mathbf{x}) = \begin{bmatrix} L_{g_1} L_f^{r_1-1} h_1(\mathbf{x}) & \cdots & L_{g_m} L_f^{r_1-1} h_1(\mathbf{x}) \\ \vdots & \ddots & \vdots \\ L_{g_1} L_f^{r_m-1} h_m(\mathbf{x}) & \cdots & L_{g_m} L_f^{r_m-1} h_m(\mathbf{x}) \end{bmatrix}$$

where $\mathbf{A}(\mathbf{x})$ is the lie derivative of h along with $\mathbf{f}(\mathbf{x})$, and $\mathbf{E}(\mathbf{x})$ is the lie derivative of h along with $\mathbf{g}(\mathbf{x})$.

$\mathbf{E}(\mathbf{x})$ is also called the decoupling matrix of the system, and it is not always nonsingular, and therefore the linearization control is then achieved if and only if the decoupling matrix is invertible [29]. Therefore, writing the linearization control law in compact form as

$$\mathbf{u} = \mathbf{E}^{-1}(\mathbf{x})[-\mathbf{A}(\mathbf{x}) + \mathbf{v}] \tag{2.9}$$

reduces the input-output relationship of Equation (2.8) to

$$\begin{bmatrix} y_1^{(r_1)} \\ y_2^{(r_2)} \\ \vdots \\ y_m^{(r_m)} \end{bmatrix} = \mathbf{v} \tag{2.10}$$

where $\mathbf{v}$ is the new input control that is designed to solve regulation problems. In Equation (2.10), r_i is called the relative degree of the system, according to Definition 2.1.

Definition 2.2 (Relative degree of MIMO systems)

A MIMO nonlinear system of Equation (2.3) is said to have a relative degree $r = r_1 + r_2 + \cdots + r_m$, $1 \le r \le n$ at $\mathbf{x}$ in a region $D_0 \subset D$ if and only if [28]:

$$L_g L_f^{r_i-1} h(\mathbf{x}) = 0 \text{ for } i = 1, 2, \cdots r_i - 1 \text{ but } L_g L_f^{r_i-1} h(\mathbf{x}) \ne 0 \text{ for } r_i \le n \tag{2.11}$$

2.5 Review of Previous Works

Since the controlled environment is the main requirement to increase the plant quality in every greenhouse, many researchers are interested in designed and developed different controlling mechanisms to control the basic environmental parameters of the greenhouse, such as air temperature, humidity, and carbon dioxide. Hence, several research papers have presented on the internal climate control of a greenhouse using conventional methods like PID and optimal control methods, including predictive control [34] [35] [36], multivariable control [37] [38], fuzzy logic control [39], fuzzy and PID [40], and neural network control [41]. Some recent papers are presented in this thesis. The nonlinear greenhouse system is linearized by the feedback-feedforward technique to obtain a decoupling system. PID and fuzzy logic controllers were proposed to control the decoupling system in literature [42]. The result shows that the system's closed-loop response remains tolerable for any step change of setpoints, whatever external disturbances. However, these responses are prolonged to regulate the internal humidity and temperature of the greenhouse due to the fuzzy logic controller.

The authors in [43] designed a fuzzy logic controller to control the internal climate. The nonlinear MIMO greenhouse dynamic system was controlled by considering the temperature and humidity as input variables in this designed system. In contrast, the water spills and roof openings are output variables. A two fuzzy associative matrix was created in which the output variables are mapped to the corresponding input variables.

Based on these matrices, the fuzzy rules were formed for all combinations. This study shows that the temperature and humidity were controlled automatically by controlling the roof opening and water spills of the greenhouse. But, the response of both control signal and output signals is slow due to a large number of fuzzy rules. There is also a stability problem due to controlling the nonlinear system. The other drawback of this study is that it didn't discuss the effect of disturbances in the greenhouse.

An automated greenhouse temperature controller was proposed to control the ideal greenhouse temperature for a particular crop to grow [44]. In this paper, a self-tuning of the proportional controller of the greenhouse was designed and simulated for setpoint tracking. The developed system didn't consider any disturbance rejection methods. Even though humidity has a large impact on the quality and growth of plants, this study is not focused on humidity control. Hence, controlling only the temperature of a greenhouse is the drawback of this paper. Due to the existence of a coupling relation between air temperature and humidity, it is essential to control both parameters.

An adaptive feedback linearization based on predictive control of greenhouse temperature was performed in literature [45]. The study shows that the proposed technique has a good setpoint tracking performance of indoor temperature with efficient energy inputs in an adaptive way. The system is not simulated under disturbance conditions, and internal humidity control is not considered in the system. These problems can be viewed as a limitation of the study.

The authors in [46] proposed a hybrid control strategy by combining the RBF network with a conventional PID controller. The PID gains were tuned and identified adaptively using the RBF network. The results show that the proposed technique has good adaptability, robustness, and setpoint tracking. The proposed technique used a gradient descent method to minimize the error. Since the training algorithm using a gradient descent method is timeconsuming, it is difficult to obtain a fast response during any setpoint change. It is the drawback of the study.

From the above-reviewed literature, the controller's ability to reject any disturbances that exist in a greenhouse is not discussed. Since the greenhouse environment is highly affected by external disturbances in both the summer and winter seasons, the designed control technique should have good performance in rejecting disturbances. The primary performance measures such as settling time, overshoot, and integral absolute error are not addressed in the literature. This thesis work solves the listed problems using an optimal control method that preserves the existing advantages and assimilates further performance tests by designing LQR based PI-type state feedback controller for indoor climate control of a greenhouse.

CHAPTER THREE

METHODOLOGY AND SYSTEM MODELING

This chapter deals with obtaining the mathematical model of a greenhouse climate system that has been used by most of the researchers [47] [48]. The greenhouse climate system is described in the state space form. The possibility of using feedback linearization is examined.

3.1 Methods

Before modeling and designing the proposed system, several tasks are performed, such as literature review, data collection, and analysis. The closely related papers and literature are reviewed to get more information about the greenhouse climate control system and feedback linearization technique.

Since this thesis work aims to perform different tracking and rejection tests, the setpoint values of indoor temperature and humidity for the different psychrometric processes are taken from the Floresnsis Ethiopia PLC. These data are collected by observing recorded data of the company and interviewing with the concerned bodies to get better information about the overall greenhouse and its control system. Moreover, the values of solar intercepted energy and outside temperature are taken from the company. Since this company produces cutting flowers, the proposed method can be used for only such flowers because the indoor air temperature and humidity vary from plant to plant. The greenhouse model parameter values are also taken from the literature. In general, the primary and secondary data collection methods are used in this thesis work. The collected data are analyzed mathematically and graphically for developing system modeling.

The modeling and feedback linearizing of greenhouse indoor climate control systems are analyzed. A PI-type LQR controller is also designed to control the indoor temperature and humidity of the greenhouse. The simulation results of the system are compared with those of the GA-based PID controller. The overall system is implemented on MATLAB software. The methods followed throughout this thesis work are described in the block diagram of Figure 3.1.

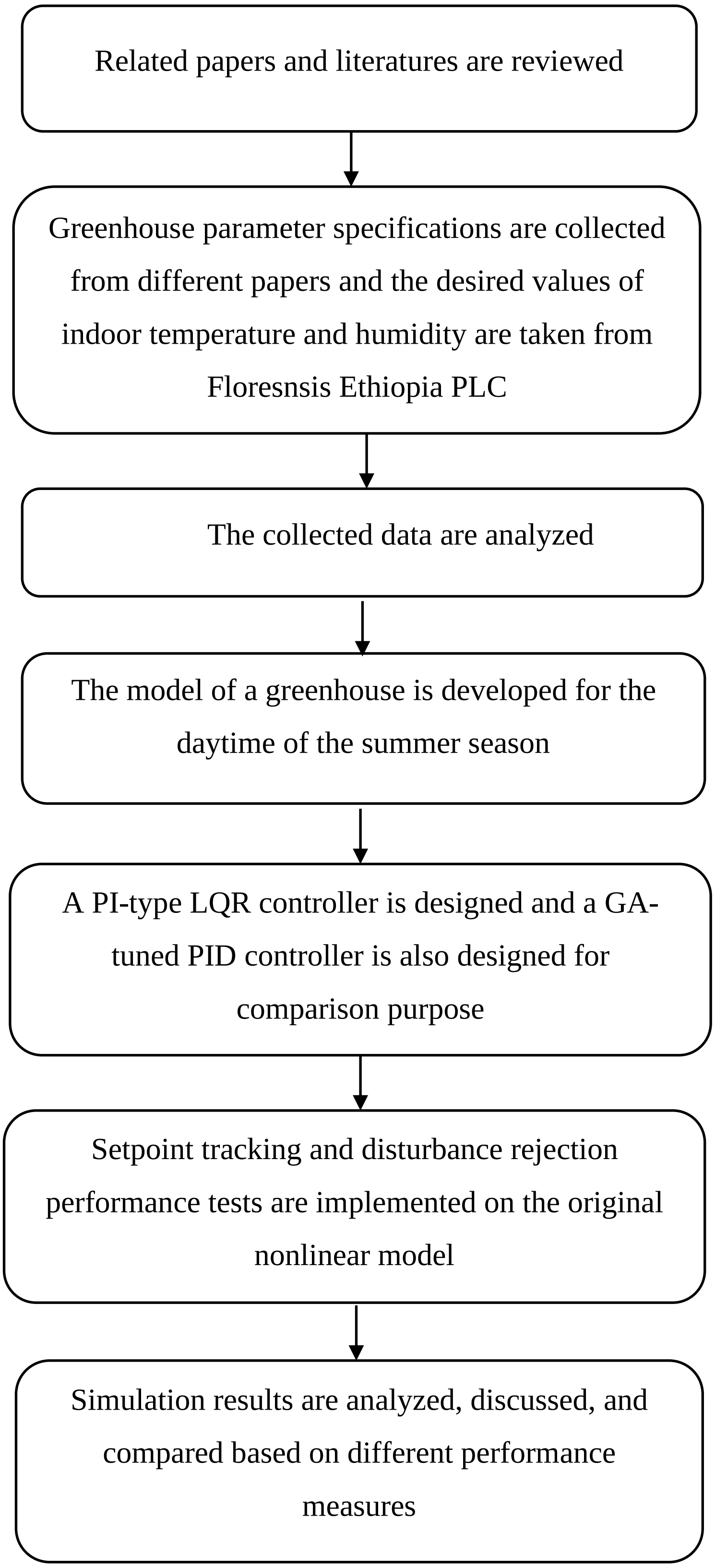

Figure 3.1 Block diagram of research methodology

3.2 Mathematical Modeling of the Greenhouse System

Since the greenhouse integrates various physical and biological phenomena, the system behaves in nonlinear characteristics [48]. As shown in Figure 3.2, the greenhouse is an MIMO system that has several state variables such as internal temperature, internal humidity, and carbon dioxide (CO_2). It consists of some physical systems for ventilation, heating, spraying, and CO_2 injection to regulate those state variables. The greenhouse system is highly prone to external disturbance unless the glazing, shading, and other disturbance rejections are chosen properly. The disturbances can be solar radiation, external temperature, external humidity, and wind speed [44] [49].

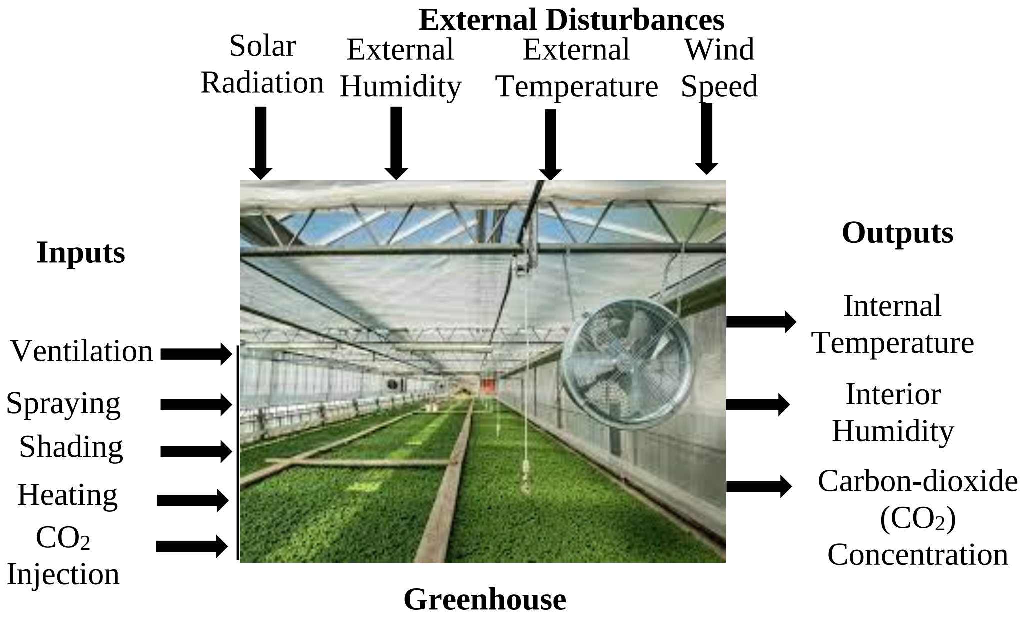

Figure 3.2 A simple greenhouse climate system representation [50] [44]

3.2.1 Greenhouse Climate Control System for Summer Season

The determination of the dynamic behavior of the greenhouse model is based on the energy balance and mass transfer equations [51] [52]. To model this complex dynamic system, the water balance and heat balance differential equations are considered.

A. Heat Balance

The air exchange between the internal air and the external environment produces losses that affect the heat and water balance. The internal heat balance is calculated by Equation (3.1):

$$\rho C_p V_T \dot{T}_{in}(t) = Q_s + Q_h - Q_V - Q_C - Q_e - Q_{fog} \tag{3.1}$$

where ρ is the air density (kgm^{-3}), C_p is the specific heat of the air ($Jkg^{-1}K^{-1}$), V_T is the temperature active mixing volume (m^3), Q_s is the solar energy entering the greenhouse (W), Q_h is the heat emanated by the floor heating system (W), Q_C is heat loss conducted through the walls, Q_e is heat loss due to water evaporation, Q_{fog} is heat loss due to the fog system, Q_V is due to the ventilation, (W), Tin is the indoor air temperature in (°C), and t is time (min) [50].

Solar gain is a natural way of recovering heat losses in the morning till dusk. Solar energy entering the greenhouse can be obtained using Equation (3.2) [48] [50].

$$Q_{sr} = S_i(t) = \alpha_c \tau_c AI \qquad (3.2)$$

where α_c is the cover absorptivity of the solar radiation, τ_c is the cover transmittance, A is the surface area (m^2), I is solar radiation (Wm^{-2}), S is intercepted solar radiant energy (W) [48].

For the summer operation, the value of Q_h in Equation (3.1) becomes zero. Equation (3.3) represents the heat ventilation losses Q_v that is a linear function of the difference between inside temperature T_{in} and outside temperature T_{out} in °C, as well as of the ventilation rate V_R in (m^3/min) [47] [2].

$$Q_V = f_V(T_{in}, T_{out}, V_R) \approx \rho C_p V_R(t)(T_{in}(t) - T_{out}(t)) \qquad (3.3)$$

The conductive heat losses Q_C are a linear function of the temperature difference T_{int} and T_{out} and it can be expressed using Equation (3.4) [47] [42].

$$Q_C = f_C(T_{in}, T_{out}) \approx UA(T_{in}(t) - T_{out}(t)) \qquad (3.4)$$

where UA is the heat transfer coefficient of the enclosure (W/K).

The heat losses due to the fog system Q_{fog} are related to the water capacity of the fog system (rate of vaporization of water by the fog system) q_{fog}, through Equation (3.5) [47].

$$Q_{fog} = \lambda q_{fog}(t) \qquad (3.5)$$

where λ is the latent heat of vaporization in (kJ/kg)

The heat losses due to evaporation of the water from the floor Q_e is negligible in this system because it has little influence on the thermal and moisture processes of the greenhouse indoor climate. Equation (3.1) can be expressed as [42] [53] [54].

$$\rho C_p V_T \dot{T}_{in}(t) = S_i(t) - \rho C_p V_R(t)(T_{in}(t) - T_{out}(t)) - UA(T_{in}(t) - T_{out}(t)) - \lambda q_{fog}(t) \quad (3.6)$$

B. Water Balance

After the heat balance, the dynamics of the humidity inside the greenhouse need to be modeled. This is based on Equation (3.7):

$$\rho V_H \dot{H}_{in}(t) = W_{fog} + W_e - W_{airin} + W_{airout} \quad (3.7)$$

where V_H is actively mixing air volume humidity (m^3), H_{int} is inside humidity ratio in (g H_2O/kg of dry air), W_{fog} ($q_{fog}(t)$) is the water capacity of the fog system (g [H_2O] s^{-1}), W_{airout} and, W_{airin} are the rates of moisture transfer from the outside air entering the greenhouse, and from the inside air leaving the greenhouse respectively in (g [H_2O] s^{-1}), and W_e are the rates of moisture due to evaporation water from the floor in (g [H_2O] s^{-1}) [53].

The rates of moisture due to evaporation water from the floor is expressed as Equation (3.8) and also the evapotranspiration rate is primarily related to the intercepted solar radiant energy, through the simplified relation that expressed in Equation (3.8):

$$W_e = f(S_i(t), H_{in}(t)) = \alpha \frac{S_i(t)}{\lambda} - \beta_T H_{in}(t) \quad (3.8)$$

where α is an overall coefficient to account for shading and leaf area index (dimensionless), and β_T is the overall coefficient to account for thermodynamic constants and other factors affecting evapotranspiration (i.e., stomata and air motion) [47] [2] [42].

The rates of moisture transfer from outside air W_{airout} and inside air W_{airin} are also linear functions and depend on V_R, H_{in}, and H_{out}, so that [47]:

$$W_{airout} = f_{out}(V_R, H_{out}) \approx V_R(t) H_{out}(t) \quad (3.9a)$$

$$W_{airin} = f_{in}(V_R, H_{in}) \approx V_R(t) H_{in}(t) \quad (3.9b)$$

The differential equation of inside humidity of greenhouse can be rewritten as [42] [54]:

$$\rho V_H \dot{H}_{in}(t) = q_{fog}(t) + \alpha \frac{S_i(t)}{\lambda} - \beta_T H_{in}(t) - V_R(t)(H_{in}(t) - H_{out}(t)) \quad (3.10)$$

Based on Equations (3.1) - (3.10), the mathematical model describing the heat and moisture processes of the indoor climate of the greenhouse can be expressed as [47]:

$$\dot{T}_{in}(t) = f_T(T_{in}, T_{out}, H_{out}, q_{fog}, V_R) \quad (3.11a)$$

$$\dot{H}_{in}(t) = f_H(H_{in}, S_i, H_{out}, q_{fog}, V_R) \tag{3.11b}$$

The overall system differential equations for coupled energy and water vapor mass balances are defined below:

$$\dot{T}_{in}(t) = \frac{1}{C_o}[S_i(t) - \lambda q_{fog}(t)] - \frac{\rho C_p V_R(t)}{C_o}(T_{in}(t) - T_{out}(t)) - \frac{UA}{C_o}(T_{in}(t) - T_{out}(t)) \tag{3.12a}$$

$$\dot{H}_{in}(t) = \frac{1}{\rho V_H} q_{fog}(t) + \frac{\alpha}{\lambda \rho V_H} S_i(t) - \frac{\beta_T}{\rho V_H} H_{in}(t) - \frac{V_R(t)}{\rho V_H}(H_{in}(t) - H_{out}(t)) \tag{3.12b}$$

where $C_o = 1/\rho C_p V_T$ represents the thermal capacity of the greenhouse [47] [42].

The model described by Equation (3.12) is rewritten in Equation (3.13).

$$\dot{T}_{in}(t) = \frac{1}{C_o}[S_i(t) - \lambda' q_{\%fog}(t)] - \frac{V_{R,\%}(t)}{t_v}(T_{in}(t) - T_{out}(t)) - \frac{UA}{C_o}(T_{in}(t) - T_{out}(t)) \tag{3.13a}$$

$$\dot{H}_{in}(t) = \frac{q_{\%fog}(t)}{V'} + \alpha' S(t) - \frac{V_{R\%}(t)}{t_v}(H_{in}(t) - H_{out}(t)) \tag{3.13b}$$

where t_v represents the inverse of the number of air changes per unit time, $q_{\%fog}$ defined as a percentage of the maximum capacity of the fog system, λ' is a product of λ and $q_{fog,\,max}$, $V' = V_H/q_{fog,\,max}$ is greenhouse volume per unit of the maximal fog water supply, and $\alpha' = 1/\alpha V_H$ which is the contribution of evapotranspiration to the balance of the absolute humidity [2] [53].

3.3 State Space Representation

The greenhouse considered in Section 3.2 is a two-input, two-output system with three external disturbances, as shown in Figure 3.3 and was modeled for the daytime of the summer season. During the hot season, the indoor temperature and humidity are changed due to changes in the outside temperature and solar radiation. At this time, fog spray and ventilation are used for adjusting the indoor climate of a greenhouse.

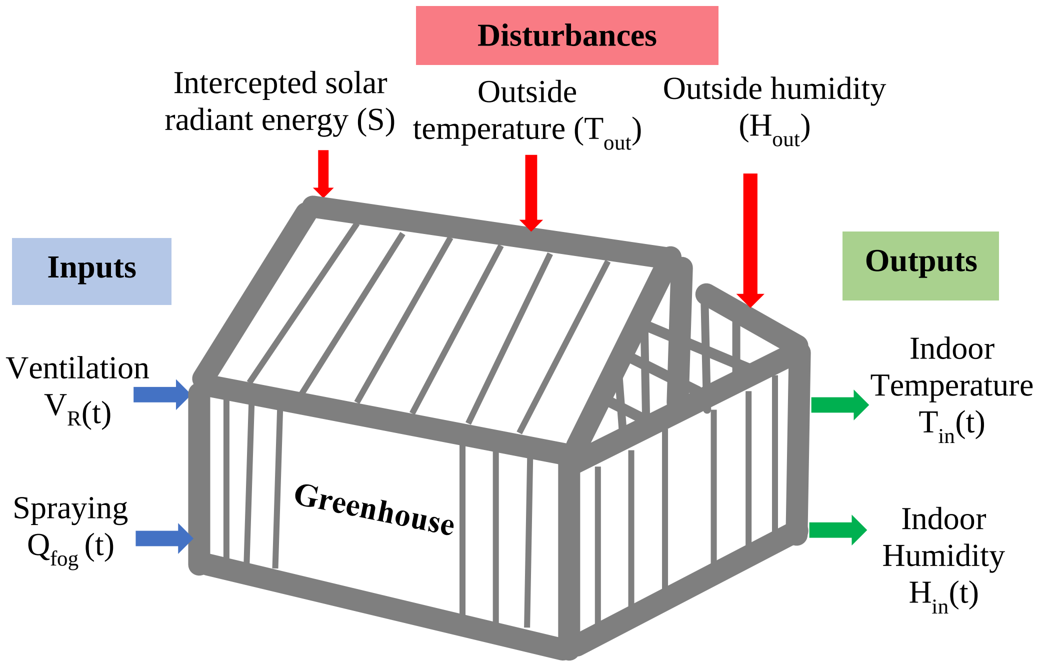

Figure 3.3 Model of a greenhouse indoor climate system [43]

As in Equation (3.13), the physical model of the greenhouse is described by coupled nonlinear equations. These equations can be effectively expressed by assigning the indoor temperature T_{in} and interior humidity H_{in} as the state variables, $x_1(t)$ and $x_2(t)$, respectively. The ventilation rate V_R and the fog rate q_{fog} as the control variables, $u_1(t)$ and $u_2(t)$, respectively. Also, the intercepted solar radiant energy S, the outside temperature T_{out}, and the outside humidity ratio H_{out} are taken as the disturbances, $d_i(t)$, i = 1, 2, 3. Equation (3.13) can alternatively be rewritten in the state-space form:

$$\dot{x}_1(t) = -\frac{UA}{C_o}x_1(t) - \frac{1}{t_v}x_1(t)u_1(t) - \frac{\lambda'}{C_o}u_2(t) + \frac{1}{C_o}d_1(t) + \frac{UA}{C_o}d_2(t) + \frac{1}{t_v}u_1(t)d_2(t) \quad (3.14a)$$

$$\dot{x}_2(t) = -\frac{1}{t_v}x_2(t)u_1(t) + \frac{1}{V'}u_2(t) + \alpha' d_1(t) + \frac{1}{t_v}u_1(t)d_3(t) \quad (3.14b)$$

Defining the state vector as $\mathbf{x} = [x_1 \;\; x_2]^T \in \Re^2$, Equation (3.14) can be rewritten in a compact form:

$$\dot{\mathbf{x}} = \mathbf{f}(\mathbf{x}) + \sum_{i=1}^{m} \mathbf{g}_i(\mathbf{x})u_i \quad (3.15a)$$

$$\begin{aligned} y_1 &= h_1(\mathbf{x}) \\ y_2 &= h_2(\mathbf{x}) \end{aligned} \tag{3.15b}$$

where y_1 and y_2 are the outputs,

$$\mathbf{f}(\mathbf{x}) = \begin{bmatrix} -\frac{UA}{C_o}x_1 + \frac{1}{C_o}d_1 + \frac{UA}{C_o}d_2 \\ \alpha' d_1 \end{bmatrix} \tag{3.15c}$$

$$g_1(\mathbf{x}) = \begin{bmatrix} \frac{1}{t_v}(d_2 - x_1) \\ -\frac{\lambda'}{C_O} \end{bmatrix}, g_2(\mathbf{x}) = \begin{bmatrix} \frac{1}{t_v}(d_3 - x_2) \\ \frac{1}{V'} \end{bmatrix} \tag{3.15d}$$

$$\begin{aligned} h_1(\mathbf{x}) &= x_1 \\ h_2(\mathbf{x}) &= x_2 \end{aligned} \tag{3.15e}$$

and m is the dimension of the control input vector $\mathbf{u} = [u_1 \quad u_2]^T \in \Re^2$ with m= 2

3.4 Input-Output Feedback Linearization

As mentioned previously in Section 2.4, input-output feedback linearization is used for obtaining the linear behavior of the given nonlinear system by nonlinear coordinate transformation [31]. Equations (3.15a) and (3.15b) show that the outputs are indirectly related to the inputs through the state variables and the state equation. Hence, it is not easy to see how the inputs can be designed to control the tracking behavior of the outputs. This difficulty can be solved by finding a direct relationship between the system outputs and the control inputs using input-output feedback linearization.

To check whether feedback linearization can be applied to the system in Equation (3.15) or not, we examine the relative degree of the system through Theorem 3.1.

Theorem 3.1:

Consider the MIMO nonlinear system in Equation (3.15). Then, the system is fully feedback linearizable if the following condition is satisfied:

Relative degree $r= r_1+r_2= 2$

Proof: Finding the first derivative of the outputs in Equation (3.15b) yields

$$\begin{bmatrix} \dot{y}_1 \\ \dot{y}_2 \end{bmatrix} = L_f h(\mathbf{x}) + L_g h(\mathbf{x})\mathbf{u} \tag{3.16a}$$

where

$$L_f h(\mathbf{x}) = \begin{bmatrix} L_f h_1(\mathbf{x}) \\ L_f h_2(\mathbf{x}) \end{bmatrix} = \begin{bmatrix} \frac{d_1}{C_o} + \frac{UA}{C_o} d_2 - \frac{UA}{C_o} x_1 \\ \alpha' d_1 \end{bmatrix} \tag{3.16b}$$

$$L_g h(\mathbf{x}) = \begin{bmatrix} L_{g_1} L_f h_1(\mathbf{x}) & L_{g_2} L_f h_1(\mathbf{x}) \\ L_{g_1} L_f h_2(\mathbf{x}) & L_{g_2} L_f h_2(\mathbf{x}) \end{bmatrix} = \begin{bmatrix} \frac{1}{t_v}(d_2 - x_1) & -\frac{\lambda'}{C_o} \\ \frac{1}{t_v}(d_3 - x_2) & \frac{1}{V'} \end{bmatrix} \tag{3.16c}$$

Rewriting Equation (3.16) gives

$$\begin{aligned} \dot{y}_1 &= L_f h_1(\mathbf{x}) + \frac{1}{t_v}(d_2 - x_1)u_1 - \frac{\lambda'}{C_o} u_2 \\ \dot{y}_2 &= L_f h_2(\mathbf{x}) + \frac{1}{t_v}(d_3 - x_2)u_1 + \frac{1}{V'} u_2 \end{aligned} \tag{3.17}$$

Since at least one of the inputs appears in both $\dot{y}_1$ and $\dot{y}_2$, it is clearly shown that the relative degree of each output is 1, that is, $r_1 = r_2 = 1$. Hence, the total relative degree r becomes $r_1 + r_2 = 2$ and according to Definition 2.2, the full state feedback controller design is possible. ■

CHAPTER FOUR

CONTROLLER DESIGN

In this chapter, the augmented system for the linear model is explained in detail. The PI-type controller is designed for the augmented system after checking its controllability. Furthermore, the stability of the closed-loop system is discussed. Finally, a GA- based PID controller is designed for performance comparison.

4.2 Augmented System

By Theorem 3.1 and Definition 2.2, we know that the full state feedback controller design is possible for the MIMO system given by Equation (3.15). From Equation (3.16a), if **v**= [v_1 v_2]^T is chosen as

$$\mathbf{v} = \mathbf{A}(\mathbf{x}) + \mathbf{E}(\mathbf{x})\mathbf{u} \tag{4.1a}$$

where

$$\begin{aligned} \mathbf{A}(\mathbf{x}) &= L_f h(\mathbf{x}) - \begin{bmatrix} -\dfrac{UA}{C_o} x_1 \\ 0 \end{bmatrix} \\ \mathbf{E}(\mathbf{x}) &= L_g h(\mathbf{x}) \end{aligned} \tag{4.1b}$$

The linear system is obtained by substituting Equation (4.1) into Equation (3.16a) as follow:

$$\begin{bmatrix} \dot{y}_1 \\ \dot{y}_2 \end{bmatrix} = \begin{bmatrix} -\dfrac{UA}{C_o} x_1 \\ 0 \end{bmatrix} + \mathbf{v} \tag{4.2}$$

Defining the state variables as $z_1 = y_1$, and $z_2 = y_2$ with the fact that $y_1 = x_1$, and $y_2 = x_2$ yields:

$$\dot{z}_1 = -\frac{UA}{C_o} z_1 + v_1 \tag{4.3a}$$

$$\dot{z}_2 = v_2 \tag{4.3b}$$

Equations (4.3) can be rewritten in the following form:

$$\dot{\mathbf{z}} = \mathbf{Az} + \mathbf{Bv} \tag{4.4a}$$

$$\mathbf{y} = \mathbf{Cz} \tag{4.4b}$$

where

$$\mathbf{z} = \begin{bmatrix} z_1 \\ z_2 \end{bmatrix}, \mathbf{A} = \begin{bmatrix} -\dfrac{UA}{C_o} & 0 \\ 0 & 0 \end{bmatrix}, \mathbf{B} = \begin{bmatrix} 1 & 0 \\ 0 & 1 \end{bmatrix}, \text{ and } \mathbf{C} = \begin{bmatrix} 1 & 0 \\ 0 & 1 \end{bmatrix} \tag{4.4c}$$

State feedback involves the use of the state vector, that is, a linear combination of the state variables to compute a control law for the system given in Equation (4.4). To check the existence of such a control law, its controllability of the pair of (**A**, **B**) has to be checked. From the following controllability matrix

$$\mathbf{U} = \begin{bmatrix} \mathbf{B} & \mathbf{AB} \end{bmatrix} = \begin{bmatrix} 1 & 0 & -\dfrac{UA}{C_o} & 0 \\ 0 & 1 & 0 & 0 \end{bmatrix} \tag{4.5}$$

the rank of **U** is equal to 2. Hence, the linear system in Equation (4.4) is controllable.

In designing a greenhouse indoor climate control system, exhibiting a particular desired response of the inside air temperature and humidity is the principal issue in the presence of either setpoint or disturbance changes. A state feedback controller is straightforward in design, gives good performance in the presence of uncertainty, and improves system characteristics such as rise time, overshoot, and settling time [55] [45]. One of the common problems that occurred in state feedback control is not only stabilizing the system against disturbances but also making the output track to setpoint changes. For the output to follow the desired setpoint, new state variables are defined as

$$q_1 = \int (y_1 - y_{r_1}) dt \tag{4.6a}$$

$$q_2 = \int (y_2 - y_{r_2}) dt \tag{4.6b}$$

Differentiating both sides of the Equations (4.6) gives

$$\dot{q}_1 = y_1 - y_{r_1} \tag{4.7a}$$

$$\dot{q}_2 = y_2 - y_{r_2} \tag{4.7b}$$

Adding Equation (4.7) to Equation (4.4) forms a linear augmented equation as

$$\dot{\tilde{\mathbf{x}}} = \tilde{\mathbf{A}}\tilde{\mathbf{x}} + \tilde{\mathbf{B}}\mathbf{v} - \begin{bmatrix} \mathbf{0} \\ \mathbf{I} \end{bmatrix} \mathbf{y}_r \tag{4.8a}$$

$$\mathbf{y} = \tilde{\mathbf{C}}\tilde{\mathbf{x}} \tag{4.8b}$$

where

$\tilde{\mathbf{x}} = [z_1 \quad z_2 \quad q_1 \quad q_2]^T, \mathbf{y_r} = [y_{r1} \quad y_{r2}]^T$,

$$\tilde{\mathbf{A}} = \begin{bmatrix} \mathbf{A} & 0 \\ \mathbf{C} & 0 \end{bmatrix} = \begin{bmatrix} -\frac{UA}{C_o} & 0 & 0 & 0 \\ 0 & 0 & 0 & 0 \\ 1 & 0 & 0 & 0 \\ 0 & 1 & 0 & 0 \end{bmatrix}, \ \tilde{\mathbf{B}} = \begin{bmatrix} \mathbf{B} \\ 0 \end{bmatrix} = \begin{bmatrix} 1 & 0 \\ 0 & 1 \\ 0 & 0 \\ 0 & 0 \end{bmatrix}, \text{ and } \tilde{\mathbf{C}} = \begin{bmatrix} \mathbf{C} & 0 \end{bmatrix} = \begin{bmatrix} 1 & 0 & 0 & 0 \\ 0 & 1 & 0 & 0 \end{bmatrix}$$

Finally, the greenhouse climate system is expressed by Equation (4.8), and we design a state feedback controller based on this linear equation, so it is necessary to check the controllability of the pair ($\tilde{\mathbf{A}}$, $\tilde{\mathbf{B}}$) in Equation (4.8). The following theorem verifies the controllability of the augmented system.

Theorem 4.1 (Controllability of the linear augmented system)

Consider the augmented system expressed by Equation (4.8). This system is controllable if and only if the pair (**A**, **B**) of the original system in Equation (4.4) has the rank of n [56]:

$$\text{rank}\begin{bmatrix} \mathbf{B} & \mathbf{AB} & \cdots & \mathbf{A}^{n-1}\mathbf{B} \end{bmatrix} = n \tag{4.9}$$

and the following condition is satisfied

$$\text{rank}\begin{bmatrix} \mathbf{B} & \mathbf{A} \\ 0 & -\mathbf{C} \end{bmatrix} = n + p \tag{4.10}$$

where n denotes the order of the original system and p the dimension of **y**.

Proof:

Obtaining the rank of Equation (4.10) gives

$$\text{rank}\begin{bmatrix} \mathbf{B} & \mathbf{A} \\ 0 & -\mathbf{C} \end{bmatrix} = \text{rank}\begin{bmatrix} 1 & 0 & -\frac{UA}{C_o} & 0 \\ 0 & 1 & 0 & 0 \\ 0 & 0 & -1 & 0 \\ 0 & 0 & 0 & -1 \end{bmatrix} = n + p = 4 \tag{4.11}$$

From the fact that Equation (4.5) has the rank of 2 and Equation (4.11) has the rank of 4, the pair ($\tilde{\mathbf{A}}$, $\tilde{\mathbf{B}}$) of the augmented system is controllable. ■

Note that from Equation (4.4), n is 2 (two-state variables z_1 and z_2) and p is also 2 (two output elements y_1 and y_2).

4.2 Design of a PI-type LQR Controller

With the augmented system of Equation (4.8), the control law for both indoor air temperature and humidity control can be of the form

$$\mathbf{v} = -\tilde{\mathbf{K}}\tilde{\mathbf{x}} = -\mathbf{K}_p\mathbf{x} - \mathbf{K}_i\mathbf{q} \tag{4.12}$$

where $\tilde{\mathbf{K}} = [\mathbf{K_p} \quad \mathbf{K_i}]$, and $\mathbf{K_p}$ and $\mathbf{K_i}$ denote the proportional gain matrix and the integral gain matrix, respectively. The poles of the feedback system matrix $(\tilde{\mathbf{A}} - \tilde{\mathbf{B}}\tilde{\mathbf{K}})$ must be stable, suitably damped locations in the complex plane. Theorem 4.1 guarantees that a PI-type state feedback control law can be synthesized. There are some appropriate methods for designing a state controller based on a state-space representation of the linear model of Equation (4.12) such as pole assignment, LQR, eigenvalue assignment, and so on [57] [58]. In the pole assignment method, the gain matrix is obtained from the user-supplied poles. LQR is one of the fascinating control methods. It is essentially an automated way of finding a state feedback controller that assures stability robustness with full state feedback. In this thesis, the LQR design method is adopted.

In the LQR method, $\tilde{\mathbf{K}}$ is obtained such that the following quadratic cost function is minimized

$$J = \frac{1}{2}\int_0^\infty (\tilde{\mathbf{x}}^\mathbf{T}\mathbf{Q}\tilde{\mathbf{x}} + v^\mathbf{T}\mathbf{R}v)dt \tag{4.13}$$

where $\mathbf{Q} \in \Re^{4\times4}$ is a semi-positive definite and symmetric state weight matrix ($\mathbf{Q} \geq 0$) and $\mathbf{R} \in \Re^{2\times2}$ is a symmetric and positive definite control weight matrix ($\mathbf{R} > 0$). We need to specify the right weighting matrices that deliver specified performance for the linear system.

The optimal feedback gain $\tilde{\mathbf{K}}$ is evaluated by:

$$\tilde{\mathbf{K}} = \mathbf{R}^{-1}\tilde{\mathbf{B}}^\mathbf{T}\mathbf{P} \tag{4.14}$$

where $\mathbf{P} \in \Re^{4\times4}$ is the solution of Riccati equation and a symmetric positive definite matrix [59] [60]:

$$\tilde{\mathbf{A}}^{\mathbf{T}}\mathbf{P}+\mathbf{P}\tilde{\mathbf{A}}-\mathbf{P}\tilde{\mathbf{B}}\mathbf{R}^{-1}\tilde{\mathbf{B}}^{\mathbf{T}}\mathbf{P}+\mathbf{Q}=\mathbf{0} \tag{4.15}$$

As shown in Equation (4.13), the weighting matrix **Q** is used to penalize the bad performance by minimizing the state/error signal of the system. On the other hand, the weighting matrix **R** is used for penalizing the actuator's effort (fan and fog spray). The weighting matrices of the following diagonal form are used in this thesis.

$$\mathbf{Q}=\begin{bmatrix} q_{11} & 0 & 0 & 0 \\ 0 & q_{22} & 0 & 0 \\ 0 & 0 & q_{33} & 0 \\ 0 & 0 & 0 & q_{44} \end{bmatrix}, \text{ and } \mathbf{R}=\begin{bmatrix} r_{11} & 0 \\ 0 & r_{22} \end{bmatrix} \tag{4.16}$$

where q_{11}, q_{22}, q_{33}, q_{44}, r_{11}, and r_{22} denote the real positive number. From Equation (4.13), the energy expenditure of the system related to the quadratic cost function is determined by the weighting matrices [60]. Hence, the proper selection of these weighting matrices is required for a successful LQR design.

Finally, the overall control input is calculated using Equations (4.1a) and (4.12) as

$$\begin{aligned}\mathbf{u}&=\mathbf{E}^{-1}(\mathbf{x})[\mathbf{v}-\mathbf{A}(\mathbf{x})]\\ &=\mathbf{E}^{-1}(\mathbf{x})[-\mathbf{K_p}\mathbf{x}-\mathbf{K_i}\mathbf{q}-\mathbf{A}(\mathbf{x})]\end{aligned} \tag{4.17a}$$

where

$$\begin{aligned}\mathbf{E}(\mathbf{x})&=\begin{bmatrix} \frac{1}{t_v}(d_2-x_1) & -\frac{\lambda'}{C_o} \\ \frac{1}{t_v}(d_3-x_2) & \frac{1}{V'} \end{bmatrix}\\ \mathbf{A}(\mathbf{x})&==\begin{bmatrix} \frac{d_1}{C_o}+\frac{UA}{C_o}d_2 \\ \alpha' d_1 \end{bmatrix}\end{aligned} \tag{4.17b}$$

Finally, substituting Equation (4.6) to Equation (4.16a) gives

$$\mathbf{u}=\mathbf{E}^{-1}(\mathbf{x})[-\mathbf{K_p}\mathbf{x}+\mathbf{K_i}\begin{bmatrix} \int(y_{r_1}-y_1)dt \\ \int(y_{r_2}-y_2)dt \end{bmatrix}-\mathbf{A}(\mathbf{x})] \tag{4.18}$$

The block diagram of the proposed system is illustrated in Figure 4.1 as shown below:

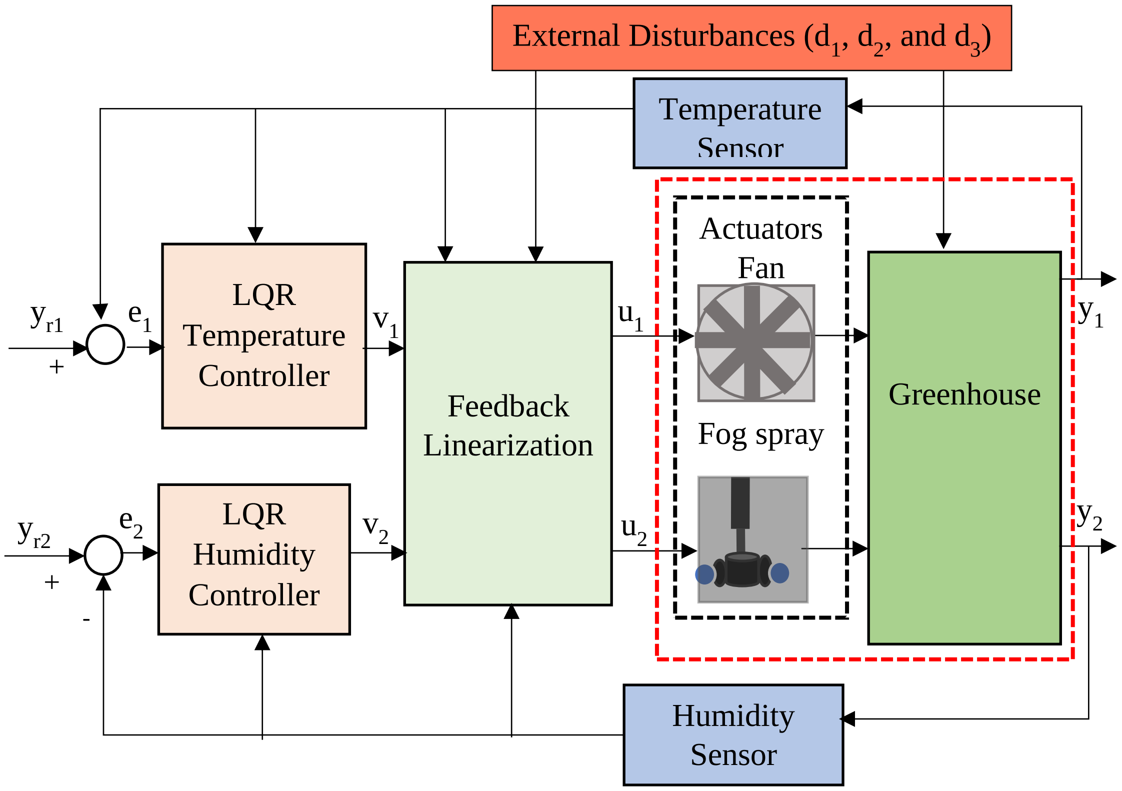

Figure 4.1 Design of the overall proposed system

4.3 Stability Analysis of the Closed-Loop System

When designing a controller, one of the important factors to be considered is the stability of the closed-loop system. It is known that the main advantage of LQR control is to stabilize the given system by selecting eigenvalue locations of the closed-loop system. Now, the stability of the proposed closed-loop system is checked.

Substituting Equation (4.1) into Equation (3.23a) gives the closed-loop equation:

$$\dot{\tilde{\mathbf{x}}} = (\tilde{\mathbf{A}} - \tilde{\mathbf{B}}\tilde{\mathbf{K}})\tilde{\mathbf{x}} - \begin{bmatrix} \mathbf{0} \\ \mathbf{I} \end{bmatrix} \mathbf{y}_r \tag{4.19}$$

Under the assumption that the setpoint $\mathbf{y}_r$ is step-type, differentiating both sides once give the following equation:

$$\ddot{\tilde{\mathbf{x}}} = (\tilde{\mathbf{A}} - \tilde{\mathbf{B}}\tilde{\mathbf{K}})\dot{\tilde{\mathbf{x}}} \tag{4.20}$$

The solution of the above equation is written by

$$\dot{\tilde{\mathbf{x}}}(t) = e^{(\tilde{\mathbf{A}} - \tilde{\mathbf{B}}\tilde{\mathbf{K}})t}\dot{\tilde{\mathbf{x}}}(t_0) \tag{4.21}$$

The LQR control allows all eigenvalues of the feedback system matrix ($\tilde{\mathbf{A}}$-$\tilde{\mathbf{B}}\tilde{\mathbf{K}}$) to have negative real values, so the following condition holds.

$$\lim_{t\to\infty}\left\|\dot{\tilde{\mathbf{x}}}(t)\right\| = \lim_{t\to\infty}\left\|e^{(\tilde{\mathbf{A}}-\tilde{\mathbf{B}}\tilde{\mathbf{K}})t}\tilde{\mathbf{x}}(t_0)\right\| \le \lim_{t\to\infty}\left\|e^{(\tilde{\mathbf{A}}-\tilde{\mathbf{B}}\tilde{\mathbf{K}})t}\right\|\cdot\left\|\tilde{\mathbf{x}}(t_0)\right\| \to \mathbf{0} \tag{4.22}$$

That is,

$$\lim_{t\to\infty}\left\|\dot{\tilde{\mathbf{x}}}(t)\right\| = \lim_{t\to\infty}\left\|\begin{bmatrix}\dot{z}_1(t)\\ \dot{z}_2(t)\\ \dot{q}_1(t)\\ \dot{q}_2(t)\end{bmatrix}\right\| \to \mathbf{0} \tag{4.23}$$

Equation (4.23) implies

$$\begin{aligned}\lim_{t\to\infty}\dot{q}_1(t) &= \lim_{t\to\infty}[y_1(t)-y_{r_1}(t)] = 0\\ \lim_{t\to\infty}\dot{q}_2(t) &= \lim_{t\to\infty}[y_2(t)-y_{r_2}(t)] = 0\end{aligned} \tag{4.24a}$$

that is,

$$\begin{aligned}\lim_{t\to\infty} y_1(t) &= y_{r_1}(t)\\ \lim_{t\to\infty} y_2(t) &= y_{r_2}(t)\end{aligned} \tag{4.24b}$$

This means that the proposed controller can either track step-type setpoint changes or reject step-type disturbance changes that exist in the indoor climate of a greenhouse. Since the linear augmented system becomes asymptotically stable after applying the LQR technique, accordingly, if the decoupling matrix **E**(**x**) in Equation (4.1b) is nonsingular, then the overall system becomes stable.

4.4 Equilibrium States

Equilibrium denotes the condition of a system when its state, its control input, and disturbances do not change with time. The equilibrium states of the greenhouse system at a nominal operating point must satisfy the following equilibrium equations expressed by Equation (3.14).

$$0 = -\frac{UA}{C_O}x_1 - \frac{1}{t_v}x_1u_1 - \frac{\lambda'}{C_O}u_2 + \frac{1}{C_O}d_1 + \frac{UA}{C_O}d_2 + \frac{1}{t_v}u_1d_2 \tag{4.25a}$$

$$0 = -\frac{1}{t_v}x_2u_1 + \frac{1}{V'}u_2 + \alpha'd_1 + \frac{1}{t_v}u_1d_3 \tag{4.25b}$$

Rearranging Equation (4.25) in the form of **Ax** = **b**, and the nominal control input $\mathbf{u}_0(t)$ yields:

$$\begin{bmatrix} \frac{1}{t_v}(d_2-\mathbf{x}_1) & -\frac{\lambda'}{C_o} \\ \frac{1}{t_v}(d_3-\mathbf{x}_2) & \frac{1}{V'} \end{bmatrix} \begin{bmatrix} u_{01}(t) \\ u_{02}(t) \end{bmatrix} = \begin{bmatrix} \frac{UA}{C_O}\mathbf{x}_1(t) - \frac{1}{C_O}d_1(t) - \frac{UA}{C_O}d_2(t) \\ -\alpha' d_1(t) \end{bmatrix} \tag{4.26}$$

As long as matrix **A** is nonsingular, $\mathbf{u}_0$ (t) exists and it is obtained by:

$$\mathbf{u}_0(t) = \begin{bmatrix} u_{01}(t) \\ u_{02}(t) \end{bmatrix} = \begin{bmatrix} \frac{1}{t_v}(d_1-\mathbf{x}_1) & -\frac{\lambda'}{C_o} \\ \frac{1}{t_v}(d_3-\mathbf{x}_2) & \frac{1}{V'} \end{bmatrix}^{-1} \begin{bmatrix} \frac{UA}{C_O}\mathbf{x}_1(t) - \frac{1}{C_O}d_1(t) - \frac{UA}{C_O}d_2(t) \\ -\alpha' d_1(t) \end{bmatrix} \tag{4.27}$$

4.5 PID Controller Design for Performance Comparison

4.5.1 Practical PID Controller

The proportional-integral-derivative (PID) controller is the most commonly used form in the process industry. Today, more than 95% of controllers used in the control loops are of PID type [61]. The PID controller has three terms: proportional, integral, and derivative terms. The proportional is used for determining the reaction of the controller to the current error. The integral term determines the reaction depend on the sum of errors to remove offset, and the derivative term determines the reaction based on the rate at which the error has been changing [61]. The time-domain mathematical equation is expressed in both standard and parallel form in Equations (4.28a) and (4.28b), respectively.

Standard form:

$$u(t) = K_p[e(t) + \frac{1}{T_i}\int_0^t e(\tau)d\tau + T_d\frac{de(t)}{dt}] \tag{4.28a}$$

Parallel form:

$$u(t) = K_p e(t) + K_i\int_0^t e(\tau)d\tau + K_d\dot{e}(t) \tag{4.28b}$$

where u (t) is the control input, and e (t) is the current error that is the difference between the reference input $y_r(t)$ and the process output y (t), K_p is the proportional gain, T_i is the integral time, T_d is the derivative time, $K_i = K_p/T_i$ is the integral gain, and $K_d = K_p \cdot T_d$ is the derivative gain.

Equation (4.28b) can be rewritten in the transfer function form:

$$\frac{U(s)}{E(s)} = K_p + \frac{K_i}{s} + K_d s \tag{4.29}$$

In general, the result of the ideal differentiator would be a spike. Sudden changes of the setpoint and/or disturbances or high-frequency noises can cause the derivative of the error to be instantaneously large and the controller output saturates actuators for some cycles. This phenomenon known as derivative kick causes low performance such as large overshoot, long settling time, and instability.

For showing the effect of the ideal differentiator to frequency, the magnitude of the ideal derivative term $U_d(s)/E(s) = K_d s$ is

$$\left|\frac{U_d(j\omega)}{E(j\omega)}\right| = |K_d j\omega| = K_d \omega \tag{4.30}$$

Figure 4.2 shows the magnitude plot for ω= 0.01~100 [rad/sec]. It can be seen in Figure 4.2 that since the magnitude plot increases in proportion to ω, the ideal differentiator amplifies high-frequency signals or noises.

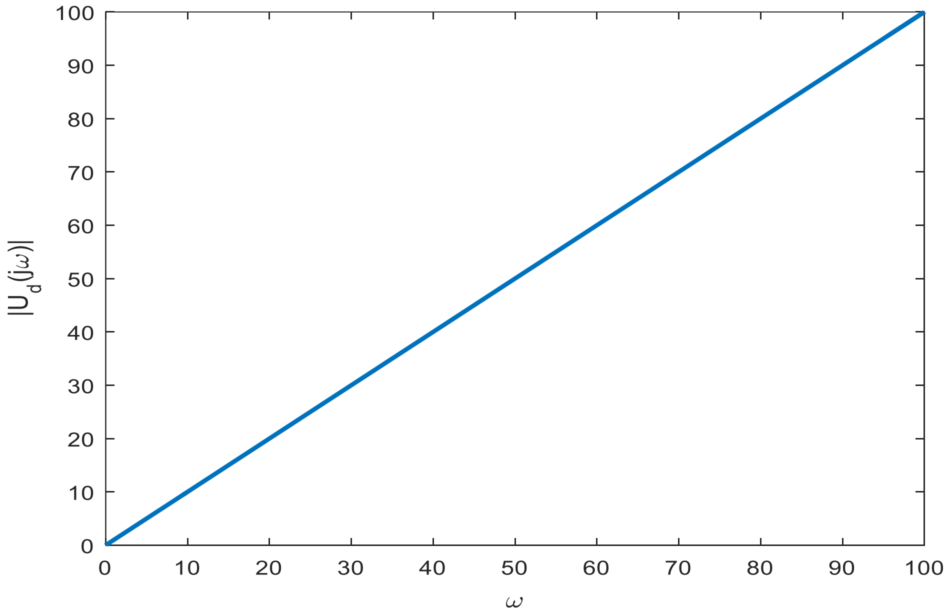

Figure 4.2 Magnitude plot of the ideal derivative term (K_d= 1)

Due to the *derivative kick* phenomenon, a built-in derivative filter with a time constant is often used in combination with the standard PID controller in industrial control loops. In this thesis, to overcome the disadvantages of the standard PID controller, a practical PID controller is designed to manipulate the system outputs, namely the indoor air temperature and humidity, to their setpoint values y_{r1} and y_{r2}, respectively.

The practical PID controller is expressed in the time-domain as

$$u(t) = u_p(t) + u_i(t) + u_d(t) \tag{4.31a}$$

$$u_p(t) = K_p e(t) \tag{4.31b}$$

$$u_i(t) = K_i \int e(t)dt \tag{4.31c}$$

$$\frac{T_d}{N}\dot{u}_d(t) + u_d(t) = K_d \dot{e}(t) \tag{4.31d}$$

Equation (4.31) can be rewritten in the frequency domain as:

$$\frac{U(s)}{E(s)} = K_p + \frac{K_i}{s} + \frac{K_d s}{1 + \frac{T_d}{N}s} \tag{4.32}$$

where the derivative filter divisor N is usually set to N = 5~50 [61] but N= 10 is used in this thesis. To see the effect on the filter, finding the magnitude of the frequency response of $U_d(s)/E(s)$ yields

$$\left|\frac{U_d(j\omega)}{E(j\omega)}\right| = \left|\frac{K_d j\omega}{1 + \frac{T_d}{N} j\omega}\right| = \frac{K_d \omega}{\sqrt{1 + (T_d \omega / N)^2}} \tag{4.33}$$

It is seen in Equation (4.33) that $|U_d(j\omega)/E(j\omega)| \rightarrow K_d N$, as $\omega \rightarrow \infty$. For high frequencies, the gain of the practical differentiator approaches to $K_d N$. Due to this, the effects of high-frequency errors or noises on the input are limited to some extent. Figure 4.3 shows the magnitude plot of the practical PID derivative term for three typical N with K_d=1 and T_d=1.

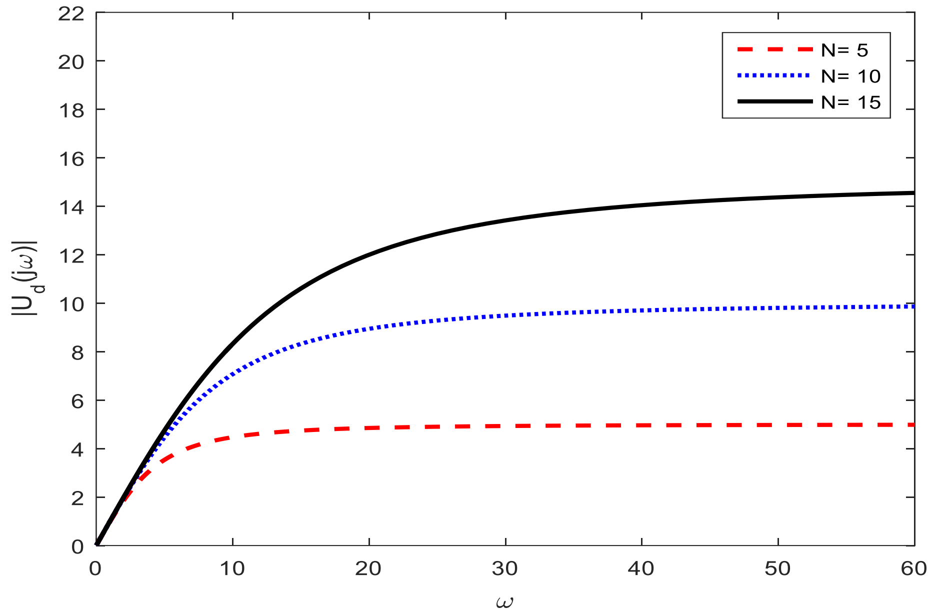

Figure 4.3 Magnitude plot of the practical derivative term for three typical N

Therefore, two PID controllers of the form Equation (4.32) are used

Temperature controller:

$$U_1(s) = (K_{pT} + \frac{K_{iT}}{s} + \frac{K_{dT}s}{1+\frac{T_{dT}}{N}s})E_1(s) \quad (4.34a)$$

Humidity controller:

$$U_2(s) = (K_{pH} + \frac{K_{iH}}{s} + \frac{K_{dH}s}{1+\frac{T_{dH}}{N}s})E_2(s) \quad (4.34b)$$

where K_{pT}, K_{iT}, and K_{dT} are the proportional, integral, and derivative gains of the temperature controller, respectively. K_{pH}, K_{iH}, and K_{dH} are the proportional, integral, and derivative gains of the humidity controller, respectively. Also, $e_1= y_{r1}-y_1$ is error signal for temperature and $e_2= y_{r2}-y_2$ is error signal for humidity.

Figure 4.4 depicts the PID control system for a greenhouse climate. The sensors constantly monitor the outputs of the system and pass this information back to the PID controller. When the setpoint is abruptly and largely changed, the controller output becomes large and exceeds the limit values of the actuator input. Hence, input saturation is used to limit the actuator input signals. Both ventilation rate and fog rate are in the range [0, 1].

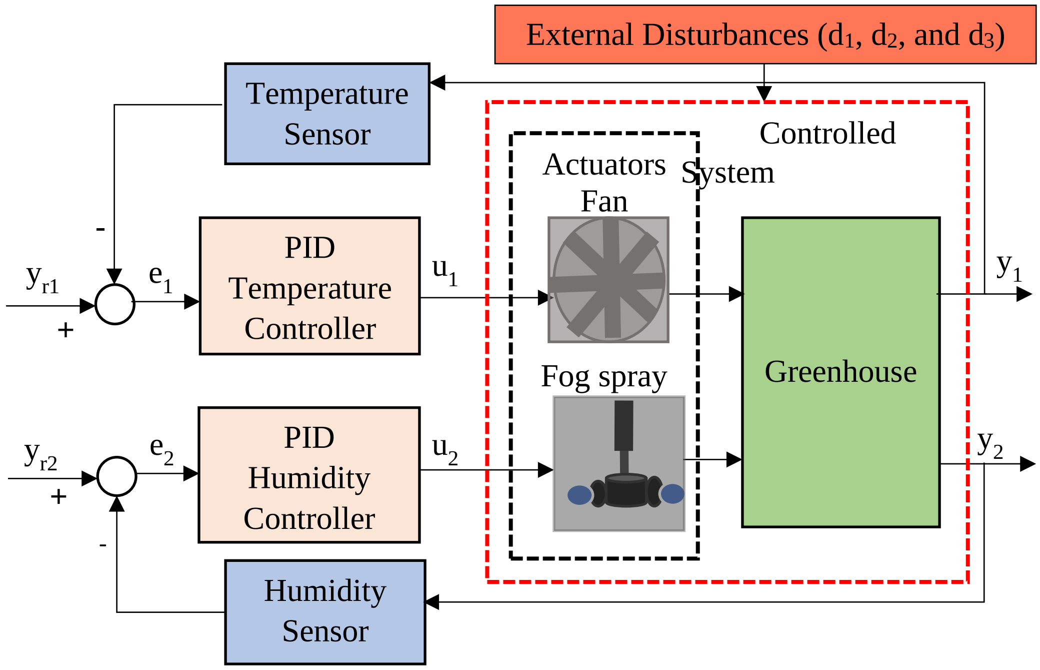

Figure 4.4 PID control of a greenhouse control system

4.5.2 Genetic Algorithm as an Optimization Tool

As can be seen in Equation (4.34), the two PID controllers have a total of 6 gains (K_{pT}, K_{iT}, and K_{dT} for the temperature controller; K_{pH}, K_{iH}, and K_{dH} for the humidity controller) to be tuned. Tuning them to improve the performance of the overall control system in terms of minimizing a performance index becomes a multivariable optimization problem and requires an optimization method. For this, GA is used. A GA is based on natural evolution and natural mutation, producing an essential solution for many optimization problems. GA uses only payoff information (objective function). Hence, this algorithm can be applied to any discrete or continuous optimization problem. In GA, the risk of becoming trapped in a stationary point is reduced because the GA always operates on a population of points (strings). Encoding exists in GA, representing solutions for the corresponding optimization problems as a population point (chromosomes). The encoding method can be binary, real number, and symbolic. The reproduction process is used for obtaining the best solution by evolving those chromosomes [62] [63]. Figure 4.5 depicts the structure of a genetic algorithm.

```
Genetic Algorithm ()
    Set k= 0;
    Initialize an initial population, P(k);
    Evaluate chromosomes in the population P(k);
    While < termination condition not met >
    {
        Set k= k+1;
        Select chromosomes from P(k);
        Crossover chromosomes;
        Mutate chromosomes;
        Evaluate chromosomes in the population P(k);
    }
    Return the best chromosome in P(k)
```

Figure 4.5 Structure of a genetic algorithm

Each of these operations will be described in the following:

Population Initialization: At the starting of the evolution process, an initial population is generated either randomly or heuristically. The heuristic method is used to solve real optimization problems, whereas the random is mainly used for research purposes to test a new GA performance. During many populations, the search space area is large, and the generation is less and vice versa. Hence, the number of generations should be considered in assigning the number of populations.

Fitness Evaluation: A fitness function is defined and calculated from the objective function used to guide the simulation towards the optimal solution. This function evaluates every individual in the population. Evaluation of the fitness function is essential to decide how best the solution is concerning the problem. For example, the problem can be either maximization or minimization problems.

Selection: This is more related to natural selection, which is about better individuals have more chances for survival. Depend on the individual fitness; many individuals are selected using many selection operators such as tournament, roulette wheel, ranking-based, stochastic sample, and affine. The Roulette wheel operator is the most common method.

Crossover: In this stage, two individuals from the parent population exchange information between chromosomes to create a new individual. The new individuals may be better than their parents. Based on the encoding type of chromosomes, many crossover operators like one-point, two-point, uniform, simple, flat, and arithmetic crossover.

Mutation: GA mutation is also related to biological mutation. A mutation is used to maintain the genetic diversity from one generation to the successive [62] [64].

In both tests, the GA is applied to minimize those errors by tuning six parameters (K_{pT}, K_{iT}, K_{dT}, K_{pH}, K_{iH}, and K_{dH}). In each iteration, GA adjusts the gain values to minimize the fitness values to the smallest value as much as possible. Thus, the design aims to eliminate the error and obtain the desired response. Around 8-10 iterations are performed in this thesis until the best fitness value of each performance index is obtained.

4.5.3 Tuning of the PID Controller

In designing a PID controller, tuning is required for adjusting the control parameters (gains) to optimum values until the system performance is satisfactory. A plenty of different methods have been used for tuning purposes, such as Ziegler Nicholas, GA, and Particle Swarm Optimization (PSO). Here a GA is applied to have optimal gain values since it is easy to understand and simple to use. Since GA optimization is required to minimize the values of performance indices by adjusting the gains, two performance indices, that is, IAE and ISE are used in this work.

$$IAE = \int_0^\infty \left(|e_1(t)| + |e_2(t)| \right) dt \tag{4.35}$$

$$ISE = \int_0^\infty \left(e_1^2(t) + e_2^2(t) \right) dt \tag{4.36}$$

where $e_1(t) = y_{r1}(t) - y_1(t)$ and $e_2(t) = y_{r2}(t) - y_2(t)$

Since the Equations (4.35) and (4.36) are used as objective functions, the PID gains are tuned as these performance indices are minimized by GA. The tuning process is required for determining the PID gains that produce the desired outputs. Hence, the population is evaluated by minimizing the following performance indices criteria:

$$J_{IAE} = \int_0^{t_f} \left(|e_1(t)| + |e_2(t)| \right) dt \tag{4.37}$$

$$J_{ISE} = \int_0^{t_f} \left(e_1^2(t) + e_2^2(t) \right) dt \tag{4.38}$$

where t_f is a sufficiently large time

CHAPTER FIVE

RESULTS AND DISCUSSIONS

This chapter deals with the simulation and analysis of the proposed LQR for the indoor climate control of the greenhouse. In addition, for the comparison purpose, the PID controller is designed and optimally tuned using a GA. The simulation results of the proposed control system are compared with that of the GA-tuned PID controller to fulfill the specific objectives of the thesis. The overall simulation is done using MATLAB script.

5.1 Specification of the Controlled Object

For a set of simulation works, the parameters and their values of the greenhouse climate system model at a nominal condition are used and summarized in Table 5.1. The disturbances of intercepted solar radiant energy, outside air temperature, and external humidity ratio used in this simulation have an initial value of 300W, 35℃, and 4g [H_2O]/kg [air], respectively. The initial values of inside air temperature and internal humidity ratio are set to 30℃ and 18g [H_2O]/kg [dry air] for daytime of the summer season, respectively. Also, the ventilation rate and fog rates are taken in the range of 0 and 1.

Figure 5.1 Parameter and values of the greenhouse system model for summer season operation [41]

Parameters	Values with unit
UA	29.81[W/°C]
C_o	-324 [minW/°C]
t_v	3.41 [min]
V'	0.0752 [g/m^{3}min]
α'	0.0033 [g/m^{3}minW]
λ'	465 [W]

With these values, the control inputs at the nominal condition for ventilation rate $u_1(t)$ and fog rate $u_2(t)$ are calculated using Equation (4.27). The results are obtained as

$$u_0(t) = \begin{bmatrix} 0.7806 \\ 0.1665 \end{bmatrix} \tag{5.1}$$

After obtaining the initial conditions and the nominal control inputs, the performance measures of the proposed controller and the PID controller are evaluated for both setpoint tracking and disturbance rejection tests.

5.2 Controller Settings

5.2.1 LQR Setting

As mentioned earlier, although LQR provides control input in terms of minimizing the quadratic performance index, **Q** and **R** are user-defined weighting matrices and affect the overall performance. The higher the state error term, the faster the closed-loop response becomes and the more oscillation it has due to bigger control input, whereas the higher the actuator effort term, the slower the closed-loop response becomes with less oscillation [65] [66] [67].

In this work, the following matrices are selected

$$\mathbf{Q} = \begin{bmatrix} 1 & 0 & 0 & 0 \\ 0 & 1 & 0 & 0 \\ 0 & 0 & 1.7 & 0 \\ 0 & 0 & 0 & 1 \end{bmatrix}, \text{ and } \mathbf{R} = \begin{bmatrix} 0.04 & 0 \\ 0 & 0.0001 \end{bmatrix} \tag{5.2}$$

With this selection of **Q** and **R**, Equation (4.3) yields the feedback gain matrix

$$\tilde{\mathbf{K}} = \begin{bmatrix} \mathbf{K_p} & \mathbf{K_i} \end{bmatrix} = \begin{bmatrix} 6.2600 & 0 & 6.5192 & 0 \\ 0 & 100.9950 & 0 & 100 \end{bmatrix} \tag{5.3}$$

where

$$\mathbf{K_p} = \begin{bmatrix} 6.2600 & 0 \\ 0 & 100.9950 \end{bmatrix}, \mathbf{K_i} = \begin{bmatrix} 6.5192 & 0 \\ 0 & 100 \end{bmatrix} \tag{5.4}$$

5.2.2 PID Controller Setting

Since each PID controller has the three gains, the total six gains are tuned by a GA based on the nonlinear MIMO system model of Equation (3.14). The response is obtained for calculating two performance criteria, IAE and ISE, while the setpoint y_{r1} is changed from 30℃ to 28℃ and y_{r2} from 18g [H_2O]/kg [air] to different setpoint conditions and disturbances remain constant. The parameters of the GA used in the simulation are shown in Table 5.2.

Table 5.1 Parameter settings of the GA

Parameter	Value
Maximum generation	20
Population size	30
Number of parameters	6
Lower bounds of parameters	[0 0 0 0 0 0]
Upper bounds of parameters	[3 0.5 3 3 0.5 3]

As a result, the PID controller gains tuned for IAE and ISE performance criteria are shown in Table 5.3. Based on these gain values, all the simulation results are presented in the next section for both setpoint tracking and disturbance rejection performances tests. It helps to see the ability of these tuned controller gains to control the system in case of both tracking and rejection.

Table 5.2 PID controller settings tuned by a GA

PID gains / Performance Index	Temperature controller			Humidity controller		
	K_{pT}	K_{iT}	K_{dT}	K_{pH}	K_{iH}	K_{dH}
IAE	1.6157	0.0295	0.7078	1.0424	0.0573	0.2995
ISE	2.0314	0.0616	1.9945	1.4976	0.0377	0.1952

5.3 Performance Tests

In this section, a set of simulation works are done using MATLAB based on two performance tests, that is, setpoint tracking and disturbance rejection tests. The performances of the proposed controller are compared with those of the PID controllers. The tracking performance is measured in terms of the peak time t_p, rise time t_r, settling time t_s, overshoot M_p and IAE. The regulation performance is measured in terms of the peak time t_p, recovery time t_{rcy}, perturbance peak M_{peak} and IAE are measured. M_{peak} denotes $|y_{max}-y_r|$ or $|y_{min}-y_r|$ and t_{rcy} does the time that it takes for y to recover within 2% of y_r.

5.3.1 Setpoint Tracking Performance Test

In the setpoint tracking tests, the setpoints y_{r1} and y_{r2} are changed while disturbances remain constant, and the simulation is done for 30min.

5.3.1.1 Setpoint Change of Indoor Temperature at a Constant Humidity

When indoor air temperature increases due to intense sunlight at the daytime of the summer season, it is better to reduce it to the required temperature for plants in the greenhouse. For this reason, it requires a sensible cooling process. In this simulation, the setpoint y_{r1} for indoor air temperature is decreased from 30℃ to 28℃ while the setpoint y_{r2} of the indoor humidity ratio is fixed at 18g [H_2O]/kg [dry air].

Figure 5.1 depicts the closed-loop responses of the LQR and the PID controllers tuned for IAE and ISE with their control input signals.

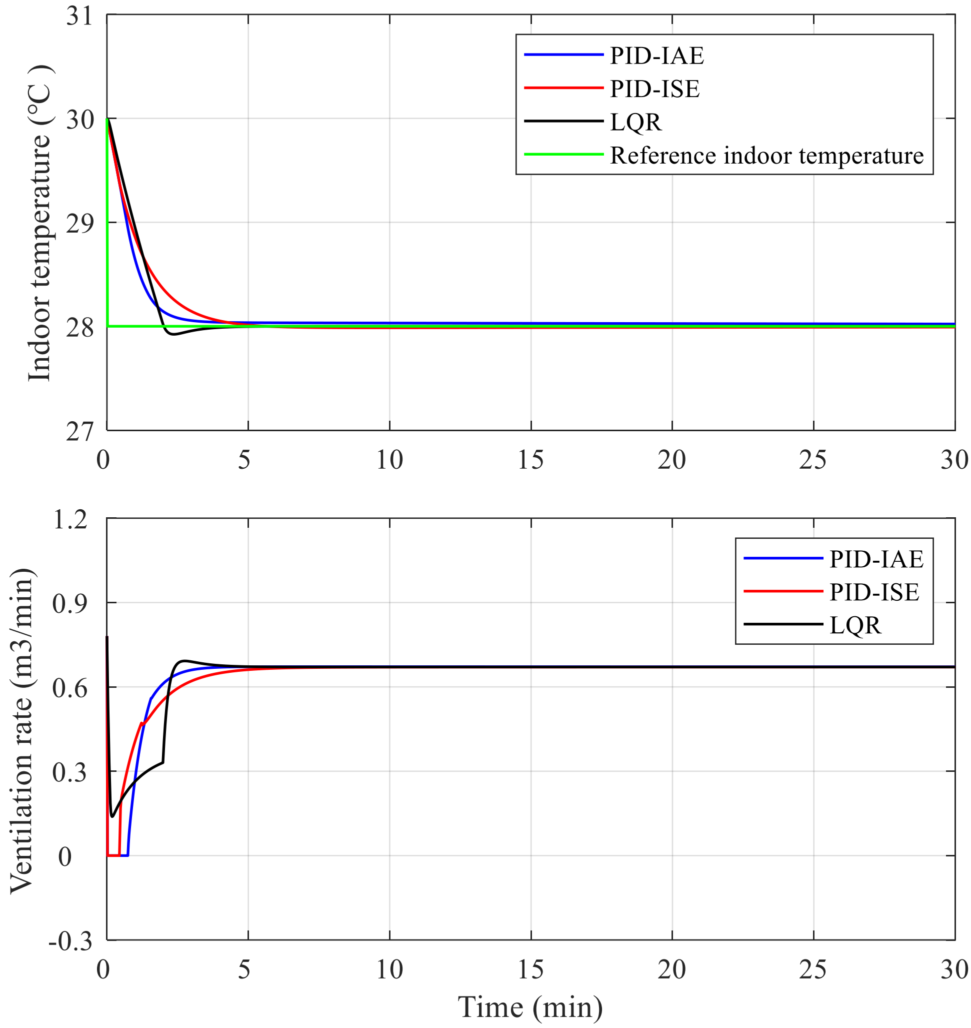

Figure 5.2 Tracking responses of the closed-loop system to a step-type temperature change while y_{r2} is fixed at 18 g [H_2O]/kg [dry air]

It can be seen in the Figure 5.1 that all three controllers show satisfactory performance. The result shows that the LQR provides a quick response for the setpoint change of temperature with acceptable overshoot than the PID controller.

The quantitative comparison of the control methods is summarized in Table 5.4. The LQR gives a shorter rise time and settling time, and a smaller IAE than those of the PID controller.

Table 5.3 Performance measures when y_{r1} is changed from 30°C to 28°C with y_{r2}= 18 g [H_2O]/kg [dry air]

Temperature controllers	Performance measures				
	t_p	t_r	M_p	t_s	IAE
PID - IAE	29.5	1.5980	0	3.7803	2.9801
PID - ISE	9.70	2.4907	0.7357	4.2043	2.7249
LQR	2.36	1.5665	3.8603	3.0634	2.0366

Figure 5.2 illustrates the responses of indoor humidity when y_{r1} is changed while y_{r2} remains constant. From the figure, it can be seen that the LQR provides better regulatory performance. The quantitative performance measures listed in Table 5.5 imply that the LQR takes a shorter recovery time to settle down within 2% of its steady-state value than the PID controllers. Moreover, M_{peak} and IAE are less in LQR as shown in Table 5.5. These results indicate that the LQR has better performance in tracking indoor temperature setpoint change.

Table 5.4 Performance measures when y_{r1} is changed from 30°C to 28°C

Humidity controllers	Performance measures			
	t_p	M_{peak}	t_{rcy}	IAE
PID - IAE	0.92	0.8500	7.0308	1.3345
PID - ISE	0.56	0.5047	5.9316	0.8078
LQR	0.76	0.1384	5.6829	0.2693

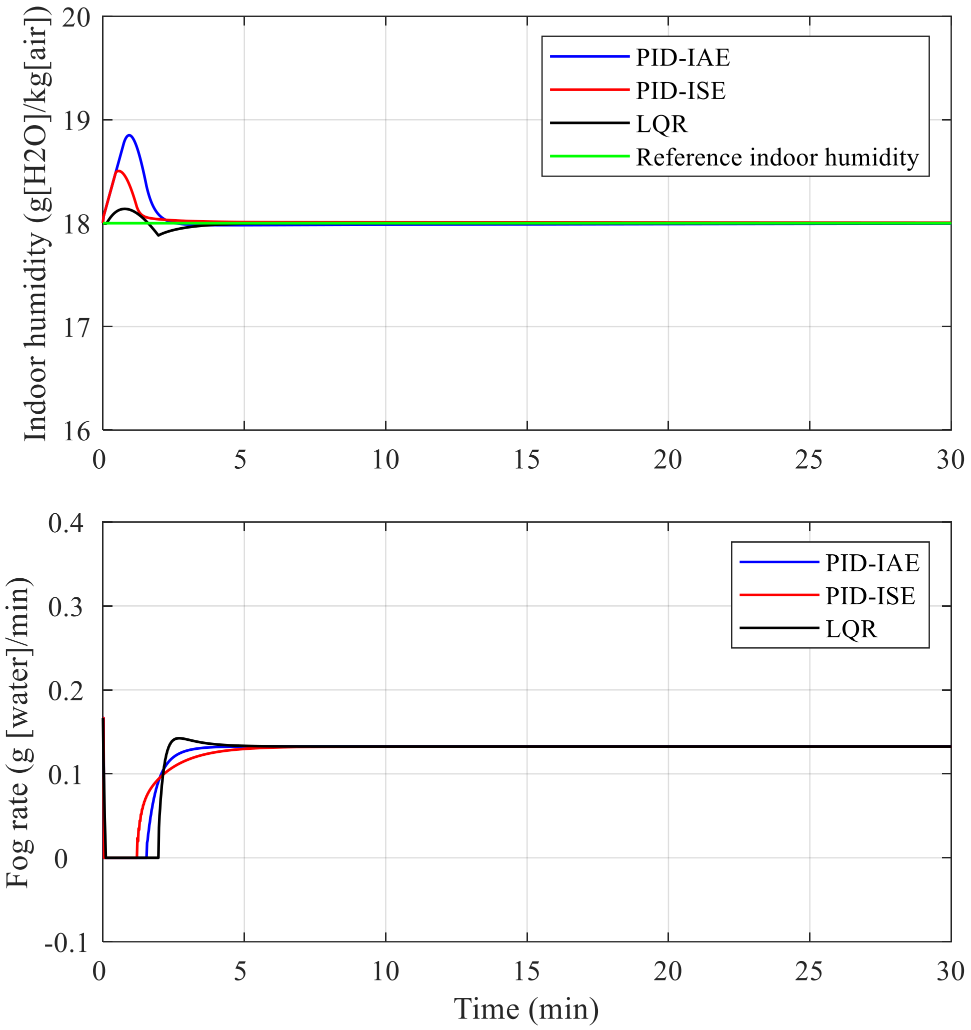

Figure 5.3 Tracking responses of the closed-loop system to a step-type temperature change while the humidity is fixed at 18 g [H_2O]/kg [dry air]

5.3.1.2 Setpoint Change of Indoor Humidity at a Fixed Indoor Temperature

As the next simulation, the humidification is added to the previous scenario. In another word, the operator decreases the setpoint y_{r1} of the indoor temperature from 30℃ to 28℃ and increases the setpoint y_{r2} of the indoor humidity from 18g [H_2O]/kg [dry air] to 20g [H_2O]/kg [dry air]. This process is called the cooling and humidification process. During humidification process, cool water is sprayed in the air stream. The responses of indoor temperature and their control signals are illustrated in Figure 5.3.

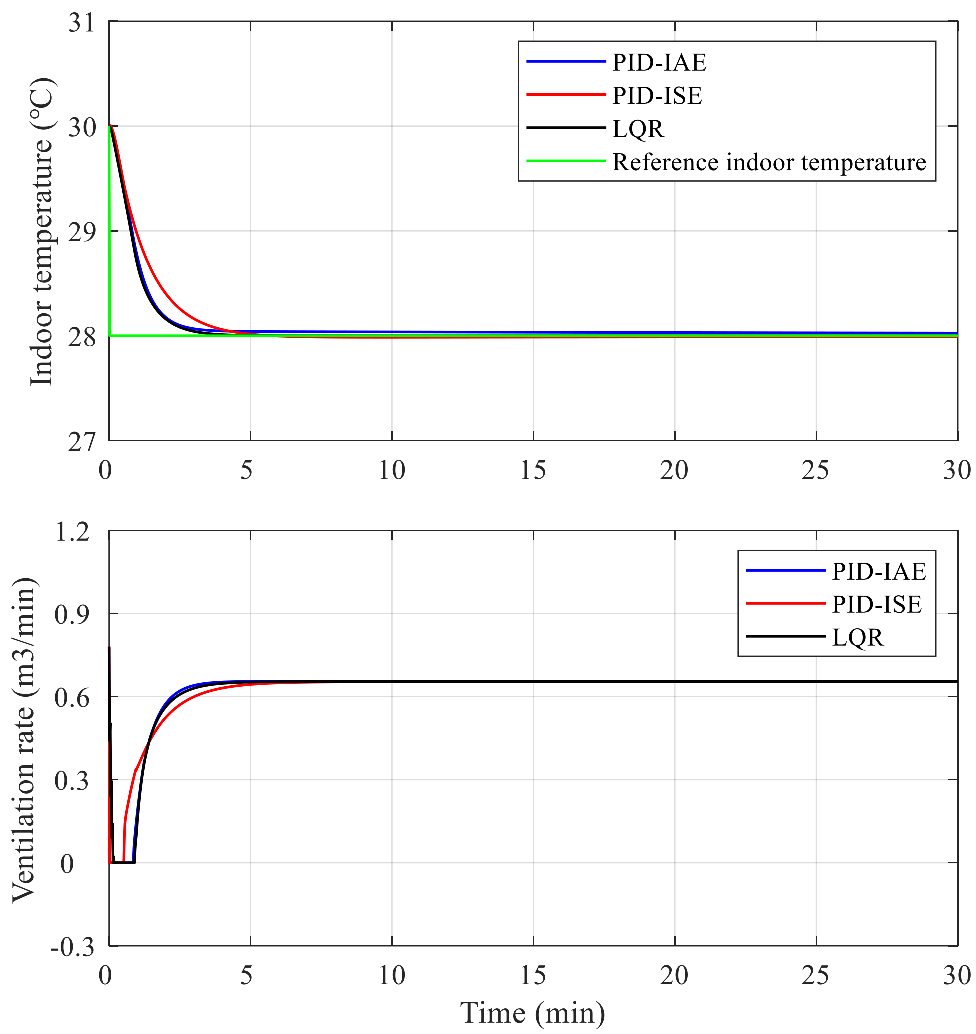

Figure 5.4 Tracking responses of the closed-loop system to a step-type humidity change while the temperature is fixed at 28°C

Figure 5.3 shows that the LQR gives quicker response than the PID controller. The responses in Figure 5.3 are further zoomed-in between 0 and 8 min as shown in Figure 5.4. It can be seen that the LQR takes a short time to settle the temperature within 2% of the steady state value. The result also implies that the selected **Q** and **R**, appropriately penalize the state error and vent effort.

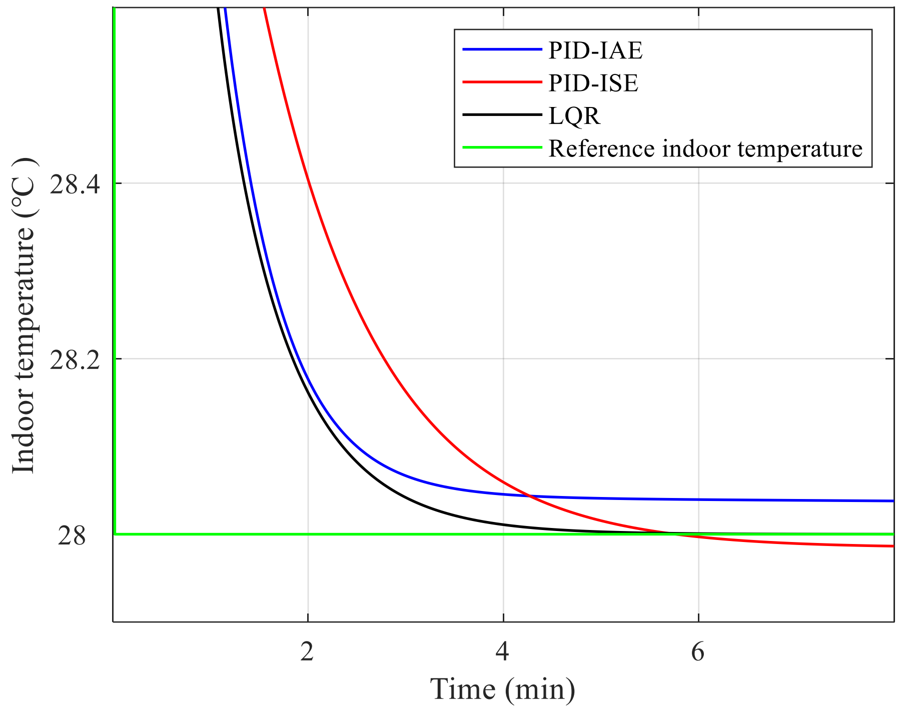

Figure 5.5 Indoor temperature zoomed result using the LQR and PID controllers

The quantitative comparison of the control methods is listed in Table 5.6. The LQR gives better tracking performance than the GA-tuned PID controllers since all the performance measures are small in LQR compared to the PID.

Table 5.5 Performance measures when y_{r2} is changed from 18 to 20 g [H_2O]/kg [dry air]

Temperature controllers	Performance measures				
	t_p	t_r	M_p	t_s	IAE
PID - IAE	29.5610	1.6640	0	5.4882	3.4229
PID - ISE	9.8200	2.5065	0.7353	4.3386	2.9912
LQR	23.1000	1.6369	0	3.0330	1.8523

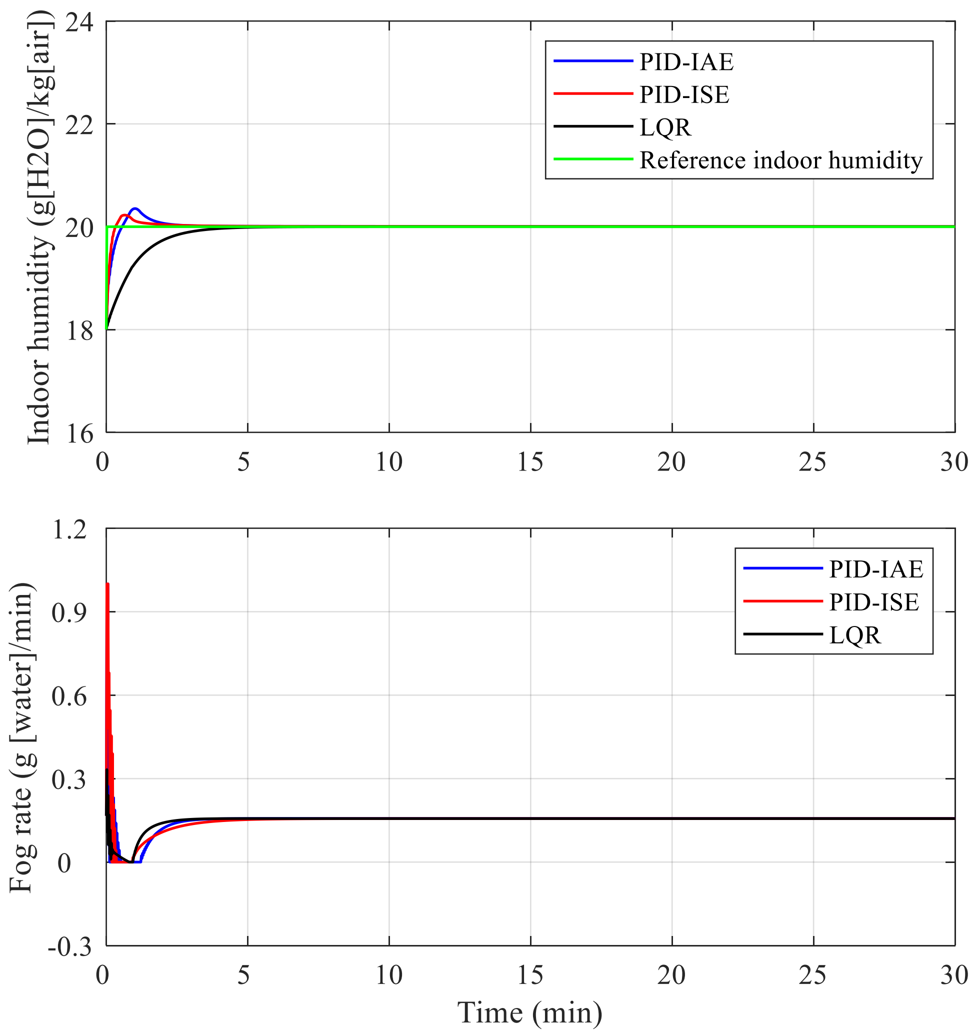

Figure 5.6 Tracking responses of the closed-loop system to a step-type humidity change while the temperature is fixed at 28℃

Figure 5.5 shows the humidity responses of the three methods. The LQR shows slower response with zero overshoot as compared to the PID controller but it is acceptable. Since **R** penalizes the fog spray effort and limits the fog rate signal from reaching its maximum value, this results in slower response and zero overshoot in LQR. Figure 5.6 shows the zoomed-in responses of the indoor humidity between 0 and 7 min. It indicates that the LQR takes much time to attain its setpoint even though IAE is smaller compared to the PID controller.

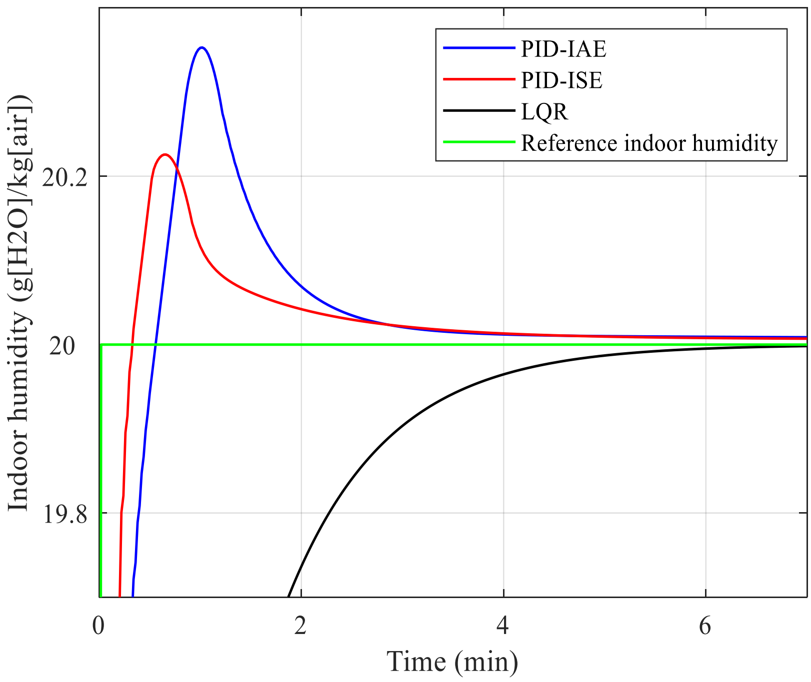

Figure 5.7 The indoor humidity zoomed response when indoor humidity is increased at a fixed temperature

The quantitative comparison is summarized in Table 5.7. Even though the LQR gives large tr, tp, and ts, the IAE, and overshoot remain smaller than the PID controller.

Table 5.6 Performance measures when y_{r2} is changed from 18 to 20 g [H_2O]/kg [dry air]

Humidity controllers	Performance measures				
	t_p	t_r	M_p	t_s	IAE
PID - IAE	1.02	0.3774	17.6418	2.3862	0.8183
PID - ISE	0.66	0.2059	11.2839	2.0681	0.6459
LQR	10.53	2.1778	0	3.8772	0.5814

The heat amount in the air becomes less as the day riding. At this condition, the operator needed to decrease the internal humidity ratio through dehumidification process. Figures 5.7~5.9 demonstrate the result of indoor temperature and humidity corresponding to their input signals for both LQR and PID controllers when y_{r2} is decreased 18g $[H_2O]$/kg [dry air] to 16g $[H_2O]$/kg [dry air].

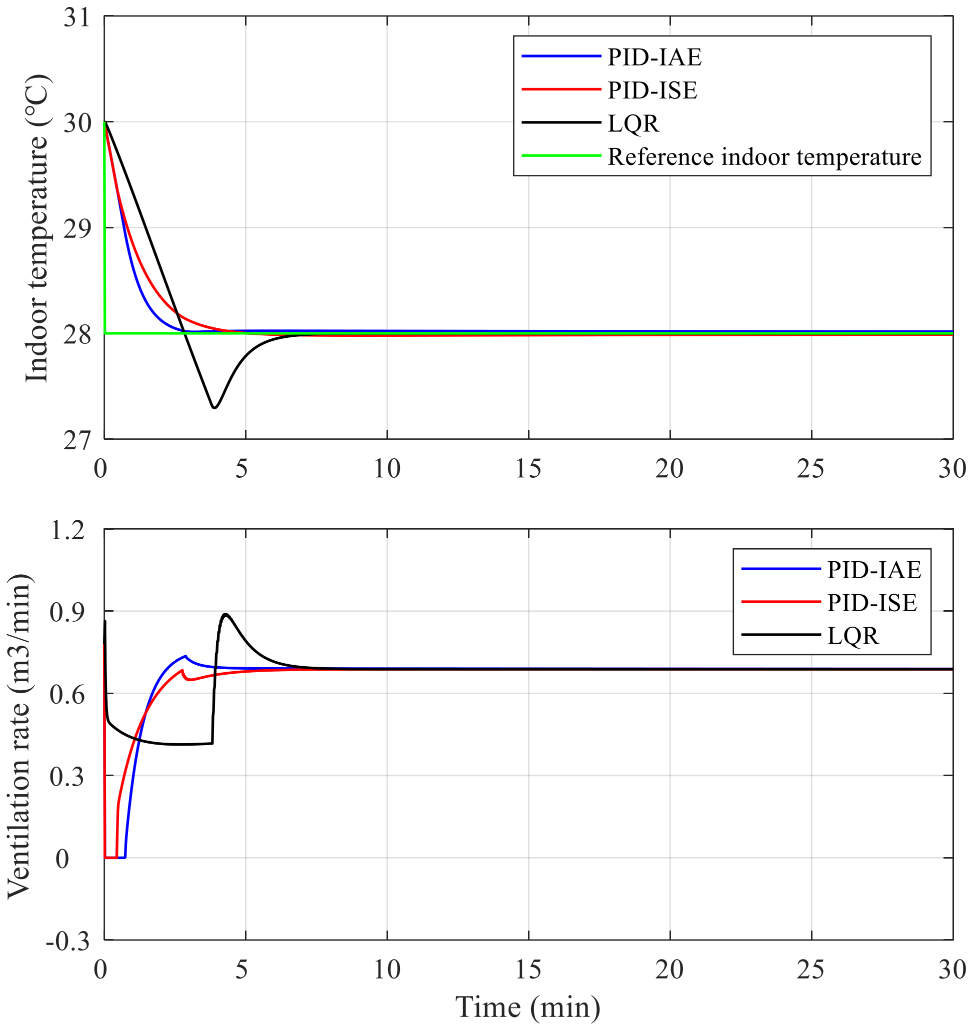

Figure 5.8 Tracking responses of the closed-loop system to a step-type humidity change while the temperature is fixed at 28°C

To keep the indoor temperature in its desired value while the humidity is decreased from 18g $[H_2O]$/kg [dry air] to 16g $[H_2O]$/kg [dry air], the fan should be turned on and cooled the environment. Due to this reason, the ventilation rate is increased, as shown in Figure 5.7. The LQR turns on the fan quickly and works at a 0.4 ventilation rate for 2.78 min. After 3.82min, it becomes increases to a 0.8885 m^3/min vent rate. Due to the R weighting matrix, the ventilation rate is minimized from 0.8885 to 0.6885 m^3/min.

At this time, an undershot occurs in the indoor temperature response. However, the temperature attains its steady-state value than PID quickly. The indoor temperature is zoomed from 27.2 to 28.5°C with 13min of the simulation time as shown in Figure 5.8.

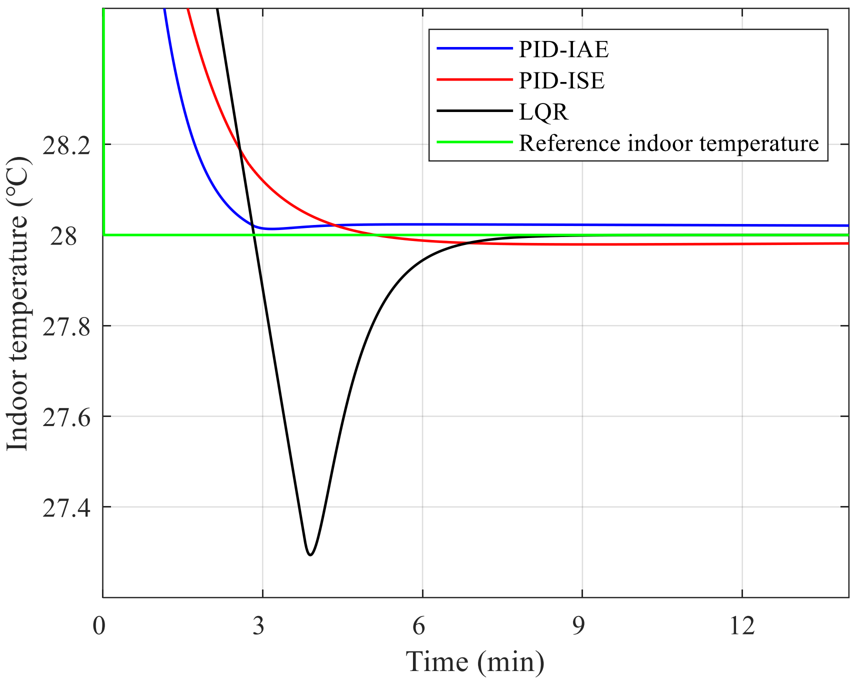

Figure 5.9 The indoor temperature zoomed result when indoor humidity is decreased while the temperature is fixed at 28°C

Figure 5.8 depicts that the indoor temperature response in LQR reaches its steady-state value within a short period compared to PID. It implies the LQR gives a faster response even though an undershoot exists in the temperature response. Moreover, the proposed controller also has a good performance in minimizing IAE than PID. The performance measures for both temperature controllers are summarized in Table 5.8.

Table 5.7 Performance measures when y_{r2} is changed from 18 to 16g [H_2O]/kg [dry air]

Temperature controllers	Performance measures				
	t_p	t_r	M_p	t_s	IAE
PID - IAE	30	1.5807	0	2.5722	2.5689
PID - ISE	9.18	2.3754	1.0414	3.9531	2.8401
LQR	3.90	2.2234	35.3133	6.2494	1.9654

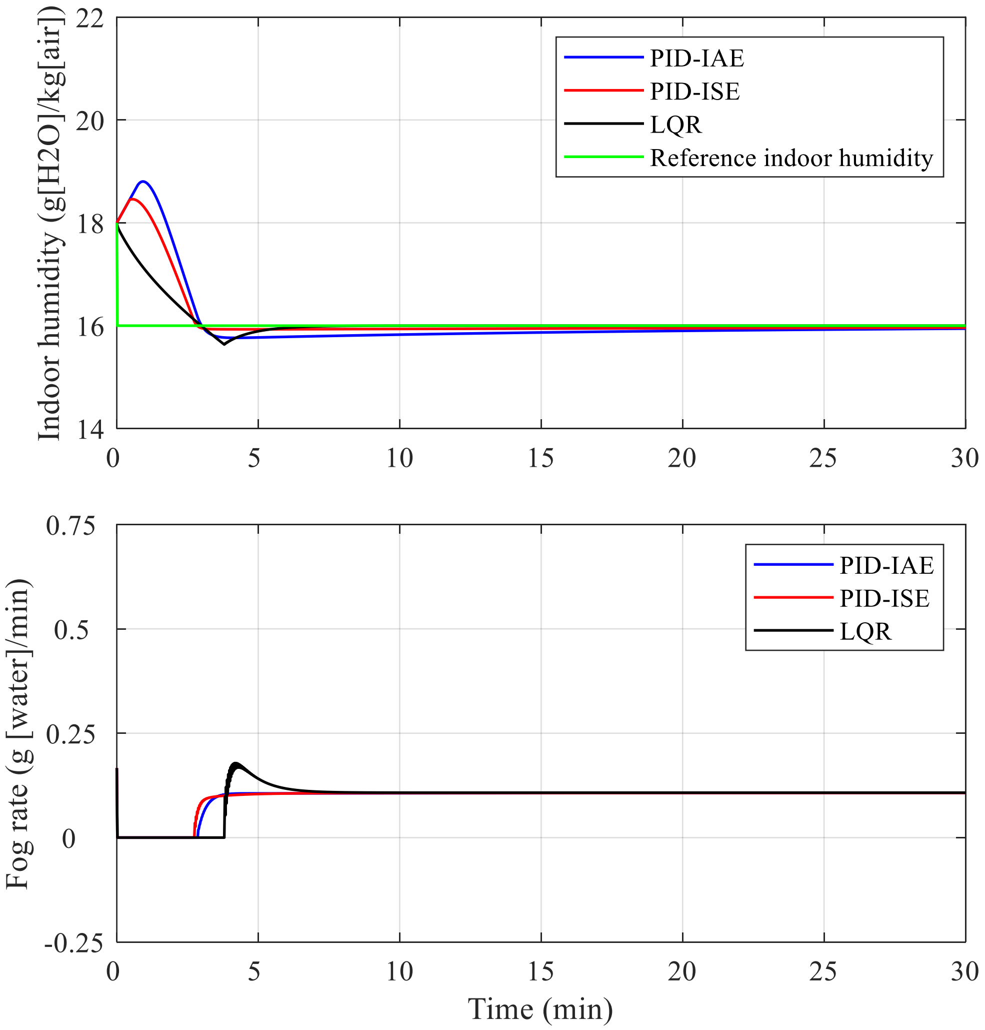

Figure 5.10 Tracking responses of the closed-loop system to a step-type humidity change while the temperature is fixed at 28°C

The above simulation result shows that the LQR gives a small peak time and settling time with a tolerable overshoot than the PID. This implies the proposed controller gives a quick response for the setpoint change of indoor humidity from 18 to 16 g [H_2O]/kg [dry air]. Furthermore, the IAE is small in LQR in comparison to PID. Table 5.9 shows the setpoint tracking performance parameters of the humidity controllers for the dehumidification process.

Table 5.8 Performance measures when y_{r2} is changed from 18 to 16 g [H_2O]/kg [dry air]

Humidity controllers	Performance measures				
	t_p	t_r	M_p	t_s	IAE
PID - IAE	4.18	0.9571	11.8157	28.5394	9.9211
PID - ISE	4.68	1.1692	3.5154	20.1903	6.8254
LQR	3.80	2.4260	18.3390	6.0048	2.9997

The setpoint tracking performance of the indoor temperature and humidity controller is summarized in Figure 5.10. The figure illustrates the tracking performance in terms of settling time for both temperature controllers by considering the setpoint change condition of humidity. The graph shows that the LQR controller has better tracking performance with a short settling time than the PID.

The overall setpoint tracking performance tests imply that the LQR has good performance in terms of settling time, rise time, peak time, IAE, and overshoot than PID. Since the LQR is designed for a linear model of a greenhouse indoor climate system, its tracking performance is better compared to PID. Moreover, the optimal control input is quickly synthesized in the proposed controller since the open-loop augmented with the integral error is controllable, as it is proofed in theorem 3.2. Hence, the LQR gives a faster response during setpoint change.

Figure 5.10 demonstrates the settling time graphical results of each temperature and humidity controller. The graph shows that the LQR temperature and humidity controllers have better tracking performance than the others. It implies that the LQR gives faster response than PID.

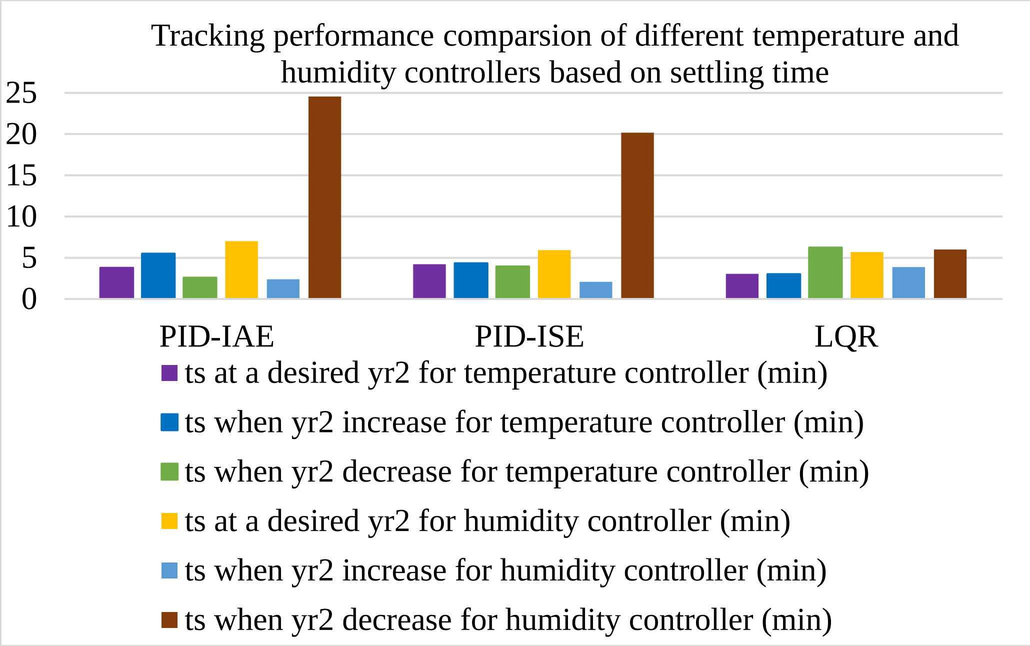

Figure 5.11 Graphical representation of indoor temperature and humidity controllers tracking performance based on settling time

5.3.2 Disturbance Rejection Performance Test

As can be expected, greenhouse systems are highly affected by external disturbances, mainly solar radiation, outside temperature, and outside humidity. Solar radiation and outside temperature have an immense effect on the greenhouse system during the daytime of the summer season. In this thesis, the robustness of the proposed controller to reject those disturbances is shown and compared with the PID controllers using different performance measures. The simulation is done for 30min.

Similar to the case of the setpoint tracking performance test, disturbances are changed while setpoints are kept constant, and performances in terms of perturbance peak M_{peak}, recovery time t_{rcy}, and IAE are gauged.

5.3.2.1 Disturbances Increase at a Fixed Indoor Temperature and Humidity

During the daytime of the summer season, the plants cannot resist a large amount of temperature that is increased by intercepted solar radiant energy and outside temperature. Accordingly, the role of the controller is to keep the indoor temperature and humidity at their desired value whenever the intercepted solar radiant energy and outside temperature have existed in the system.

.

The first simulation was carried out by considering that the intercepted solar radiant energy is increased from 300W to 400W while the outside temperature remains constant at 35℃, and the system operates at 28℃ and 18 g [H_2O]/kg [dry air].

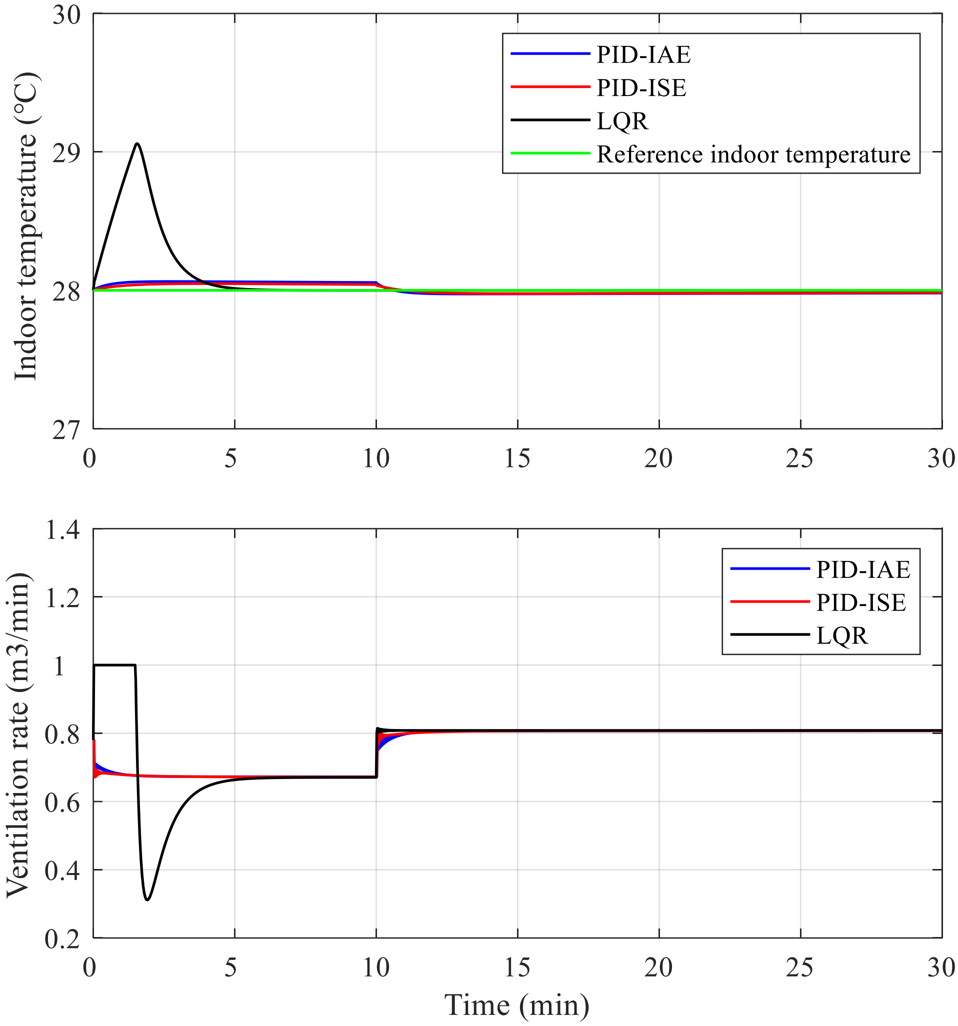

Figure 5.12 Rejection response of the feedback system when intercepted solar radiant energy increases while the outside temperature is fixed at 35℃

Figures 5.11 shows that the LQR and PID temperature controllers produce the control signal after 10min of the simulation time to reject the effect of disturbance on the indoor temperature. When the intercepted solar radiant energy becomes increases, the indoor temperature is also increased. Hence, the fan requires more energy to keep the temperature at its desired value. As shown in Figure 5.11, the ventilation rate increases at 10min to minimize the effect of solar radiant energy on the indoor temperature. During this change, the ventilation rate that is produced by the PID temperature controller has some oscillation compared to LQR.

The quantitative comparison of the control methods is summarized in Table 5.10. In PID controller, there is not a finite time which is required to recover the response to less than 2% of the desired response. But, the LQR requires 4.6748 min to recover the response as shown in Table 5.10. Even though the LQR has large IAE and M_{peak}, it takes small time to reach to its first peak. Disturbance rejection performance is better in LQR than PID since LQR has small peak time and recovery time.

Table 5.9 Performance measures when d_1 changes from 300 to 400W

Temperature controller	Performance measures			
	t_p	M_{peak}	t_{rcy}	IAE
PID - IAE	2.72	0.0639	-	1.6815
PID - ISE	3.96	0.0484	-	1.2227
LQR	1.54	1.0598	4.6748	1.8923

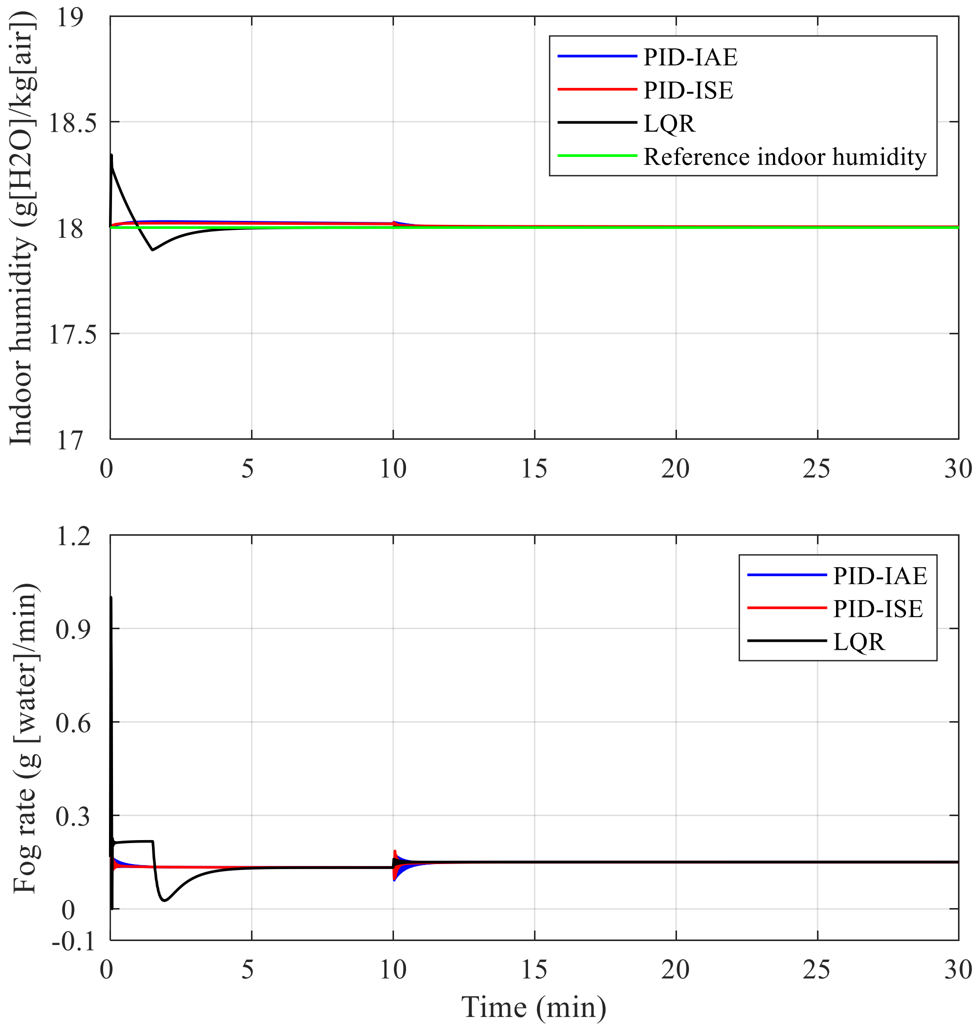

Figure 5.13 Rejection response of the feedback system when intercepted solar radiant energy increases while the outside temperature is fixed at 35°C

The simulation result of the indoor humidity with its control signal is shown in Figure 5.12. Like the fan, the fog spray rate is also increased as the intercepted solar energy increases to cool the indoor climate of a greenhouse. But a small amount of fog rate is added to the environment compared to the ventilation rate since the system operates at 18g [H_2O]/kg [dry air]. The LQR humidity controller turns on the spray nozzle as quickly as possible to recover the humidity response to 17.98g [H_2O]/kg [dry air] than PID. Besides, the LQR has less peak time and error than PID, as described in Table 5.11. Figure 5.13 shows the zoomed-in responses of the indoor humidity between 0 and 15 min. It indicates that the LQR has large perturbance peak even though t_p, t_{rcy}, and IAE is smaller compared to the PID controller.

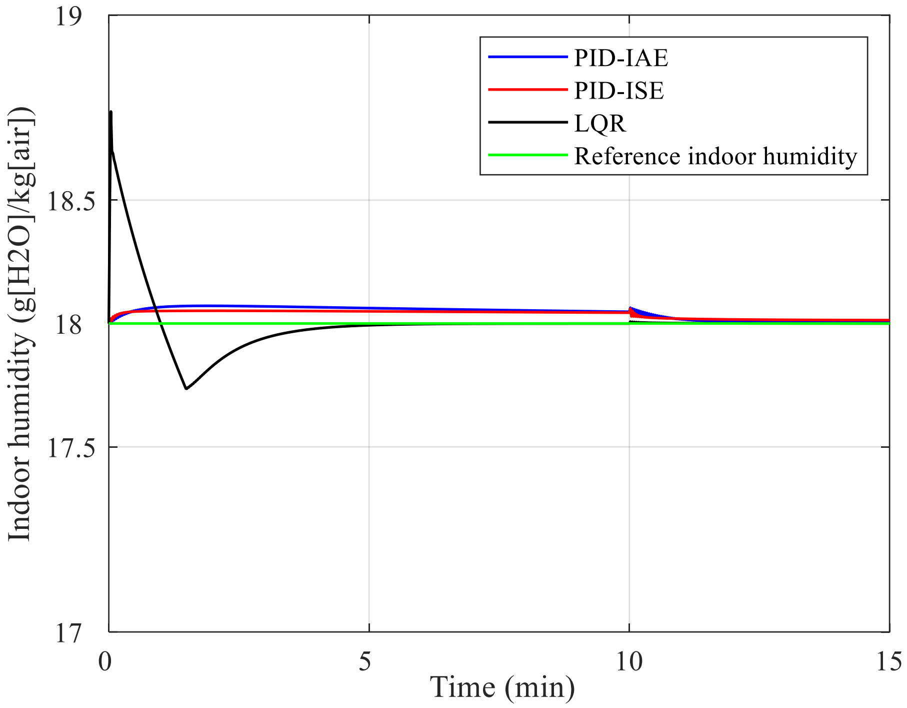

Figure 5.14 The indoor humidity zoomed result when intercepted solar radiant energy increases while the outside temperature is fixed at 35°C

Table 5.10 Performance measures when d_1 changes from 300 to 400W

Humidity controller	Performance measures			
	t_p	M_{peak}	t_{rcy}	IAE
PID - IAE	1.88	0.0286	32.4606	0.2857
PID - ISE	10.02	0.0241	-	0.3929
LQR	0.04	0.3436	4.1572	0.2725

Furthermore, it is a well-known fact that solar radiation is directly related to air temperature. Hence, the next simulation is performed by considering the midday of the summer season. Due to this reason, both intercepted solar radiant energy and outside temperature are increased from 300W to 400W and 35°C to 37°C while the setpoints are kept constant, respectively. The closed-loop responses of the outputs with corresponding control signals are illustrated in Figures 5.14 and 5.15.

From the closed-loop response of the indoor temperature, as illustrated in Figure 5.14, it is realized that the LQR recovers the indoor temperature quickly by minimizing the energy consumption of the fan. Whereas the optimized PID controller increases the ventilation rate signal with some oscillations. As a result, the recovery time of the indoor temperature is high in PID. On the other hand, the PID controller has a small perturbance peak value compared to the LQR, as shown in Table 5.12. Table 5.12 also indicates that the LQR has a small error than PID because the selected weighting matrix **Q** properly penalizes the temperature error signal. Hence, LQR has a good rejection performance in minimizing the error signal than that of PID. Even though the PID rejection performance in terms of obtaining a fast response is less compared to LQR, it shows a satisfactory performance.

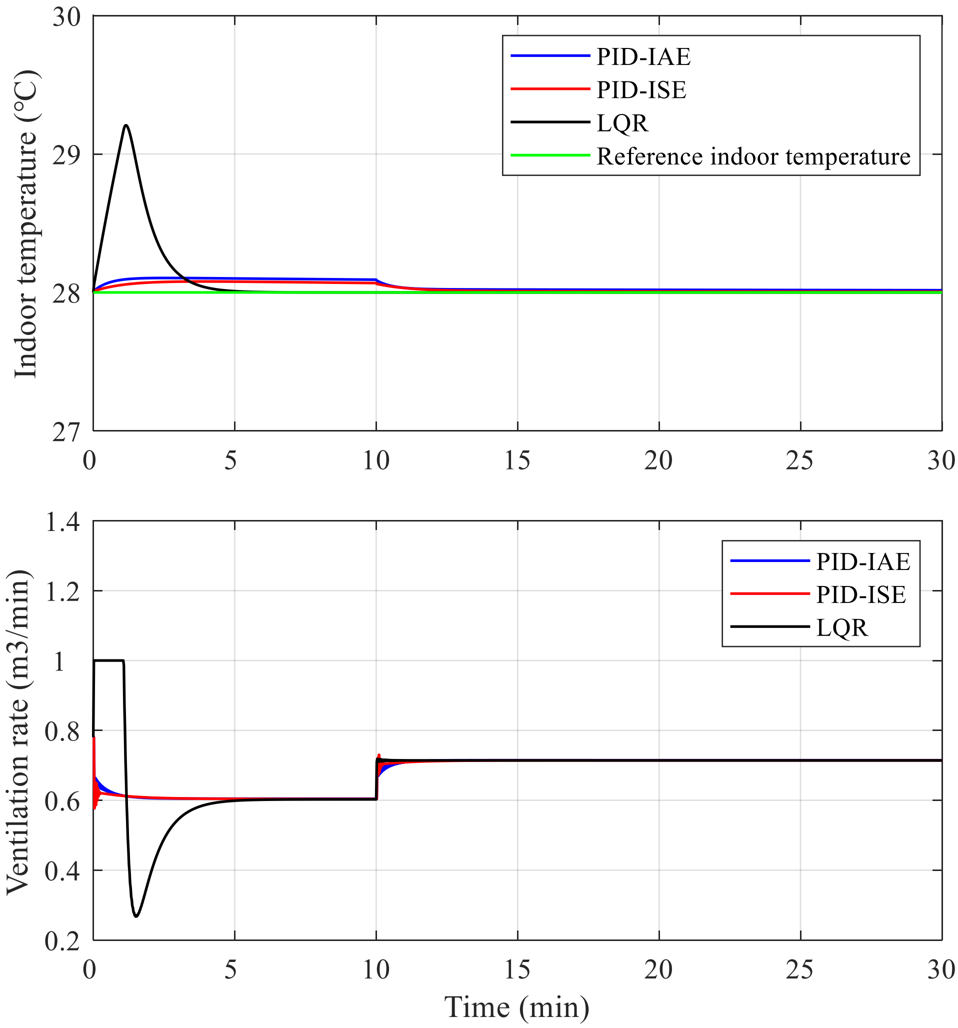

Figure 5.15 Rejection response of the feedback system when both step-type disturbances increase while setpoints are kept constant at 28℃ and 18g [H_2O]/kg [dry air]

The quantitative comparison of the control methods is summarized in Table 5.12. Table 5.12 implies that the LQR controller has a better performance than PID in obtaining fast response.

Table 5.11 Performance measures when both d_1 and d_2 increase at 28°C and 18g [H_2O]/kg [dry air]

Temperature controller	Performance measures			
	t_p	M_{peak}	t_{rcy}	IAE
PID - IAE	2.56	0.1044	-	1.8959
PID - ISE	3.88	0.0790	69.3938	1.8427
LQR	1.16	1.2075	4.2819	1.0923

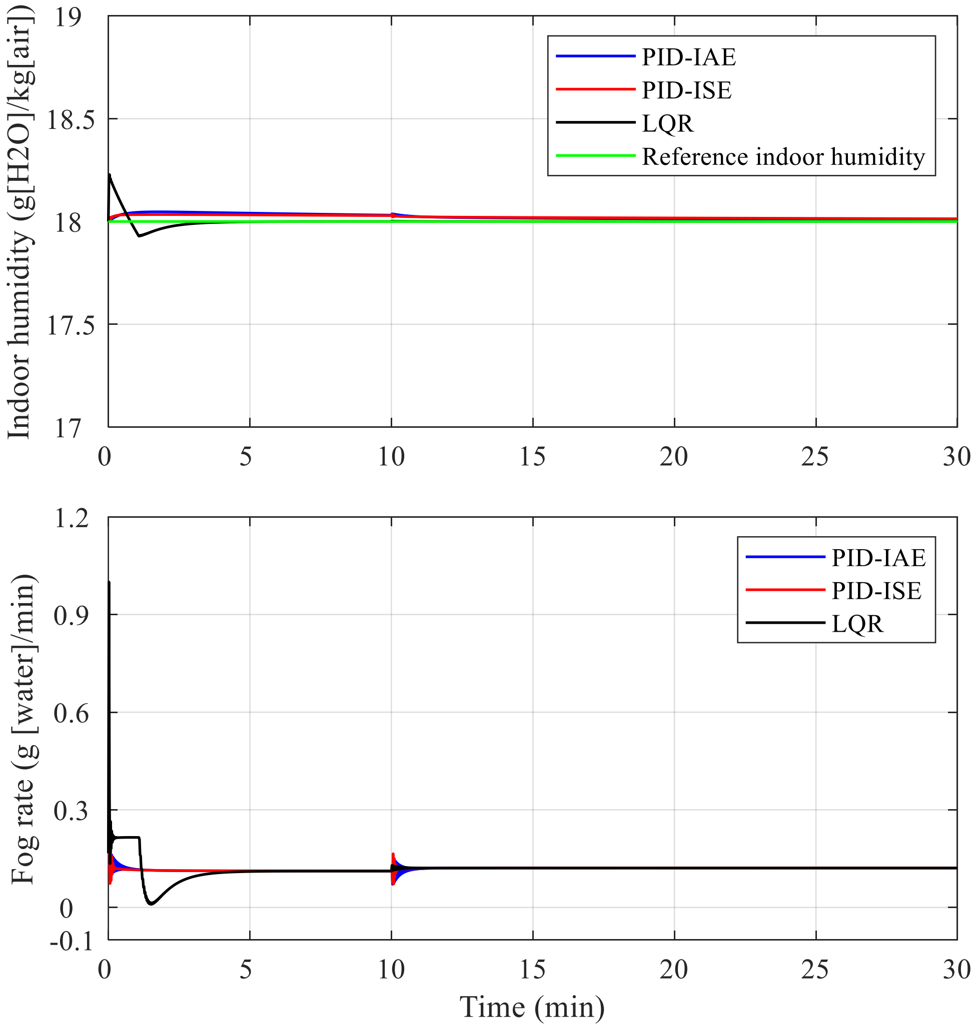

Figure 5.16 Rejection response of the feedback system when both step-type disturbances increase while setpoints are kept constant at 28°C and 18g [H_2O]/kg [dry air]

Figure 5.15 depicts that all the humidity controllers increase the fog rate signal with some oscillation after 10min of the simulation time to reject the effect of disturbance on the indoor temperature. However, the fog rate signal that LQR produces has less fluctuation since the weighting matrix **R** is used in LQR. It minimizes the energy consumption of the spray nozzle, so the fog spray works with less oscillation and recovers the indoor humidity quickly as much as possible to its desired value. As a result, the closed-loop response of the indoor humidity takes a considerable time to recover to 17.98g [H_2O]/kg [dry air] of indoor humidity. Table 5.13 indicates that the LQR has better rejection performance with short recovery time, peak time and small error signal. Since the weighting matrix **Q** penalizes the humidity error signal, the IAE is very small in LQR. It demonstrates that the selected **Q** matrix appropriately penalizes the state error.

Table 5.12 Performance measures when both d_1 and d_2 increase at 28°C and 18g [H_2O]/kg [dry air]

Humidity controller	Performance measures			
	t_p	M_{peak}	t_{rcy}	IAE
PID - IAE	1.76	0.0471	67.4936	0.7813
PID - ISE	10.02	0.0350	-	1.0483
LQR	0.04	0.2285	3.7231	0.1680

5.3.2.2 Disturbances Decrease at a Fixed Indoor Temperature and Humidity

The amount of solar radiation decreases as the time of the day is getting rid of. Because of the direct relation between solar radiation and air temperature, the outside temperature is reduced when the solar radiation reduces. Hence, the simulation is done by reducing intercepted solar radiant energy from 400W to 200W and outside temperature from 37 to 32°C while the indoor temperature and humidity are kept constant at 28°C and 18g [H_2O]/kg [air], respectively.

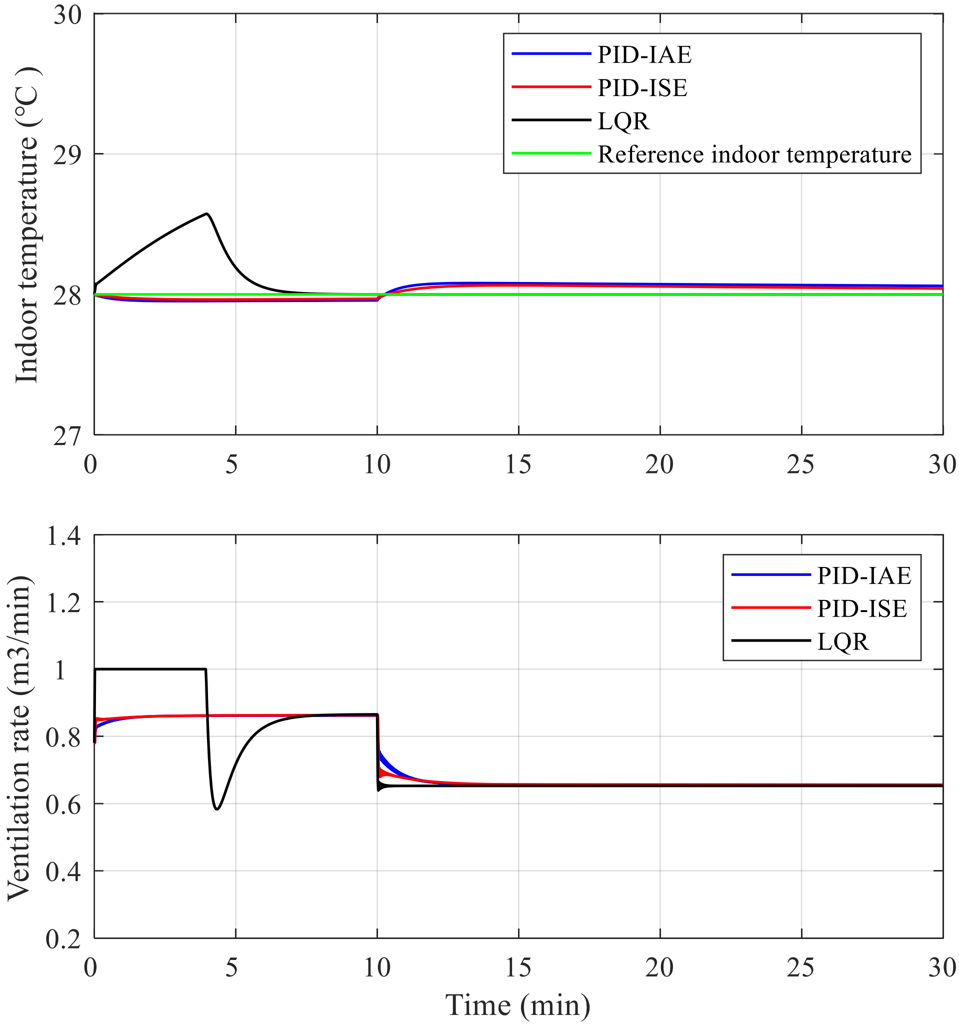

Figure 5.17 Rejection response of the feedback system when both step-type disturbances decrease at 28°C and 18g [H_2O]/kg [dry air]

The ventilation rate signal in Figure 5.16 depicts that the PID controller takes a large time to produce a ventilation signal and reject the disturbances. On the other hand, the weighting matrix **R** in LQR has a small ventilation rate signal within a short period; hence the fan works in its operational range after 3.8636min of the simulation time. A short recovery time with a small error is obtained in LQR than PID.

Figure 5.17 shows the zoomed-in responses of the indoor temperature between 0 and 15 min. It indicates that the LQR takes short time to recover the response to less than 2% of its setpoint even though M_{peak} is larger compared to the PID controller. The PID takes an infinite time to recover the temperature response hence it is difficult to obtain fast response.

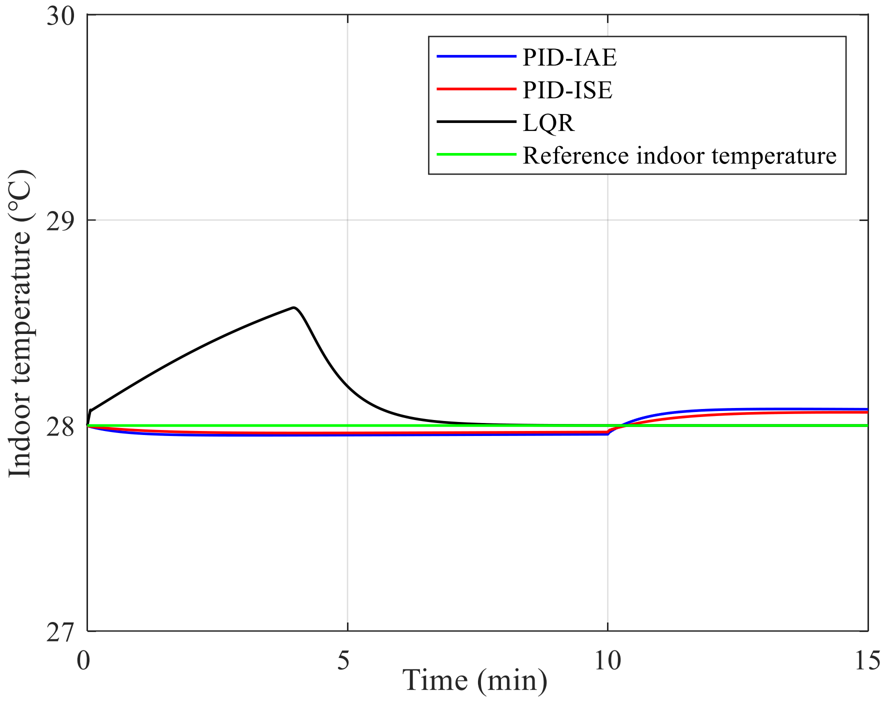

Figure 5.18 Indoor temperature zoomed response when both step-type disturbances decrease at 28°C and 18g [H_2O]/kg [dry air]

Table 5.14 shows the quantitative comparison of the control methods based on disturbance rejection performance measures. The LQR gives fast response with less peak time compared to PID controller. From the table, it is observed that LQR has better rejection performance than PID.

Table 5.13 Performance measures when both d_1 and d_2 decrease at 28°C and 18g [H_2O]/kg [dry air]

Temperature controllers	Performance measures			
	t_p	M_{peak}	t_{rcy}	IAE
PID - IAE	13.44	0.0804	-	3.8124
PID - ISE	14.66	0.0643	-	2.4272
LQR	3.96	0.5736	7.0895	1.8923

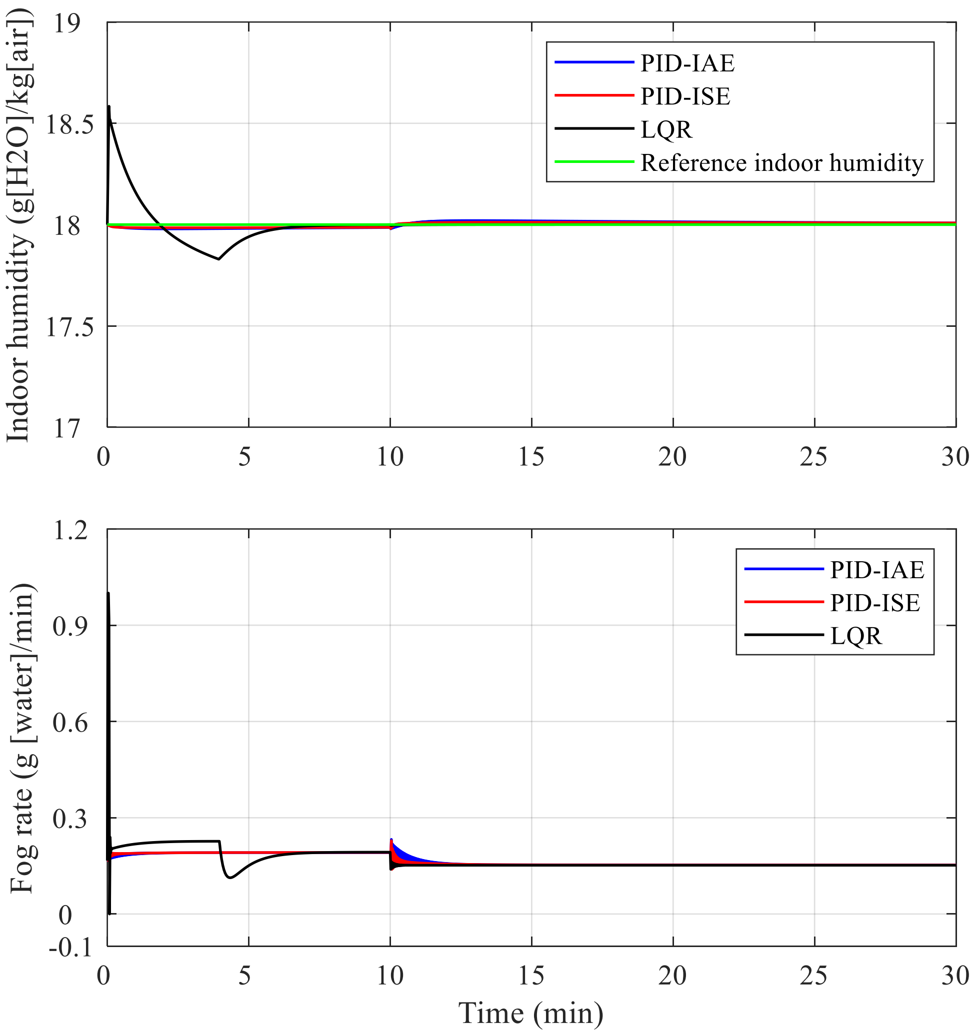

Figure 5.19 Rejection response of the feedback system when both step-type disturbances decrease at 28°C and 18g [H_2O]/kg [dry air]

Figure 5.18 shows the humidity responses of the three methods. The LQR shows fast response with 0.5842 perturbance peak as compared to the PID controller. Since LQR has small peak time, it has better swiftness behavior than PID. Also, the simulation result in Figure 5.18 shows that the LQR can minimize the integral absolute error using the state weighting matrix **Q**. Since **Q** is appropriately selected in this thesis work, the IAE is very small compared to PID. The zoomed-in response in Figure 5.19 depicts that the PID takes infinite time to recover the response. As a result, the output response cannot match the setpoint. In LQR, the recovery time is finite and small hence the LQR has better closeness property than PID. Furthermore, Table 5.15 summarizes the performance parameter values of the humidity controllers.

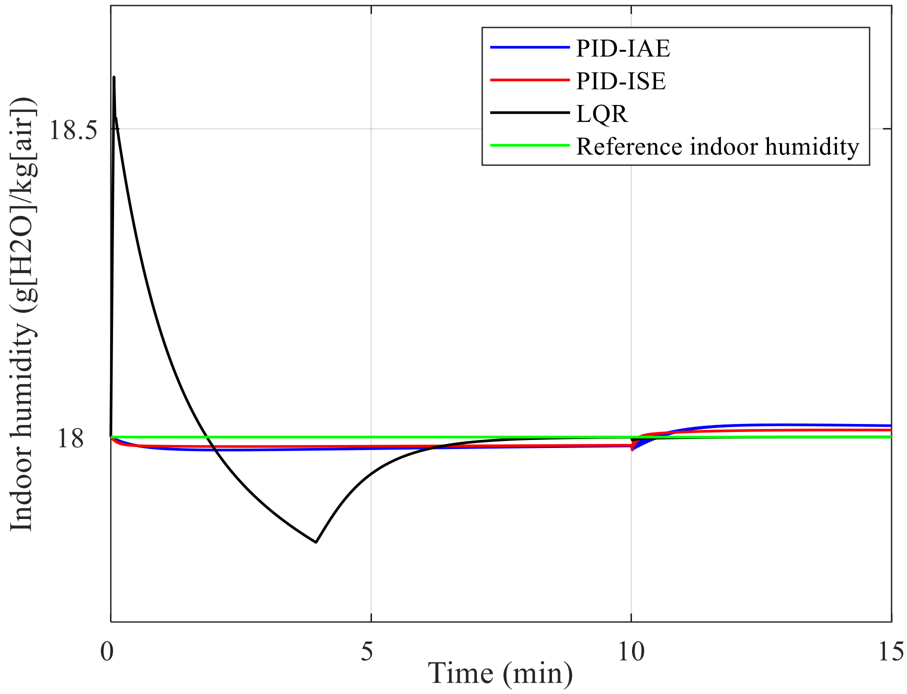

Figure 5.20 Indoor humidity zoomed response when both step-type disturbances decrease at 28°C and 18g [H_2O]/kg [dry air]

Table 5.14 Performance measures when both d_1 and d_2 decrease at 28°C and 18g [H_2O]/kg [dry air]

Humidity controller	Performance measures			
	t_p	M_{peak}	t_{rcy}	IAE
PID - IAE	12.88	0.0199	-	0.5953
PID - ISE	14.26	0.0114	-	0.5767
LQR	0.06	0.5842	6.5865	0.4649

The overall disturbance rejection performance test implies that the LQR takes a short time to recover the output response with an acceptable perturbance peak than PID. Therefore, the proposed method shows better performance in disturbance rejection than tracking performance. Furthermore, since this thesis work is designed for the daytime of the summer season, the controller performance should be larger in rejecting a high amount of disturbances within a short period. Figure 5.20 demonstrates the disturbance rejection performance in terms of the peak time of each humidity and temperature controllers when both disturbances increase and decrease at 28°C and 18g [H_2O]/kg [dry air].

The graph shows that the LQR temperature and humidity controller gives faster response than the PID since the LQR has small peak time. It also implies that the responses have better swiftness behavior in LQR.

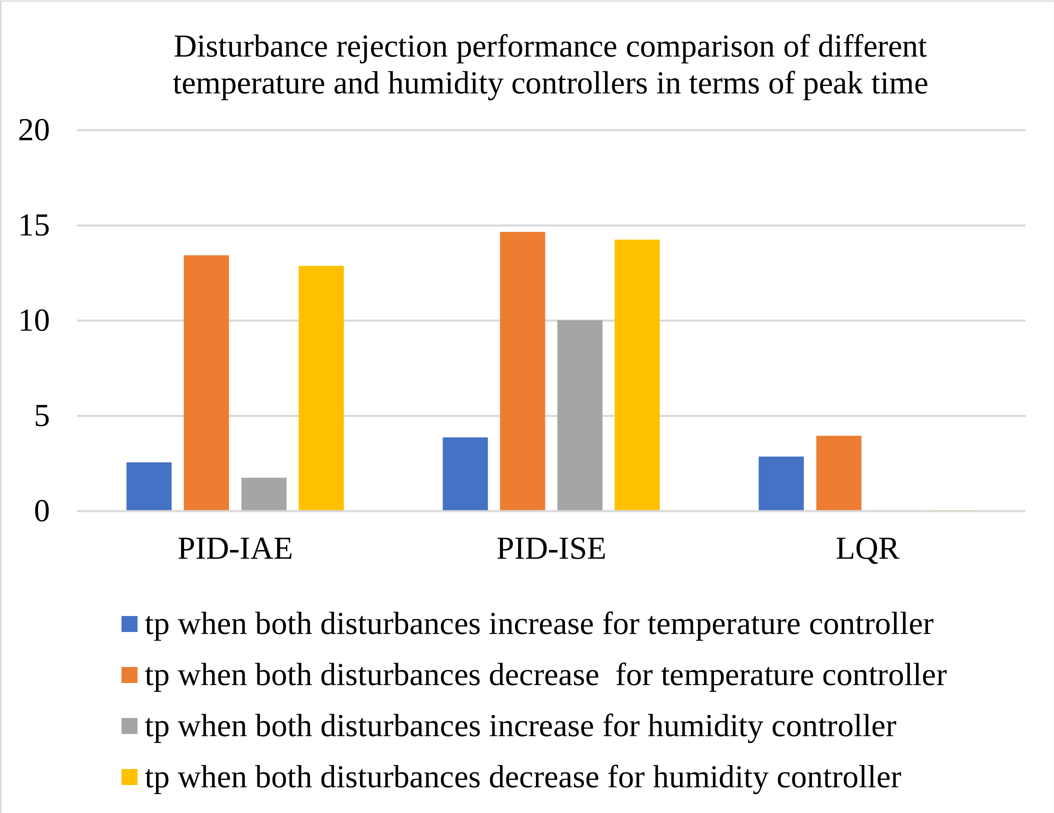

Figure 5.21 Graphical representation of indoor temperature and humidity controller's disturbance rejection performance based on peak time

CHAPTER SIX

CONCLUSIONS AND RECOMMENDATIONS

6.1 Conclusions

The greenhouse is a highly nonlinear system whose dynamics is affected by the factors of greenhouse parameters like air temperature, air humidity, carbon dioxide, and light intensity varying between day and night. Among these parameters, indoor air temperature and humidity are the basic parameters that influence the growth and quality of greenhouse plants. Due to the principle of psychrometric law, there is a coupling relation between these parameters.

In this work, the LQR for indoor climate control for a greenhouse has been presented. The greenhouse system was formulated by an MIMO nonlinear model and the input-output feedback linearization technique was used to transform the nonlinear model to its equivalent linear model. An augmented system model was obtained to eliminate the steady-state error from disturbances, and its controllability was confirmed. Then, the PI-type LQR was designed based on the linear augmented model for controlling indoor temperature and humidity of the greenhouse.

In addition, to compare the performance of the proposed method, two practical PID controllers were designed based on greenhouse system's nonlinear model. The parameters of the PID controller were optimally tuned using a genetic algorithm by minimizing the performance indices, namely IAE and ISE. The controllers' performance was analyzed by doing both setpoint tracking and disturbance rejection performance tests.

In setpoint tracking, the performance of the LQR and the GA-tuned PID controller were compared using performance measures such as rise time, settling time, IAE, and overshoot. The setpoint tracking tests show that the LQR has better performance than the PID controller, especially giving a faster response with acceptable overshoot.

For the disturbance rejection test, the intercepted solar radiant energy and outside temperature were changed by considering different setpoints, and different performance measures were taken, such as recovery time, perturbance peak, and IAE. In the disturbance rejection test, the LQR showed robustness with less perturbance peak and short recovery time than the GA-tuned PID controller.

It was found from the overall results of this work that the LQR provides better performance when both setpoint and disturbance conditions exist in the greenhouse system.

6.2 Recommendations

The greenhouse environment control system needs continuous controlling and monitoring of its environmental parameters. Hence, this thesis work can be further improved by considering the winter and nighttime operations control system. Hence, designing an advanced control technique such as a model predictive control for controlling the other parameters like carbon dioxide, soil temperature, and humidity is recommended. Since the proposed system is implemented only in MATLAB software, the hardware implementation of this work is also recommended. Nowadays, several greenhouse industries are built in different parts of Ethiopia, including urban areas like Addis Ababa. Even though the climatic condition of Ethiopia is suitable for crop production, the indoor climate of a greenhouse always needs a better control system. Accordingly, it is also recommended that the student practice, update, and implement the proposed control system by doing experiments.

Research Fund Acknowledgment

This research thesis was funded by Adama Science and Technology University under the grant number of **ASTU/SM-R/162/20**, Adama, Ethiopia.

REFERENCES

[1] Abdeen Mustafa Omer, "Sustainable Food Production in Greenhouses and its Relations to the Environment," *Advances in Plants & Agriculture Research*, vol. 5, no. 3, pp. 538-542, 2016.

[2] Yuxian Gao, Chaoying Liu, Xueling Song, and Siwu He, "Feedback Feed-forward Linearization and Decoupling for Greenhouse Environment Control," *IEEE*, pp. 179-183, 2014.

[3] T. Goldammer, "Greenhouse Glazing Greenhouse Management: A Guide to Operations and Technology," U.S.A, Apex Publishers, 2019, p. 460.

[4] "ScienceDirect," 25 May 2015 [Online]. Available: https://www.sciencedirect.com/topics/engineering/psychrometric-chart. [Accessed 10 February 2021].

[5] R. Shamshiri and Wan Ishak Wan Ismail, "A Review of Greenhouse Climate Control and Automation Systems in Tropical Regions," *Journal of Agricultural Science and Applications*, vol. 02, no. 03, pp. 175-182, 2013.

[6] Ashwini, "Agriculture Information," 25 March 2010. [Online]. Available: https://www.agricultureinformation.com/forums/threads/green-house-cultivation.44034/. [Accessed 15 Feburary 2021].

[7] Dejenie Fikir, "Fuzzy Model Based Predictive Control of Greenhouse Temprature and Humidity," 2019.

[8] Anil Kumar, G.N Tiwari, Subodh Kumar, and Mukesh Pandey, "Role of Greenhouse Technology in Agricultural Engineering," *International Journal of Agricultural Research*, vol. 1, no. 4, pp. 364-372, 2006.

[9] "Classification of Greenhouses," [Online]. Available: https://indoorgardening.com/. [Accessed 07 March 2021].

[10] " Gothic Arch Greenhouses," Greenhouse Manufacturer, Project Consulting, and Design [Online]. Available: https://www.gothicarchgreenhouses.com/gable-greenhouses.htm. [Accessed 07 March 2021].

[11] Saeed, and Sara Abdelgadir, "Design A Greenhouses Temperature Control System," 2017.

[12] "Morn Glass," Qingdao Morn Building Materials, 28 February 2019. [Online]. Available: https://www.cnmorn.com/greenhouse-glass-types.html. [Accessed 07 March 2021].

[13] "Gardening Channel," [Online].Available: https://www.gardeningchannel.com/types-of-greenhouse-coverings/. [Accessed 07 March 2021].

[14] "Focus Technology," Qingzhou Xinhe Greenhouse Horticulture, [Online]. Available: https://chinagreenhouse.en.made-in-china.com/product/DvFJkqnoHrpu/China-Greenhouse-PC-Corrugated-Types-of-Polycarbonate-Sheet-Ghana-Popular-Roofing-Sheet.html. [Accessed 07 March 2021].

[15] "ebay,"[Online]. Available: https://i.ebayimg.com/images/g/5cEAAOSwjVVVr~cl/s-l640.jpg. [Accessed 21 March 2021].

[16] "Gothic Arch Greenhouses," Greenhouse Manufacturer, Project Consulting, Design, and Products Sale Service, [Online]. Available: https://www.gothicarchgreenhouses.com/bk-greenhouse-controls.html. [Accessed 07 March 2021].

[17] D.T Santosh, K.N Tiwari, Vikas Kumar Singh, and A.Raja Gopala Reddy, "Micro Climate Control in Greenhouse," *International Multidisciplinary Scientific GeoConference Surveying Geology and Mining Ecology Management,* vol. 6, no. 3, pp. 1730-1742, 2017.

[18] Tronchin, Fabbri, and Chiara Bertolli, "Controlled Mechanical Ventilation in Buildings: A Comparison between Energy Use and Primary Energy among Twenty Different Devices," *Energies,* pp. 1-19, 2018.

[19] A. Both, "Greenhouse Management," 9 June 2011. [Online]. Available: https://www.greenhousemag.com/article/greenhouse-0611-cooling-ventilation/. [Accessed 21 March 2021].

[20] Yerbol Telebayey, and Altai Shaltabaey, "Science Society Defense," [Online]. Available:http://www.rusnauka.com/16_PN_2016/Tecnic/12_212713.doc.htm. [Accessed 21 March 2021].

[21] "India MART," India MART InterMESH, [Online]. Available: https://www.indiamart.com/locus-green/naturally-ventilated-greenhouse.html. [Accessed 27 March 2021].

[22] Kittas, Katsoulas, and Bartzanas, "Greenhouse Climate Control in Mediterranean Greenhouses," *ISSN*, pp. 89-114, 2012.

[23] E. Labbate, "Climate Control Systems," A nebula group company, [Online]. Available: https://www.climatecontrol.com/blog/greenhouse-control-systems/. [Accessed 21 March 2021].

[24] "IKEUCHI USA," IKEUCHI USA INC, [Online]. Available: https://www.ikeuchi.us/eng/products/system/1116. [Accessed 27 March 2021].

[25] Sentelhas, Ester Holcman, and Paulo, "Microclimate under different shading screens in greenhouses cultivated with bromeliads," *R. Bras. Eng. Agríc. Ambiental*, vol. 16, no. 8, pp. 858-863, 2012.

[26] "OKorder," Global Materials and Equipment Supplier, [Online]. Available: https://www.okorder.com/p/hdpe-aluminium-shade-net-for-greenhouse-5years-guarantee_589278.html. [Accessed 27 March 2021].

[27] David Shelton, "Air Properties: Temperature and Relative Humidity," University of Nebraska-Lincoln Extension, U.S.A, 2008.

[28] Boufadene Mourad, Nonlinear Control, New York: CRC Press Taylor and Francis Group, 2019.

[29] Wafa Ghozlane, and Jilani Knani, "Nonlinear control via input-output feedback linearization of a robot manipulator," *Advances in Science, Technology and Engineering Systems*, vol. 3, no. 5, pp. 374-381, 2018.

[30] M. Viking, "Wikipedia," Wikipedia, 10 January 2021. [Online]. Available: https://en.wikipedia.org/wiki/Feedback_linearization. [Accessed 25 February 2021].

[31] K.M. Hangos, J. Bokor, and G.Szederkenyi, Analysis Control of Nonlinear Process Systems, London: Springer, 2004.

[32] Freddy Garces, Victor M. Becerra, Chandrasekhar Kambhampati, and Kevin Warwick, Strategies for Feedback Linearisation, Verlag London: Springer, 2003.

[33] Khalil, and Hassan K, Nonlinear Systems, New Jersey: Prentice Hall, 2002.

[34] Lidia Roca, Jorge A. Sánchez , Francisco Rodríguez , Javier Bonilla , Alberto de la Calle , and Manuel Berenguel, "Predictive Control Applied to a Solar Desalination Plant Connected to a Greenhouse with Daily Variation of Irrigation Water Demand," *Energies*, vol. 9, no. 3, pp. 1-17, 2016.

[35] Chiara Bersani, Ahmed Ouammi, Roberto Sacile, and Enrico Zero, "Model predictive control of smart greenhouses as the path towards near zero energy consumption," *Energies*, vol. 13, no. 14, pp. 1-17, 2020.

[36] Kazuhisa Ito, and Yuma Hara, "Multipoint-measurement multipoint-heating greenhouse temperature control with wooden pellet fuel using an adaptive model predictive control approach with a genetic algorithm," *Mediterranean Conference on Control and Automation*, 2017.

[37] Sergio, Castaño Giraldo, Rodolfo C. Flesch, and Julio E. Normey-Rico, "Multivariable Greenhouse Control Using the Filtered Smith Predictor," *Journal of Control, Automation and Electrical Systems,* vol. 27, no. 4, pp. 349-358, 2016.

[38] Dimitris S, Paraforos, and Hans W. Griepentrog, "Multivariable greenhouse climate control using dynamic decoupling controllers Dimitris," *IFAC Conference on Modelling and Control in Agriculture*, Finland, 2013.

[39] Azaza, K. Echaieb, F. Tadeo, E. Fabrizio, A. Iqbal, and A. Mami, "Fuzzy Decoupling Control of Greenhouse Climate," *Arabian Journal for Science and Engineering,* vol. 40, no. 9, pp. 2805-2812, 2015.

[40] Gopal Chaudhary, Surinder Kaur, Bhawna Mehta, and Rachna Tewani, "Observer based fuzzy and PID controlled smart greenhouse," *Journal of Statistics and Management Systems*, vol. 22, no. 2, pp. 393-401, 2019.

[41] Haigen Hu, Lihong Xu, Ruihua Wei, and Bingkun Zhu, "Multi-Objective Tuning of Nonlinear PID Controllers for Greenhouse Environment using Evolutionary Algorithms," *IEEE Congress on Evolutionary Computation*, 2010.

[42] Medjber Ahmed, Moualdia Abdelhafidh, and Ould Cherchali Noureddine, "Climate Control of Greenhouse Using Fuzzy Logic and PID Controllers," *International Journal of Electrical Energy*, vol. 2, no. 3, pp. 232-237, 2014.

[43] Indu Chhipa, and Devendra Somwanshi, "Fuzzy Logic Controller to Control Internal Climate of a Greenhouse," *International Conference and Workshops on Recent Advances and Innovations in Engineering*, 2019.

[44] Amshu Vinayak, PG Scholar, and Yasha Jyothi M Shirur, "Automatic Control for Greenhouse Farming," *International Journal of Engineering Research & Technology*, vol. 6, no. 09, pp. 192-197, 2017.

[45] Chen Lijun, Du Shangfeng, Liang Meihui, and He Yaofeng, "Adaptive feedback linearization-based predictive control for greenhouse temperature," *International Agricultural Engineering Journal*, vol. 27, no. 2, pp. 360-367, 2018.

[46] Songwei Zeng, Haigen Hu, Lihong Xu, and Guanghui Li, "Nonlinear Adaptive PID Control for Greenhouse Environment Based on RBF Network," *Sensors*, vol. 12, pp. 5328-5348, 2012.

[47] Daskalov, K.G. Arvanitis, G.D. Pasgianos, and N.A. Sigrimis, "Non-linear Adaptive Temperature and Humidity Control in Animal Buildings," Biosystems Engineering, vol. 93, no. 1, pp. 1-24, 2006.

[48] Tooba Nazir, Muhammad Arslan, and Umar S. Khan, "Design of An Automated Greenhouse Temperature Controller; A Renewable, Robust and Cost Effective Scheme," International Conference on Control, Automation and Robotics, 2019.

[49] Takehiko Hoshi, Ken-Ichiro Yasuba, Hideto Kurosaki, and Takashi Okayasu, "Ubiquitous Environment Control System: An Internet-of- Things–Based Decentralized Autonomous Measurement and Control System for a Greenhouse Environment," Automation in Agriculture - Securing Food Supplies for Future Generations, pp. 107-123, 2018.

[50] Jamel Riahi, Silvano Vergura, Dhafer Mezghani, and Abdelkader Mami, "Intelligent Control of the Microclimate of an Agricultural Greenhouse Powered by a Supporting PV System," *Applied Sciences,* vol. 10, no. 4, pp. 1-20, 2020.

[51] Haigen Hu, Lihong Xu, Erik D. Goodman, and Songwei Zeng, "NSGA-II-based nonlinear PID controller tuning of greenhouse climate for reducing costs and improving performances," *Neural Computing and Application*, 2012.

[52] Athanasios Sapounas, Nikolaos Katsoulas, Bart Slager, Robert Bezemer, and Charlotte Lelieveld, "Design, Control, and Performance Aspects of Semi-Closed Greenhouses," *Agronomy Review,* pp. 1-22, 2020.

[53] Revathi S, Radhakrishnan T K, and Sivakumaran N, "Climate Control in Greenhouse using Intelligent Control Algorithms," *Proceedings of the American Control Conference*, no. 2, pp. 887-892, 2017.

[54] Eugen Horatiu Gurban, and Gheorghe-Daniel Andreescu, "Comparison study of PID controller tuning for greenhouse climate with feedback-feedforward linearization and decoupling," *International Conference on System Theory, Control and Computing*, 2012.

[55] Murray, and Karl Johan Astrom Richard, Feedback Systems, 2019.

[56] Porter, and Bradshaw, "Design of linear multivariable continuous-time tracking," *International Journal of Systems Science,* vol. 5, no. 12, pp. 1155-1164, 2013.

[57] Melih AKTAŞ, Yusuf ALTUN, and Oğuz EROL, "LQR Control of Liquid Level and Temperature Control for Coupled-Tank System," *International Conference on Hydraulics and Pneumatics*, 2017.

[58] Mohamed Essahafi, and Mustapha Ait Lafkih, "Evaluation Performance of PID, LQR, Pole Placement Controllers for Heat Exchanger," *International Journal of Electrical and Computer Engineering,* vol. 8, no. 6, pp. 939-943, 2014.

[59] Vinodh Kumar E, and Jovitha Jerome, "Algebraic Riccati equation based Q and R matrices selection algorithm for optimal LQR applied to tracking control of 3rd order magnetic levitation system," *Archives of Electrical Engineering,* no. 1, pp. 151-168, 2016.

[60] Omer Saleem, Khalid Mahmood-ul-Hasan, and Mohsin Rizwan, "Self-Tuning State-Feedback Control of Rotary Pendulum via Online Adaptive Reconfiguration of Control Penalty-Factor," *Control Engineering and Applied Informatics*, vol. 22, no. 4, pp. 23-33, 2020.

[61] Ines Tejado, Blas M. Vinagre, Jose Emilio Traver, Javier Prieto-Arranz, and Cristina Nuevo-Gallardo, "Back to Basics: Meaning of the Parameters of Fractional Order PID Controllers," *Mathematics*, vol. 530, pp. 1-16, 2019.

[62] Jaisimha Manipatruni, and Narasimha Sampath Vedula, "Design and Implementation of PID Controller Using Genetic Algorithm," *International Journal of Engineering Research & Technology*, vol. 7, no. 11, pp. 104-107, 2018.

[63] Gun-Baek So and Gang-Gyoo Jin, " Fuzzy-based nonlinear PID controller and its application to CSTR," Korean Journal of Chemical Engineering, 2017.

[64] Naveen Kumar, Karambir, and Rajiv Kumar, "A Genetic Algorithm Approach To Study Travelling Salesman," *Journal of Global Research in Computer Science*, vol. 3, no. 3, 2012.

[65] Rafael Guardeño, Manuel J. López, and Víctor M. Sánchez, "MIMO PID controller tuning method for quadrotor based on LQR/LQG theory," *Robotics*, vol. 8, no. 2, pp. 15-21, 2019.

[66] E. Okyere, A. bousbaine, G. T. Poyi, A. Joseph and J. Andrade, "LQR controller design for quad-rotor helicopters," *The Journal of Engineering*, no. 17, pp. 4003-4007, 2019.

[67] Masoud Karimi-Ghartemani, S. Ali Khajehoddin, Praveen Jain, and Alireza Bakhshai, "Linear quadratic output tracking and disturbance rejection," *International Journal of Control*, vol. 84, no. 8, pp. 1442-1449, 2011.

APPENDICES

APPENDIX A

A. 1 Appendixes related to input-output feedback linearization

MATLAB code for obtaining lie derivatives of vector field h along the vector fields f(x) and g(x)

```
% Enter parameters, number of states and number of inputs
par= input ('Parameters ','s');
eval (sprint ('syms %s', par));
parameters= sprint ('%s', par);
n= input ('Number of states= ');
nin= input ('Number of inputs= ');
x= sym (zeros (1, n));
u= sym (zeros (1, nin));
for j= 1: n
eval (sprint ('syms x%d', j))
x (:, j) = sprint ('x%d', j);
end
for k= 1: nin
eval (sprint ('syms u%d', k));
u (:, k) = sprint ('u%d', k);
end
% Enter the functions
fx= input('f(x)= ','s');
gx= input('g(x)= ','s');
hx= input('h(x)= ','s');
% Represent these on a symbolic format
fx= str2sym(fx);
gx= str2sym(gx);
hx= str2sym(hx);
% Generate the desired functions
[Lhf, Lhg] = Feedback Linearization (fx, gx, hx, x)
```

APPENDIX B

B. 1 Appendixes related to proposed system design

The MATLAB code for obtaining operating values

```
% Calculates u1(t) and u2(t) at an operating point
% Assume that the operating point is
C0= -324.67; UA= 29.81; tv= 3.41; lam= 465;
alpha= 0.0033; V= 1/13.3; % Parameters
x1= 30; x2= 18; % Initial outputs
d1= 300; d2= 35; d3= 4; % disturbances
% In the steady-state, xdot (1) = xdot (2) = 0 and obtain u1(t) and u2(t)
a11= -x1/tv+d2/tv; a12= -lam/C0;
a21= -x2/tv+d3/tv; a22= 1/V;
A= [a11 a12; a21 a22];
b1= UA/C0*x1-d1/C0-UA*d2/C0;
b2= -alpha*d1;
B= [b1; b2];
format long
x= A\B
format short
```

% Greenhouse modeling

```
function xdot= GH_Model(t, x, u)
global C0 UA tv lam alpha V d1 d2 d3
% State-space representation of greenhouse dynamic model
xdot= zeros(2,1);
xdot(1)= -UA/C0*x(1)-x(1)*u(1)/tv-lam*u(2)/C0+...
    d1/C0+UA*d2/C0+u(1)*d2/tv;
xdot(2) = -x(2)*u(1)/tv+ u(2)/V+alpha*d1+u(1)*d3/tv;
```

% Equivalent linear model of greenhouse system

```
% The lie derivative of the vector field h along f(x)
    ax= [d1/C0+(UA*d2)/C0; alpha*d1];
 % The lie derivative of the vector field h along f(x)
    bx= inv([(d2-x(1))/tv -lam/C0; -x(2)/tv 1/V]);
    u= bx*(-ax+v); % control input to the actuators
```

APPENDIX C

C. 1 Appendixes related to Magnitude plot of PID controller

% Magnitude plot of ideal PID controller derivative term

```
w= logspace(-2,2,200);
s= j*w; Kd= 1;
g= Kd*s;
mag= abs(g);
plot(w,mag,'linewidth',2)
xlabel('\omega'), ylabel('|U_d(j\omega)|')
```

% Magnitude plot of practical PID controller derivative term

```
w= logspace(-2,2,200);
s= j*w;
Kd= 1; Td= 1;
mag= [];
N= 5; g= Kd*s./(1+Td*s/N); mag= [mag abs(g')];
N= 10; g= Kd*s./(1+Td*s/N); mag= [mag abs(g')];
N= 15; g= Kd*s./(1+Td*s/N); mag= [mag abs(g')];
plot(w,mag(:,1),'--r',w,mag(:,2),':b',w,mag(:,3),'k','linewidth',2)
axis([0 60 0 22])
xlabel('\omega'), ylabel('|U_d(j\omega)|')
legend('N= 5','N= 10','N= 15')
```

C. 2 Appendixes related to objective function and GA optimization of PID indoor temperature and humidity controller

% Implementation of the object function for GA optimization

```
function Perf= Objfun_PID (pop)
% Sets PID controller parameters
KpT= pop(1); KiT= pop(2);KdT= pop(3);
KpH=pop(4); KiH=pop(5);KdH= pop(6);N=10;
gainsT= [KpT KiT KdT N];
gainsH= [KpH KiH KdH N];
for i= 1:loop
    eT= yrT-yT;
    eH= yrH-yH;
    % Measures the performance indices
    se= abs(eT)+abs(eH); % IAE
     se= eT^2+eH^2; % ISE
    if i==1 || i==loop
       Perf= Perf+0.5*h*se;
    else
      Perf= Perf+h*se;
    end
    % Calculates the PID for temperature control
    u1= PID(yrT,yT,h,gainsT,qT);
    u(1)= Saturation(u1,[0,1]);
    % Calculates the PID for humidity rate control
    u2= PID1(yrH,yH,h,gainsH,qH);
    u(2)= Saturation(u2,[0,1]);
    % Calls the greenhouse model with input u(t)
    x= RK4(@GH_Model,t,x,u,h);
    yT= x(1); yH= x(2);
    t= t+h;
end
```

% GA optimization of PID temeperature and humidity controller

```
function Tune _PID_GH
options= optimoptions('ga','PlotFcn',@gaplotbestf);
options.PopulationSize= 20;
options.MaxGenerations= 30;
nvar= 6; % Number of variables
LB= [0 0 0 0 0 0]; % Lower bound of tuning parameters
UB= [3 0.5 3 3 0.5 3]; % Upper bound of tuning parameters
[x,fval] = ga(@Objfun_PID,nvar,[],[],[],[],LB,UB,[],options)
```